EXCITATIONS IN IMPURE MAGNETIC CRYSTALS

D.E. PEPPER

BODLEIAN LIBRARY OXFORD
DEPOSITED
THESIS
17·1·73

A thesis submitted for the degree of Doctor of Philosophy at the University of Oxford

St. John's College
Oxford

August 1972

ACKNOWLEDGEMENTS

It is a pleasure to express my gratitude to my supervisor, Dr. R.J. Elliott, for his help and encouragement at all times. Most of the computation involved in Part II was carried out by Dr. W.J.L. Buyers; I am also grateful to him and to all my colleagues for many helpful discussions. I should like to thank the Chalk River Neutron Scattering Group for permission to use their results before full publication, the Oxford University Computing Laboratory for computer facilities, the Science Research Council for a Studentship and my mother for typing this thesis.

ABSTRACT

In this thesis we consider two types of magnetic system, the ferromagnet and the antiferromagnet, containing substitutional impurities. The Heisenberg Hamiltonian is used and the spin-waves are examined by means of Green function equations of motion; the coherent potential approximation (CPA) is employed to obtain expressions for self-energies which are approximately valid for all impurity concentrations. In each case, an extension of the usual CPA is made: in Part I the impurities are described by scattering potentials with matrix elements on several lattice sites, and in Part II the effects of clusters of defects are included.

In Part I, we discuss the dilute ferromagnet, and attempt to obtain an estimate of the critical concentration of magnetic ions by considering the long-wavelength spin-waves. The self-energy is calculated in such a way as to sum coherently the scattering of spin-waves from all sites affected by one impurity, although correlations between pairs of defects are neglected. We examine solutions for a single non-magnetic impurity and for small impurity concentrations; it emerges from these considerations that it is essential that the resonance which the non-magnetic ions produce at zero energy should be kept there by any approximation which is to be of use in describing the low-energy spin-waves. A generalized form of the CPA, suitable for extended defect matrices, is developed and used to derive expressions for the self-energy; detailed numerical results are presented. We find that although the CPA behaves well over most of the spin-wave band, it fails to describe the zero-energy resonance

correctly, and this failure prevents us from deducing a value for the critical concentration. Two attempts to avoid this difficulty are described: the first uses defect Green functions to fix the energy of the resonance, the second moves it away from zero and outside the spin-wave band, but neither enables us to estimate the critical concentration. We also discuss a magnetic analogue of the percolation bond problem, to which the application of the CPA is successful.

In Part II we apply the CPA to a calculation of thespin-wave energies in antiferromagnets containing either magnetic or non-magnetic impurities. Each site is allowed to have any possible number of impurities among its nearest neighbours; in order to deal with this we extend the CPA to deal with a large number of different defect types. Variations in the transverse interactions are not included in the CPA, but are treated in an approximate way afterwards. Expressions for the neutron scattering and Raman cross sections are derived in order to permit a detailed comparison of theory with experiment. The results of numerical calculations for three systems are presented: $(Mn,Co)F_2$, $K(Mn,Co)F_3$ and $(Mn,Zn)F_2$. These are compared with experimental data, and excellent agreement is found; in particular, the neutron scattering results agree extremely well, the line-shapes and widths being accurately described by the theory.

CONTENTS

Acknowledgements (ii)

Abstract (iii)

General Introduction 1

Part I - The Dilute Ferromagnet

Introduction 4

1.1 : Green Function Methods 11

A. Hamiltonian and Green Functions 11

B. Dyson Equation 14

C. Critical Concentration 17

1.2 : Small Impurity Concentrations 19

A. Theory of a Single Impurity 19

B. Finite Impurity Concentrations 21

1.3 : Coherent Potential Approximation 28

A. CPA Equations for the Self-energy 28

B. Numerical Results 31

C. Discussion 42

1.4 : Alternative Approaches 44

A. Defect Green Functions for s-modes 44

B. Infinite Impurity Potential 49

C. The Bond Problem 54

1.5 : Conclusions 60

Part II - Impure and Dilute Antiferromagnets

Introduction 62

2.1 : Green Functions 65

2.2 : Coherent Potential Approximation 70

2.3 : Neutron Cross Sections 72

2.4 : Raman Scattering 76

2.5 : Renormalization of the Transverse Interactions 79

2.6 : Results 80

A. $(Mn,Co)F_2$ 80

B. $K(Mn,Co)F_3$ 85

C. $(Mn,Zn)F_2$ 87

2.7 : Conclusions 96

Appendix A : Symmetry Transforms for the Simple Cubic Lattice 98

Appendix B : Pure Crystal Green Functions 101

Appendix C : Coherent Potential Approximation 102

Appendix D : Numerical Methods 107

Appendix E : Solution of $\Sigma'_P = -0.5$ in the CPA 109

References 112

GENERAL INTRODUCTION

The physical behaviour of crystals containing substitutional impurities has received a great deal of attention in recent years, and the principles involved are now well understood. A substantial amount of the work done on the problem has used Green function techniques; these naturally lead to a description of the effects of the impurities in terms of a multiple scattering formalism, developed originally by Edwards (1958) and Langer(1961). By these means it is possible to use the same approximations and results for several types of excitation - phonons, electrons, magnons, excitons. Consequently, much of the theoretical development has been in a form which does not directly involve any particular excitation.

The early work produced approximations valid for small defect concentrations: for example, Langer (1961) and Elliott and Taylor (1967) on phonons; Wolfram and Callaway (1963) and Izyumov (1966) on magnons; Yonezawa and Matsubara (1966) on electrons. Attempts to extend these results to higher concentrations (Davies and Langer (1963); Leath and Goodman (1966)) were not completely successful, and the most important development was the introduction by Soven (1967) and Taylor (1967) of the coherent potential approximation (CPA) in which the problem is solved self-consistently in a way which is valid throughout the concentration range. The same results were also derived independently by Yonezawa (1968) and by Onodera and Toyozawa (1967).

The CPA has been thoroughly analysed since its first appearance (Velický et al. 1968; Leath 1968, 1970) and is now

understood to be the best approximation which does not include any correlation between scattering by pairs of defects. It is at its worst when the number of impurities is in the region of the percolation concentration, as it is then that impurity clusters are most important and a "mean environment" treatment is least appropriate. Various attempts have been made to extend it to include the effects of pairs, triplets, etc. (Aiyer et al. 1969; Nickel and Krumhansl 1971; Schwartz and Siggia 1972); the formulae produced are rather cumbersome to use, but such an extension is now possible in principle.

In its original form, the CPA could be used only where the impurity terms in the Hamiltonian were site-diagonal, which was clearly a severe limitation: it meant, for example, that changes in a phonon spectrum due to force-constant modifications could not be calculated. Takeno (1968) derived an expression to remove this difficulty, but his results do not allow inclusion of a parameter to describe impurity-impurity coupling. Recently, Blackman et al. (1971) and Foo et al. (1971) have proposed methods of doing this. The calculations in Part I of this thesis involve an extended impurity potential like that used by Takeno, as the problem considered there does not require any coupling between impurities. Takeno's equation is re-derived in a way which makes clear its relationship to the normal CPA.

Although the properties of the CPA have been fully explored, there have been no attempts to use it to describe a realistic physical system. Its application to the theory of phonons has been restricted to cases where the only impurity parameter is the atomic mass: impurity force-constants are not known in practice, and the forces involved are usually of long range.

In addition, phonon spectra are often rather complicated. Electron bands in solids are also extremely difficult to work with, except in greatly oversimplified models, and electronic spectra are not easily determined by experiment. Magnetic systems, on the other hand, provide an excellent opportunity for realistic calculations, and for testing theory against experiment. The exchange interactions are short range, and are known for many pure crystals; moreover, the spin-wave spectra are comparatively simple, and readily accessible to experiment by way of neutron diffraction.

We have chosen for this thesis two problems in which the CPA can be applied to magnetic materials. In Part I, we discuss dilute ferromagnets, and attempt to use the CPA to determine the critical concentration. As explained above, we consider the spin-wave scattering from the extended potential which describes a non-magnetic impurity, using a method which enables us to sum coherently all contributions from one defect. In doing this we are not able to treat properly neighbouring defects. In Part II, we calculate the spin-wave spectra for impure and dilute antiferromagnets: specifically, we are interested in $(Mn,Co)F_2$, $(Mn,Zn)F_2$ and $K(Mn,Co)F_3$. In order to make possible a detailed comparison of our results with experiment, we improve our treatment of neighbouring impurities; however, we are forced to make further approximations in the way we deal with off-diagonal randomness. The agreement between our theory and the experimental results is very satisfactory, and appears to justify both our use of the CPA and the extra approximations involved.

INTRODUCTION

The behaviour of dilute ferromagnetic crystals has been of interest for some time, and has been tackled by means of several techniques. The greatest attention has been paid to the determination of the critical concentration (p_c) of magnetic atoms in the lattice: that is, the minimum concentration necessary for the appearance of ferromagnetism. The variation of the Curie temperature (T_c) with concentration (p) has also been studied, and has some bearing on the relationship between the values of p_c for the Heisenberg and Ising models, which will be mentioned later.

In a discussion of previous work on this problem, the first point to be made is that it is closely related to the percolation problem of Broadbent and Hammersley (1957). This exists in two forms. In the bond problem, we consider a lattice with pipes connecting nearest-neighbour sites; some of the pipes are blocked, the choice of pipes being made at random so that each has a probability p of remaining open. We then ask for the probability P(p) that if one site is wet at random, it will wet infinitely many other sites : P(p) is called the percolation probability. In the second form, the site problem, sites are blocked at random, with probability q = 1-p, and flow is forbidden across any blocked site. In both problems, P(p) decreases from unity at p=1 and becomes zero at some critical value of p, p_o. (For a review of work on the percolation problem, see Shante and Kirkpatrick, 1971.) p_o corresponds to the point at which an infinite cluster of open (unblocked) sites appears, and it is clear that there is a strong connection

with the critical concentration for a ferromagnet. In fact, there is a formal analogy between the dilute ferromagnet with nearest-neighbour interactions and the percolation site problem, (Domb and Sykes, 1961; Fisher and Essam, 1961); the bond problem is not directly related to any physical magnetic system. We can certainly say that no ferromagnetism is possible if there are insufficient magnetic atoms present to form an infinite cluster; it is not obvious that it will necessarily occur if $p > p_o$. We shall return to this point.

Some results for p_o for the site problem, from Monte Carlo calculations and series expansions, are given in Table I for comparison with values of p_c obtained by other methods. It can be seen that p_o is always fairly close to the crude estimate of $2/z$, produced by the argument that for an infinite cluster to form, each site must have, on average, two open neighbours.

We now turn to calculations specifically for magnetic systems. Several authors (Morgan and Rushbrooke, 1961; Rushbrooke and Morgan, 1961; Elliott and Heap, 1962; Heap, 1963) have performed series expansions of the susceptibility, in powers either of p or of (J/kT). Results for the Ising model agree well with percolation values of p_o , but for the Heisenberg model the situation is less clear. Fig. [1.1] summarises the position. The curve labelled I indicates the results for the Ising model, and p_c is equal to the percolation concentration. The curve H is the result of a high-temperature expansion for the Heisenberg model. The slope is certainly greater than that of I, being about 1.33 for the simple cubic lattice, in comparison with 1.0 for the Ising model. It appears that H will have an intercept on the p-axis at p_c^* , greater than p_c, but

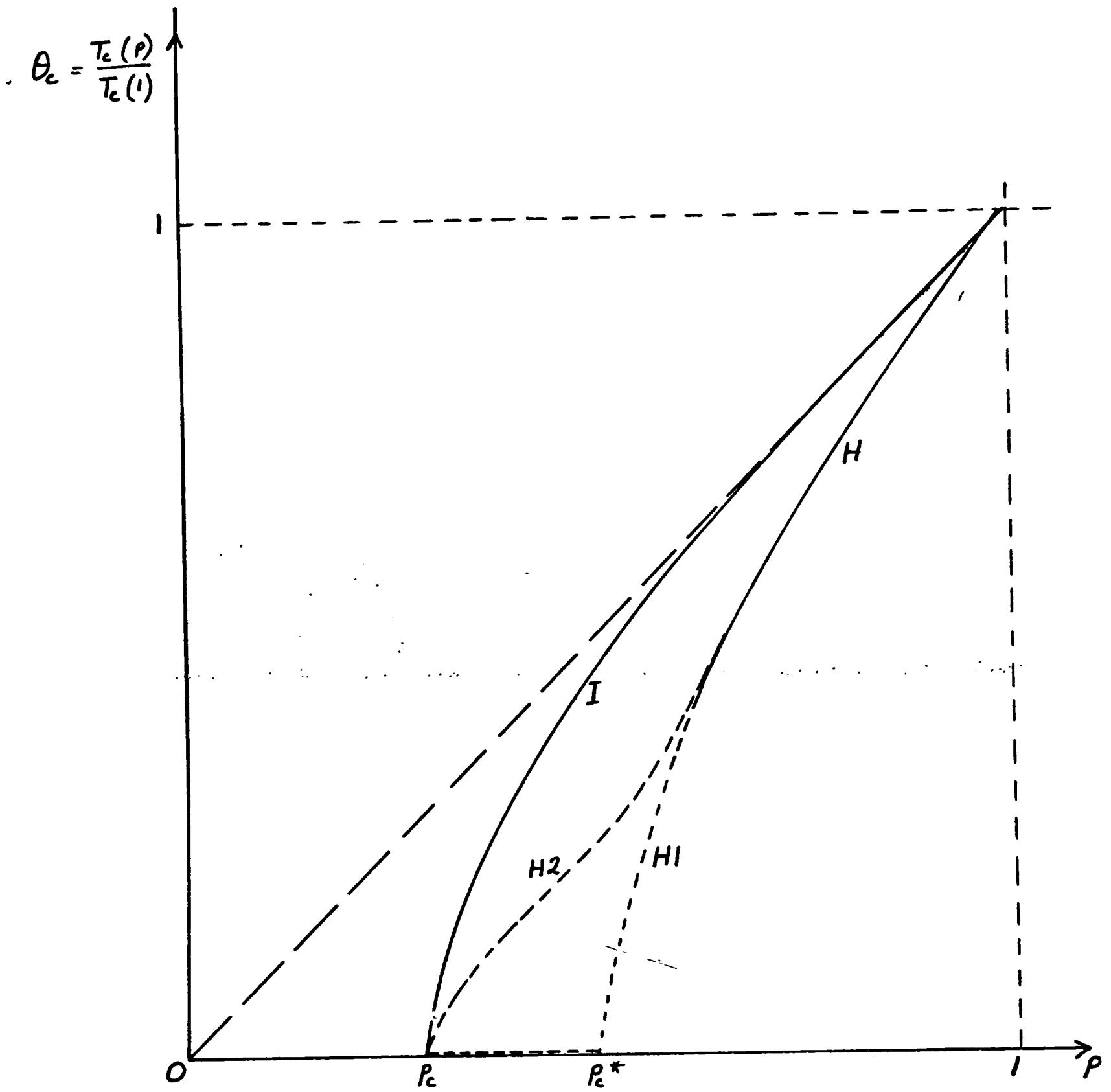


Fig. [1·1]

this cannot be stated definitely because the series are not valid for low temperatures. The expansion in p, on the other hand, diverges at p_c for both models. Elliott et al. (1960) showed that the critical concentration depends only on the lattice type, and is independent of spin and exchange interaction, but Morgan and Rushbrooke (1962) proved that this result depends on assumptions about the uniformity of convergence of the series. The question then remains whether the Heisenberg ferromagnet is unstable for $p_c < p < p_c^*$ (as in curve H1), or the Curie temperature follows curve H2.

The susceptibility has also been obtained by cluster techniques, using the well-known Bethe-Peierls-Weiss method (Smart, 1960 ; Charap, 1962; Devlin and Sawatzky, 1972). The best of these calculations is that of Charap, who included explicity the different environments possible for the outer atoms of a cluster; his results agree well with the series expansions in p. The cluster calculations also find that the slope $d\theta_c/dp$ is greater than 1 for the Heisenberg model, so that the dilemma over p_c^* is unresolved. The only experimental evidence on this point is from antiferromagnets; Baker at al. (1961) working on $(Mn,Zn)F_2$ and Breed et al. (1970) on $K(Mn,Mg)F_3$ confirm that $d\theta_c/dp > 1$, and indicate values of p_c close to those of percolation theory.

An entirely different approach relies on examining the long-wavelength spin-waves in the dilute magnet. Such a calculation could provide a check as to whether the Heisenberg ferromagnet is unstable when $p_c < p < p_c^*$. The coefficient of $(ka)^2$ in the spin-wave dispersion relation is determined as a function of p, and it is argued that this quantity becomes zero

at p_c , when the ferromagnetism becomes unstable with respect to the formation of long-wavelength spin-waves. This method was first used by Murray (1966a,b) who obtained the coefficient by means of a variational principle. Her results for p_c were much larger than those produced by other methods; however, Last (1972) has pointed out errors in the original calculation, and has shown that the variational method cannot yield a reliable estimate of p_c.

The spin-wave approach has also been adopted by Kaneyoshi (1969, 1970) and by Edwards and Jones (1971), using Green function techniques to find the dispersion relations. The most serious limitation of these calculations is the restricted number of terms included in their self-energies : only terms in p, and a few in p^2, are summed. Consequently, their application to the region $p \approx 0.3$ is questionable. This is reflected in the wide range of values which Edwards and Jones obtain for p_c by selecting various sets of terms to include in the self-energy. A rather different technique is used by Foo and Wu (1972) to obtain the self-energy; they produce a value for p_c of $\sqrt{2/z}$, which is clearly unsatisfactory.

The object of the work described in the first part of this thesis was to improve upon the existing Green function calculations for p_c. It is pointed out in the General Introduction that the best method at present available for problems of this type is the CPA, and while even that approximation includes only a sub-set of the terms in the self-energy, it could be expected to give a substantially better answer than has been obtained by related methods. In order to use the CPA for this problem, it is first necessary to extend the theory as it is normally used in order to permit treatment of off-diagonal randomness.

In the first section of Part I we develop the Green function formalism to be used. The general approach consists of studying the scattering of spin-waves by the non-magnetic impurities in a ferromagnetic medium, and describing that scattering in terms of a self-energy which embodies both an energy shift and a width. In § 1.2 some forms of the self-energy which are valid for small impurity concentrations are examined, in particular their behaviour at low energies. The development of the CPA for this problem is given in § 1.3, and detailed numerical results are presented. We show from them that the CPA cannot provide an estimate of the critical concentration, as it fails to describe the low energy spin-waves properly. This failure is shared by one of the low-concentration theories, and bedevils our attempts to solve the problem in this way. In § 1.4 we describe two ways in which we have tried to avoid the difficulty encountered in the CPA, and show why they also fail. We also consider a magnetic form of the percolation bond problem, for which the CPA can, in fact, give an answer.

TABLE I

Critical Concentrations for the Ferromagnet.

	Diamond	s.c.	b.c.c.	f.c.c.
Percolation - Monte Carlo [a]	0.436	0.325	-	0.199
Percolation - series [b]	0.425	0.307	0.243	0.195
Ising model - series [c]	0.42	0.34	0.25	-
Cluster ($S=\frac{1}{2}$) [d]	-	0.33	0.24	-
Spin-waves [e]	-	0.35-0.39	-	-

References :

(a) Frisch et al. 1961

(b) Sykes and Essam, 1964

(c) Heap, 1963

(d) Charap, 1962

(e) Edwards and Jones, 1971

1.1 : GREEN FUNCTION METHODS

In this section we shall set up the formalism and methods to be used in the problem. In subsection A, the Hamiltonian is described, and the Green functions defined and their properties derived. In subsection B we consider the effect of adding impurities to the crystal, and derive a Dyson equation to describe the impure system. The form of the solution to this equation is also discussed. In subsection C we show how the Green functions may be used to find a critical concentration for the dilute ferromagnet.

A. Hamiltonian and Green Functions

We shall describe the ferromagnet by means of the isotropic Heisenberg Hamiltonian :

$$\mathcal{H} = -\sum_{m\,n}{}' J_{mn} \left[S_m^z S_n^z + \tfrac{1}{2}\left(S_m^+ S_n^- + S_m^- S_n^+ \right) \right] \quad . \qquad (1.1)$$

S_m is the spin on the ion at site m; $S^{\pm} = S^x \pm i S^y$ are the spin raising and lowering operators; and J_{mn} is the exchange coupling between sites m and n. We shall restrict our attention to nearest-neighbour coupling, so that the summation extends only over pairs of neighbouring sites. We specify that a fraction 1-c of the sites are occupied by magnetic (host) ions, and a fraction c by non-magnetic (impurity) ions. (Note that the quantity p used in the Introduction is equal to 1-c.) The ground state of the system is taken to be the state in which all the spins are aligned parallel to the z-direction.

It will be convenient to re-write the Hamiltonian in terms of the so-called "quasi-boson operators", a_m, defined as follows (Izyumov, 1966) :

$$S_m^+ = (2S_m)^{1/2} a_m \qquad S_m^- = (2S_m)^{1/2} a_m^+$$
$$S_m^z = S_m - a_m^+ a_m \qquad (1.2)$$

We shall consider the system only at zero temperature: we may then neglect the effects of spin-wave interactions, and also replace $\langle S_m^z \rangle$ by S_m. The Hamiltonian is thus transformed into:

$$\mathcal{H} = -\sum_{m\,n} J_{mn} (S_m S_n)^{1/2} \left[-2 a_m^+ a_m + a_m^+ a_n + a_m a_n^+ \right] \qquad (1.3)$$

and the a_m have commutation relations

$$\left[a_m , a_n^+ \right] = \frac{S_m^z}{S_m} \delta_{mn} \simeq \delta_{mn} \qquad (1.4)$$

In (1.3) we have omitted an unimportant constant term, and have neglected a term of the form $a_m^+ a_m a_n^+ a_n$, which corresponds to spin-wave interactions.

To derive the properties of the Hamiltonian, we use two-time temperature-dependent Green functions of the type described by Zubarev (1960). Define :

$$G_{mn}(t) = -i\,\theta(t) \left\langle \left[a_m(t), a_n(0) \right] \right\rangle_T \equiv \ll a_m(t) ; a_n^+(0) \gg \qquad (1.5)$$

where $\theta(t)$ is the unit step-function, $a_m(t)$ is an operator at time t in the Heisenberg representation, and $\langle \cdots\cdots \rangle_T$ denotes a thermal average. The Fourier transform with respect to time of G_{mn} is defined by

$$G_{mn}(\omega) = \int_{-\infty}^{\infty} G_{mn}(t)\, e^{i\omega t}\, dt \equiv \ll a_m ; a_n^+ \gg_\omega \qquad (1.6)$$

Now, the equation of motion of G_{mn} is:

$$i \frac{dG_{mn}}{dt} = \left\langle \left[a_m, a_n^+ \right] \right\rangle \delta(t) + \ll \left[a_m(t), \mathcal{H} \right] ; a_n^+(0) \gg \qquad (1.7)$$

in units where $\hbar = 1$; if we perform a Fourier transform, and evaluate the commutator, we find

$$\omega\, G_{mn}(\omega) = \delta_{mn} + \sum_{p}{}' 2\, J_{mp} (S_m S_p)^{\frac{1}{2}} \left[G_{mn}(\omega) - G_{pn}(\omega) \right] \qquad (1.8)$$

where the summation extends over all sites which are nearest neighbours of site m.

In the impure crystal, the equation of motion is complicated by the fact that J_{mp} and S_m vary from site to site; the translational symmetry of the lattice is therefore lost, and a simple Fourier transform to $\underline{k}$ - space cannot be performed. However, in the pure crystal the symmetry is preserved, and permits a straightforward solution of (1.8). If we write the Green function with no impurities present as $g_{mn}(\omega)$, and define the $\underline{k}$-space transform by

$$g(\underline{k},\omega) = \sum_m g_{mn}(\omega)\, e^{i\underline{k}\cdot(\underline{r}_m - \underline{r}_n)} \qquad (1.9)$$

then (1.8) becomes

$$\omega g(\underline{k},\omega) = 1 + 2JS_z(1-\gamma_{\underline{k}})\, g(\underline{k},\omega) \qquad (1.10)$$

where z is the number of nearest neighbours of any site, and

$$\gamma_{\underline{k}} = z^{-1} \sum_{\Delta} e^{i\underline{k}\cdot\underline{\Delta}} \qquad (1.11)$$

summed over all nearest-neighbour vectors $\underline{\Delta}$. (1.10) then yields a solution for g :

$$g(\underline{k},\omega) = \frac{1}{\omega - 2JS_z(1-\gamma_{\underline{k}})} \qquad (1.12)$$

The usual spin-wave energies for the ferromagnet are then given by the poles of $g(\underline{k},\omega)$, viz:

$$\omega_0(\underline{k}) = 2JS_z(1-\gamma_{\underline{k}}) \qquad (1.13)$$

and the density of states is given by the imaginary part of the diagonal Green function in the site representation :

$$\rho_0(\omega) = \frac{i}{2\pi} N^{-1} \sum_{\underline{k}} \left[g(\underline{k},\omega+i\varepsilon) - g(\underline{k},\omega-i\varepsilon) \right] \qquad (1.14)$$

B. Dyson Equation

In order to solve (1.8) for the impure crystal, we first derive a Dyson equation. Writing the spin and exchange interactions for host ions as S and J, we may re-arrange (1.8) :

$$\omega G_{mn}(\omega) = \delta_{mn} + \sum_{\rho}{}' 2JS\left[G_{mn}(\omega) - G_{\rho n}(\omega)\right] + \sum_{\rho}{}' 2\left[J_{m\rho}(S_m S_\rho)^{1/2} - JS\right]\left[G_{mn}(\omega) - G_{\rho n}(\omega)\right]. \tag{1.15}$$

This may be written in matrix form

$$\omega \underset{\sim}{G} = \underset{\sim}{I} + \underset{\sim}{\Omega}\,\underset{\sim}{G} + \underset{\sim}{V}\,\underset{\sim}{G} \tag{1.16}$$

where

$$\Omega_{ij} = \sum_{\rho}{}' 2JS\,(\delta_{ij} - \delta_{\rho j}) \tag{1.17}$$

$$V_{ij} = \sum_{\rho}{}' 2\left[J_{i\rho}(S_i S_\rho)^{1/2} - JS\right](\delta_{ij} - \delta_{\rho j}) .$$

The corresponding equation for the pure-crystal Green function is

$$\omega \underset{\sim}{g} = \underset{\sim}{I} + \underset{\sim}{\Omega}\,\underset{\sim}{g} \tag{1.18}$$

Combining (1.16) and (1.18) to eliminate ω and $\underset{\sim}{\Omega}$ we obtain the required Dyson equation :

$$\underset{\sim}{G} = \underset{\sim}{g} + \underset{\sim}{g}\,\underset{\sim}{V}\,\underset{\sim}{G} \tag{1.19}$$

We shall consider the form of $\underset{\sim}{V}$ first for a general impurity, and then for the particular case of a non-magnetic impurity. The matrix $\underset{\sim}{V}$ has non-zero elements only in a (z+1)-square block around the defect, corresponding to coupling between it and its z neighbours. If we write the impurity spin as S', and the exchange coupling between host and impurity as J', then the significant block of $\underset{\sim}{V}$ has the form (Wolfram & Callaway, 1963; Izyumov 1966) :

$$\underset{\sim}{U} = 2JS \begin{bmatrix} \varepsilon z & -\gamma & -\gamma & \cdots\cdots & -\gamma \\ -\gamma & \rho & 0 & \cdots\cdots & 0 \\ -\gamma & 0 & \rho & \cdots\cdots & 0 \\ \cdots & \cdots & \cdots & \cdots & \cdots \\ -\gamma & 0 & 0 & \cdots\cdots & \rho \end{bmatrix} \qquad (1.20)$$

in which the first row (column) corresponds to the defect site, and the other z rows (columns) are its neighbours. The impurity parameters are given by

$$\varepsilon = \frac{J'}{J} - 1 \; ; \quad \rho = \frac{J'S'}{JS} - 1 \; ; \quad \gamma = \frac{J'}{J}\left(\frac{S'}{S}\right)^{\frac{1}{2}} - 1 \quad . \qquad (1.21)$$

For the special case of a non-magnetic impurity, we put $J' = S' = 0$, so that $\varepsilon = \rho = \gamma = -1$. Except in §1.4B, we shall be using these values throughout Part 1 of this thesis.

In a crystal with many impurities, $\underset{\sim}{V}$ will have blocks of elements $\underset{\sim}{y}$ distributed along the principal diagonal, corresponding to the distribution of impurities in the lattice. If the concentration c of impurities is small, these blocks are likely to be well separated and non-overlapping. However, if c is not small, there will in reality be pairs of adjacent impurities in the crystal, and larger clusters also. Such clusters are not properly accounted for by the matrix $\underset{\sim}{y}$; a neighbouring pair, for example, should be described by a 2z-square matrix, rather than by two (z+1)-square ones, and the elements on the overlap sites are not simply the sum of the corresponding elements in the smaller matrices. This effect is neglected in the present treatment; it does not seem to be possible to include it in this formalism without seriously upsetting the behaviour of the spin-waves at small $\underline{k}$, and this

is of prime importance if we are to find a critical concentration.

Later chapters will be devoted to methods for solving the Dyson equation (1.19). First, however, we shall make some general observations on the form of solution to be employed, and on how it will be used.

Equation (1.19) will in principle give G_{mn} for any particular sites in the crystal and any given configuration of impurities. However, we shall be interested in quantities such as the density of states and the neutron scattering cross section, the calculation of which involves a sum over all sites in the lattice; the density of states, for example, is $N^{-1} \sum_m G_{mm}(\omega)$. Performing such a sum is equivalent, in a macroscopic crystal, to examining one site and finding the average of G as we vary the configuration of defects around it. We shall therefore perform on (1.19) an average over all defect configurations, a process which will be represented by angular brackets $\langle \cdots \rangle$, and use the Green function thus obtained to provide information about the impure crystal.

We now want to solve the equation

$$\langle \underset{\sim}{G} \rangle = \underset{\sim}{g} + \underset{\sim}{g} \langle \underset{\sim}{V} \underset{\sim}{G} \rangle \qquad (1.22)$$

The averaging has restored translational symmetry to the lattice; we therefore seek solutions of the form

$$\langle \underset{\sim}{G} \rangle = \underset{\sim}{g} + \underset{\sim}{g} \underset{\sim}{\Sigma} \langle \underset{\sim}{G} \rangle \qquad (1.23)$$

where $\underset{\sim}{\Sigma}$ is a self-energy which is a function of ω , and is itself translationally invariant. (1.23) can now be Fourier transformed to

$$\langle G(\underline{k},\omega) \rangle = g(\underline{k},\omega) + g(\underline{k},\omega) \Sigma(\underline{k},\omega) \langle G(\underline{k},\omega) \rangle \qquad (1.24)$$

which may be arranged to give

$$\langle G(\underline{k},\omega)\rangle = \frac{1}{g^{-1}(\underline{k},\omega) - \Sigma(\underline{k},\omega)} \quad . \tag{1.25}$$

From (1.12), we may substitute for g^{-1} in (1.25) to give

$$\langle G(\underline{k},\omega)\rangle = \left[\omega - 2JS_z(1-\gamma_{\underline{k}}) - \Sigma(\underline{k},\omega)\right]^{-1} \quad ; \tag{1.26}$$

Σ thus produces a shift and a width in the spin-waves, which are described by the poles of $\langle G(\underline{k},\omega)\rangle$.

C. Critical Concentration

In the pure ferromagnet, the spin-wave energies are given by (1.13), which at small $\underline{k}$ may be approximated by

$$\omega_o(\underline{k}) \simeq 2JS\,(ak)^2 \tag{1.27}$$

where a is the lattice spacing. Now, it is known from the Goldstone theorem that for an isotropic ferromagnet the spin-wave energy $\omega(\underline{k})$ must go to zero as $\underline{k}\to 0$, and this is true even when non-magnetic impurities are present. $\omega(\underline{k})$ is given by the poles of (1.26), and as Σ is a function of concentration and will later be shown to vary as $(ak)^2$, we may write for small $\underline{k}$:

$$\omega(\underline{k}) \simeq 2JS\,\varphi(c)\,(ak)^2 \tag{1.28}$$

which is the equation used by Murray (1966b) and by Edwards and Jones (1971). The function $\varphi(c)$ is equal to unity for c=0, and falls as c is increased. There will be some value of c, say c_o, for which $\varphi(c)$ becomes zero: above c_o, $\omega(\underline{k})$ is negative for small $\underline{k}$, so that the system is unstable with respect to the formation of long-wavelength spin-waves, and the ferromagnetism must then break down. We shall take the condition

$\varphi(c)=0$ as our criterion for determining c_o. As explained by Murray, this is strictly only an upper bound on c_o, as it is possible that the order may be destroyed for some other reason at a lower value of c; this method, however, gives no information about such a possibility.

1.2 : SMALL IMPURITY CONCENTRATIONS

We now move on to derive some solutions of the Dyson equation. In subsection A we consider a single non-magnetic impurity in the lattice, and examine in particular its behaviour near zero energy. In subsection B we discuss some solutions for a small but finite impurity concentration. It is important to examine these solutions carefully, as they provide a limiting case of the coherent potential approximation, and indicate a danger which any approximate solution to this problem must avoid if it is to be of use in determining c_o.

A. Theory of a Single Impurity

We have seen that when only one impurity is present, the matrix $\underset{\sim}{V}$ has just one small block of non-zero elements. This enables us to find the poles of $G(\omega)$ very easily. The Dyson equation (1.19) may be inverted to give

$$\underset{\sim}{G} = (\underset{\sim}{1} - \underset{\sim}{g}\underset{\sim}{V})^{-1}\underset{\sim}{g} \qquad (1.29)$$

The poles of $G(\underline{k},\omega)$ will be the same as those of $g(\underline{k},\omega)$, but with the addition of any new ones produced by the factor $(\underset{\sim}{1}-\underset{\sim}{g}\underset{\sim}{V})^{-1}$. These extra poles may be found from the roots of

$$Re\{det|1 - \underset{\sim}{g}\underset{\sim}{V}|\} = 0 \qquad (1.30)$$

Because of the special form of $\underset{\sim}{V}$, this equation reduces immediately to a (z+1)-square determinant, which is easily manageable.

At this point we make two simplifications. Firstly, we restrict our attention to the simple cubic lattice, as that is the most convenient to work with and may be expected to contain all the essential features of the problem. Secondly, we set

2JS equal to 1, as this factor occurs throughout the calculations and its only effect is to scale the energy.

For the simple cubic lattice, then, the significant block of $\underset{\sim}{V}$ is found by putting $\varepsilon = \rho = \gamma = -1$ in (1.20) :

$$\underset{\sim}{\mathcal{V}} = \begin{bmatrix} -6 & 1 & 1 & 1 & 1 & 1 & 1 \\ 1 & -1 & . & . & . & . & . \\ 1 & . & -1 & . & . & . & . \\ 1 & . & . & -1 & . & . & . \\ 1 & . & . & . & -1 & . & . \\ 1 & . & . & . & . & -1 & . \\ 1 & . & . & . & . & . & -1 \end{bmatrix} \qquad (1.31)$$

It is explained in Appendix A how matrices of this form may be block-diagonalized using the symmetry of the lattice. The 7 x 7 matrix $\underset{\sim}{g}_o$ which appears in the reduced form of (1.30) has the same structure as $\underset{\sim}{A}$ in the appendix, equation (A.1). Using the methods described there, (1.30) may be reduced to the following set of three equations :-

$$Re\left\{ det\left| \begin{pmatrix} 1 & 0 \\ 0 & 1 \end{pmatrix} - \begin{pmatrix} g_{oo} & \sqrt{6}\, g_{o1} \\ \sqrt{6}\, g_{o1} & g_s' \end{pmatrix} \begin{pmatrix} -6 & \sqrt{6} \\ \sqrt{6} & -1 \end{pmatrix} \right| \right\} = 0 \qquad (1.32)$$

with $\quad g_s' = g_{oo} + g_{12} + 4\, g_{13}$

$$1 + Re\,(g_{oo} - g_{12}) = 0 \qquad (1.33)$$

$$1 + Re\,(g_{oo} + g_{12} - 2 g_{13}) = 0 \qquad (1.34)$$

Examination of the values of g_{oo}, g_{12} and g_{13} as functions of ω shows that (1.33) and (1.34) have no roots, so that there are no localized or virtual p or d modes for this system, although clearly p-wave and d-wave scattering do affect $g_{oo}(\omega)$. (See also Izyumov and Medvedev, 1966).

Evaluating the determinant in (1.32), we obtain the following condition for the s-type states :

$$Re\left[1 + 6 g_{oo} - 12 g_{o1} + g_s' \right] = 0 \quad . \qquad (1.35)$$

It is shown in Appendix B how g_{01} and g_{5}' may be expressed in terms of g_{00} ; using equations (B.2) and (B.5) in (1.35) we obtain

$$Re\left[-\frac{\omega}{6}\left(1-\omega\, g_{00}(\omega)\right)\right] = 0 \qquad (1.36)$$

This equation has only one root, $\omega = 0$. The physical origin of this root is easy to see; the impurity atom is completely decoupled from the rest of the lattice, and there is therefore zero energy associated with a spin-reversal. The other factor in (1.36) is never equal to zero, so that symmetric scattering from the shell ions does not produce a localized or virtual mode.

It is clear physically that the $\omega = 0$ mode must remain unchanged even when more impurities are added to the system. Consequently, any approximation which does not reproduce this feature is seriously in error. In particular, when we are interested in the spin-waves at low energy, as in our investigation of the critical concentration, any deviation of this mode from zero energy will prove disastrous, as will be seen in later sections.

B. Finite Impurity Concentrations

When there is a finite concentration of impurities present in the crystal, we can no longer solve the Dyson equation in the simple way used in the previous section. Instead we develop from it a series describing multiple scattering of spin-waves by impurities, and then attempt to sum this series (Langer, 1961). If we expand (1.19) by iteration, we find

$$\underset{\sim}{G} = \underset{\sim}{g} + \underset{\sim}{g}\,\underset{\sim}{V}\,\underset{\sim}{g} + \underset{\sim}{g}\,\underset{\sim}{V}\,\underset{\sim}{g}\,\underset{\sim}{V}\,\underset{\sim}{g} + \cdots\cdots \qquad (1.37)$$

Now, $\underset{\sim}{V}$ has small blocks $\underset{\sim}{v}$ distributed along the principal diagonal; if we write the (l,m) element of the block corresponding to an impurity labelled s as $v_{lm}^{(s)}$, (1.37) may be written

$$G_{ij} = g_{ij} + \sum_{s} \sum_{l,m} g_{il}\, v_{lm}^{(s)}\, g_{mj} + \sum_{r,s} \sum_{\substack{l,m \\ n,p}} g_{il}\, v_{lm}^{(s)}\, g_{mn}\, v_{np}^{(r)}\, g_{pj} \qquad (1.38)$$

If we now define the t-matrix for impurity s, representing the total scattering from that impurity, by

$$t_{lm}^{(s)} = v_{lm}^{(s)} + \sum_{np} v_{ln}^{(s)}\, g_{np}\, t_{pm}^{(s)} \qquad (1.39)$$

then the terms of (1.38) can be re-arranged to give

$$G_{ij} = g_{ij} + \sum_{s} \sum_{l,m} g_{il}\, t_{lm}^{(s)}\, g_{mj} + \sum_{r \neq s} \sum_{\substack{l,m \\ n,p}} g_{il}\, t_{lm}^{(s)}\, g_{mn}\, t_{np}^{(r)}\, g_{pj} \qquad (1.40)$$

The restriction $s \neq r$ on the summation in the second term is necessary because $\underset{\sim}{t}^{(s)}$ includes all the scattering from impurity s, and the next scattering must therefore be from a different site.

As explained in §1-1, we must now perform a configurational average on (1.38) or (1.40), and obtain a solution in the form of equation (1.23). The criterion for choosing the self-energy Σ must be that the iterated form of (1.23) should reproduce as closely as possible the terms in the configuration average of (1.38).

If the concentration of impurities is very small, the restriction on the summation in (1.40) may be neglected, and we can then write approximately :

$$\sum_{lm} = c\, t_{lm}^{(s)} \quad . \qquad (1.41)$$

This is the same approximation as that used by Izyumov (1966). Now, in (1.39), $\underset{\sim}{v}^{(s)}$ is a 7 x 7 block, and $\underset{\sim}{t}^{(s)}$ is therefore the

same size. Thus we may write for one block of $\underset{\sim}{\Sigma}$:

$$\underset{\sim}{\Sigma} = c\,\underset{\sim}{v}\left(\underset{\sim}{1} - \underset{\sim}{g}_0\,\underset{\sim}{v}\right)^{-1} \tag{1.42}$$

Some explanation of this equation is necessary. We are associating with each site in the crystal a 7 x 7 matrix $\underset{\sim}{\Sigma}$, so that the total matrix element on any site or between any pair of sites is the sum of the contributions from all neighbouring sites. However, what will appear in the denominator of G when we use Σ is the Fourier transform $\Sigma(\underline{k},\omega)$, which may be written

$$\Sigma(\underline{k},\omega) = \sum_{mn} \Sigma_{mn}(\omega)\; e^{i\underline{k}\cdot\underline{\Delta}_{mn}} \tag{1.43}$$

where the sum is over all vectors linking atoms within the 7-atom cluster.

We may now reduce (1.42) to block-diagonal form as before. The s, p and d components are given by :

$$\underset{\sim}{\Sigma}_s = c\begin{pmatrix} -6 & \sqrt{6} \\ \sqrt{6} & -1 \end{pmatrix}\left[\begin{pmatrix} 1 & 0 \\ 0 & 1 \end{pmatrix} - \begin{pmatrix} g_{00} & \sqrt{6}g_{01} \\ \sqrt{6}g_{01} & g_s' \end{pmatrix}\begin{pmatrix} -6 & \sqrt{6} \\ \sqrt{6} & -1 \end{pmatrix}\right]^{-1} \tag{1.44}$$

$$\Sigma_p = -c\left(1 + g_{00} - g_{12}\right)^{-1} \tag{1.45}$$

$$\Sigma_d = -c\left(1 + g_{00} + g_{12} - 2g_{13}\right)^{-1} \tag{1.46}$$

The 2 x 2 matrix $\underset{\sim}{v}_s$ is singular, and since $\underset{\sim}{\Sigma}_s$ is a sum of terms, each of which has the form $\underset{\sim}{v}_s(\ldots)\,\underset{\sim}{v}_s$, it simplifies to look like $\underset{\sim}{v}_s$ multiplied by a scalar. In fact :

$$\underset{\sim}{\Sigma}_s = \frac{c}{\mathcal{D}_s}\begin{pmatrix} -6 & \sqrt{6} \\ \sqrt{6} & -1 \end{pmatrix} \equiv \Sigma_s\begin{pmatrix} 6 & -\sqrt{6} \\ -\sqrt{6} & 1 \end{pmatrix} \tag{1.47}$$

$$\mathcal{D}_s = 1 + 6g_{00} - 12g_{01} + g_s' \tag{1.47a}$$

$$= -\frac{\omega}{6}\left(1 + \omega\, g_{00}\right) \tag{1.47b}$$

Thus Σ_s has the same pole at $\omega = 0$ as was observed in the single-impurity theory.

We now require the Fourier transform $\Sigma(\underline{k},\omega)$. It is shown in Appendix A how this is found from the s, p and d components; using (A.11), and noting the simplification produced by the special form of $\underset{\sim}{\Sigma}_s$, we find :

$$\Sigma(\underline{k},\omega) = \Sigma_s \varphi_s(\underline{k}) + 3\Sigma_p \varphi_p(\underline{k}) + 2\Sigma_d \varphi_d(\underline{k}) \qquad (1.48)$$

$$\left.\begin{aligned} \varphi_s(\underline{k}) &= 6(1-\gamma_{\underline{k}})^2 \\ \varphi_p(\underline{k}) &= 1-\gamma_{2\underline{k}} \\ \varphi_d(\underline{k}) &= \tfrac{3}{2}(1+\gamma_{2\underline{k}}-2\gamma_{\underline{k}}^2) \end{aligned}\right\} \qquad (1.49)$$

The new spin-wave energies are now given by the roots of (1.26), using (1.48) to provide $\Sigma(\underline{k},\omega)$. We are interested primarily in the long-wavelength solutions : for small values of $\underline{k}$, we may replace (1.49) by the approximations

$$\left.\begin{aligned} \varphi_s(\underline{k}) &\simeq (ka)^4/6 \\ \varphi_p(\underline{k}) &\simeq 2(ka)^2/3 \\ \varphi_d(\underline{k}) &\propto (ka)^4 \end{aligned}\right\} \qquad (1.50)$$

We may also approximate the dispersion relation in the pure crystal by

$$\omega_o(\underline{k}) \simeq (ka)^2 \qquad (1.51)$$

Substituting these results in (1.26), we find the equation for the new spin-wave energies :

$$\omega = (ka)^2 + \frac{c(ka)^4}{\omega(1-\omega g_{00})} - \frac{2c(ka)^2}{1+g_{00}-g_{12}} + O(ka)^4 \qquad (1.52)$$

The solution of this will be of the form $\omega(\underline{k}) \propto (ak)^2$; there is therefore a cancellation in the contribution from Σ_s, so that this term is in fact of order $(ka)^2$. The last term in (1.52), from the d-modes, gives no contribution to this order, as Σ_d does not diverge at $\omega = 0$. Thus, to leading order in

(ka), we find for the impure crystal :

$$\omega(\underline{k}) \simeq \left\{ 1 + c\left(1 - \frac{2}{1+g_{oo}-g_{12}} \right) \right\} (ka)^2 \qquad (1.53)$$

It is worth noting that an estimate of the critical concentration may be obtained from this result. We require that at c_o, the coefficient of $(ka)^2$ is zero in the limit as $\omega \to o$. Numerical calculations yield an approximate value for $g_{oo}-g_{12}$ of -0.21; if we substitute this in (1.53) and equate the term in curly brackets to zero, we obtain $c \simeq 0.35$, which is seen to be fairly close to values obtained from percolation theory. The result (1.53) is identical to one of those derived by Edwards and Jones (1971). However, we cannot place much reliance upon it as we have neglected all terms of order c^2 and higher in the self-energy.

We may attempt to improve upon (1.42) by taking some account of the summation restrictions in (1.40). Elliott and Taylor (1967) and Aiyer et al. (1969) show that a better expression for Σ is :

$$\underset{\sim}{\Sigma} = c\,\underset{\sim}{v}\left[\underset{\sim}{1} - (1-c)\,\underset{\sim}{g}_o\,\underset{\sim}{v}\right]^{-1} \qquad (1.54)$$

This form ensures that at least some of the terms in c^2, generated when (1.23) is iterated, are correct; however, the series for $\langle G \rangle$ is still not completely correct to $O(c^2)$. It also has the advantage of making Σ symmetric in c and 1-c, so that it should be valid at both ends of the concentration range. This form of solution for Σ is discussed in some detail by Schwartz et al. (1971), who refer to it as the Average t-matrix Approximation or ATA; we shall adopt this nomenclature in this thesis. (1.54) may be treated in exactly the same way as (1.42);

the s, p and d components of the self-energy then become :

$$\Sigma_s = -c\left[1 + (1-c)(6g_{00} - 12g_{01} + g_s')\right]^{-1} \tag{1.55}$$

$$\Sigma_p = c\left[1 + (1-c)(g_{00} - g_{12})\right]^{-1} \tag{1.56}$$

$$\Sigma_d = c\left[1 + (1-c)(g_{00} + g_{12} - 2g_{13})\right]^{-1} \tag{1.57}$$

Using the results of Appendix B, we can again simplify Σ_s to obtain

$$\Sigma_s = c\left[c - (1-c)\frac{\omega}{6}(1-\omega g_{00})\right]^{-1} . \tag{1.58}$$

It is clear that Σ_s no longer diverges at $\omega = 0$; the pole is shifted to $\omega \simeq 6c$. Consequently, the behaviour of the long-wavelength spin-waves is now wrong; in particular, as there is no factor of ω in the denominator of (1.58), $\Sigma_s(\underline{k})$ has no term in $(ka)^2$, but only a leading term proportional to $(ka)^4(\omega - 6c)^{-1}$. This means that we cannot obtain a meaningful estimate of the critical concentration, as we should be omitting one of the two important terms of order c in the coefficient of $(ka)^2$.

The origin of the approximation (1.54) is an attempt to compensate for some of the summation restrictions in (1.40) by correcting the single-site self-energy. For most systems this is a satisfactory procedure; but in this case we require that the position of one of the poles is given exactly, and the approximation involves an error of O(c) when there is no leading term of O(1). Equation (1.42) gave the pole correctly because we used simply the single-defect t-matrix, which is necessarily right at $\omega = 0$; in any other region this result is inferior to the ATA. It appears from this that any self-energy involving a partial correction for higher order terms is in danger of failing

to describe the $\omega = 0$ pole correctly: in whatever power of c errors in Σ appear, the pole is likely to be shifted away from zero energy by an amount proportional at least so that power of c. Of course, for $\omega \gg c$ such an error will be unimportant, but it will be crucial in the region in which we are particularly interested.

1.3 : COHERENT POTENTIAL APPROXIMATION

In the previous section we studied some forms of the self-energy applicable to small defect concentrations. We now require a solution to the Dyson equation which will be valid, in some sense, throughout the concentration range. Any approximation which is to be better than the ATA must improve our treatment of those terms in (1.40) which involve repeated scattering by one or more impurities. We could in principle attempt to do this by proceeding further along the lines of the ATA, putting into the denominator of Σ explicit correction factors for higher terms; however, this would clearly become very tedious after a very few terms had been dealt with. We use instead the coherent potential approximation, in which the self-energy is determined self-consistently in such a way as to sum a large number of multiple scattering terms correctly.

In subsection A, the equations for the self-energy are derived, and numerical solutions of them are presented in subsection B. Finally we discuss these solutions and their implications.

A : CPA Equations for the Self-energy

The basic equations of the CPA are by now well known, and so we do not give a derivation of them here; for the sake of completeness, they are presented in Appendix C. It is shown there that in the single-site CPA, the self-energy is determined by the following equation, written in an operator formalism :

$$\langle t_n \rangle \equiv \langle (1 - \tilde{V}_n G)^{-1} \tilde{V}_n \rangle = 0 \qquad (1.59)$$

t_n representing the total scattering from impurity or host n of the fully perturbed propagator G in the impure crystal.

Within our approximation of neglecting the overlap of matrices corresponding to neighbouring defects, $\tilde{V}_n$ has non-zero matrix elements only in the usual block around site n :

$$\langle \ell | \tilde{V}_n | m \rangle = \langle \ell | V_n - \Sigma_n | m \rangle = \begin{cases} v_{\ell m}^{(n)} - \Sigma_{\ell m}^{(n)} & \text{for an impurity} \\ -\Sigma_{\ell m}^{(n)} & \text{for a host} \end{cases} \quad (1.60)$$

where $\underset{\sim}{\Sigma}^{(n)}$ is the 7x7 block of $\underset{\sim}{\Sigma}$ that we require, as in (1.42). Equation (1.59) may then be written in matrix form

$$c\,(\underset{\sim}{v} - \underset{\sim}{\Sigma})\left[\underset{\sim}{1} - \underset{\sim}{G}_o(\underset{\sim}{v} - \underset{\sim}{\Sigma})\right]^{-1} - (1-c)\,\underset{\sim}{\Sigma}\left[\underset{\sim}{1} + \underset{\sim}{G}_o\,\underset{\sim}{\Sigma}\right]^{-1} = 0 \quad (1.61)$$

dropping the superscript on $\underset{\sim}{\Sigma}$ for convenience. Rearranging (1.61) we obtain

$$\underset{\sim}{\Sigma} = c\,\underset{\sim}{v}\left[\underset{\sim}{1} - \underset{\sim}{G}_o(\underset{\sim}{v} - \underset{\sim}{\Sigma})\right]^{-1} \quad (1.62)$$

which is a direct generalization of the equation used by Taylor (1967), and agrees with the expression derived by Takeno (1968). $\underset{\sim}{G}_o$ is a block of the Green function for the impure crystal, replacing the block $\underset{\sim}{g}_o$ which appeared in §1.2; it is to be understood as the configuration-averaged quantity.

We now have a self-consistent matrix equation, (1.62), to be used to determine the components of Σ. This equation may be block-diagonalized as before: the three component equations are then

$$\underset{\sim}{\Sigma}_s = c\,\underset{\sim}{v}_s\left[\underset{\sim}{1} - \underset{\sim}{G}_s(\underset{\sim}{v}_s - \underset{\sim}{\Sigma}_s)\right]^{-1} \quad (1.63)$$

$$\Sigma_p = -c\left[1 + (1+\Sigma_p)(G_{00} - G_{12})\right]^{-1} \quad (1.64)$$

$$\Sigma_d = -c\left[1 + (1+\Sigma_d)(G_{00} + G_{12} - 2G_{13})\right]^{-1} \quad (1.65)$$

(1.64) and (1.65) are scalar equations and (1.63) is a 2x2 matrix, $\underset{\sim}{v}_s$ and $\underset{\sim}{G}_s$ being the usual s-components, as in (1.44).

The form of the matrix $\underset{\sim}{v}_s$ is important: it is singular, and the off-diagonal elements are equal. The only possible solution to (1.63) is then for $\underset{\sim}{\Sigma}_s$ to be equal to $\underset{\sim}{v}_s$ multiplied by a scalar. If we write

$$\underset{\sim}{\Sigma}_s = \Sigma_s \begin{pmatrix} 6 & -\sqrt{6} \\ -\sqrt{6} & 1 \end{pmatrix} \tag{1.66}$$

then (1.63) reduces to the scalar equation

$$\Sigma_s = -c\left[1 + (1+\Sigma_s)(6G_{00} - 12G_{01} + G_s')\right]^{-1} \tag{1.67}$$

which is similar in form to (1.64) and (1.65).

We thus find that the CPA provides a set of three equations to determine the three components of Σ : (1.64), (1.65) and (1.67). The Green functions which appear in these equations involve all three components of Σ ; for example, G_{oo} is given by

$$G_{oo} = N^{-1}\sum_{\underline{k}} \frac{1}{\omega - 6(1-\gamma_{\underline{k}}) - \Sigma(\underline{k},\omega)} \tag{1.68}$$

with $\Sigma(\underline{k},\omega)$ given by (1.48). G_{01}, G_{12} and G_{13} are found from similar expressions, involving sums over $\underline{k}$-space but with different numerators. We do not have completely separate equations for the s, p and d components because a spin-wave, although it may be scattered as an s-like wave by one impurity, can subsequently be scattered in other ways by other impurities.

The solution of these three simultaneous equations must be carried out numerically; the methods employed for this are discussed in Appendix D. The results obtained are described in the following pages.

B : Numerical Results

For convenience of presentation, the description of the results in this subsection will be divided into three parts. First we discuss the behaviour of the self-energy; then we examine the line shapes for neutron scattering, predicted by the theory through $G(\underline{k},\omega)$; and finally we describe the dispersion relation for spin-waves in the dilute crystal, and the density of states.

(1) The self-energy components Σ_s, Σ_p and Σ_d, solutions of (1.64), (1.65) and (1.67), are shown in figs. [1.2] and [1.3] for c=0.1: their behaviour at this concentration is typical. Σ_p and Σ_d, fig. [1.3], are very similar both in magnitude and in their variation with ω. As expected, they show no resonances; the real parts vary little across the band, and at all concentrations are of the order of -c. The imaginary parts are small, and show a smooth hump which reflects the shape of the density of states. The small peak near $\omega=0$ corresponds to the increased density of states produced by the resonance in Σ_s. The variation of the imaginary part with concentration is very slow; the magnitude is always about the same as that at c=0.1, and the peak moves to follow the maximum in the density of states.

As is seen from fig. [1.2], Σ_s is strikingly different from Σ_p and Σ_d. Over most of the band it is very small, but it has a large resonance at low energy. When c=0.1, the peak in the imaginary part of Σ_s occurs at $\omega=0.36$; the behaviour of the real part is typical of a resonance. The height of the peak in Im Σ_s increases approximately linearly with c, but the

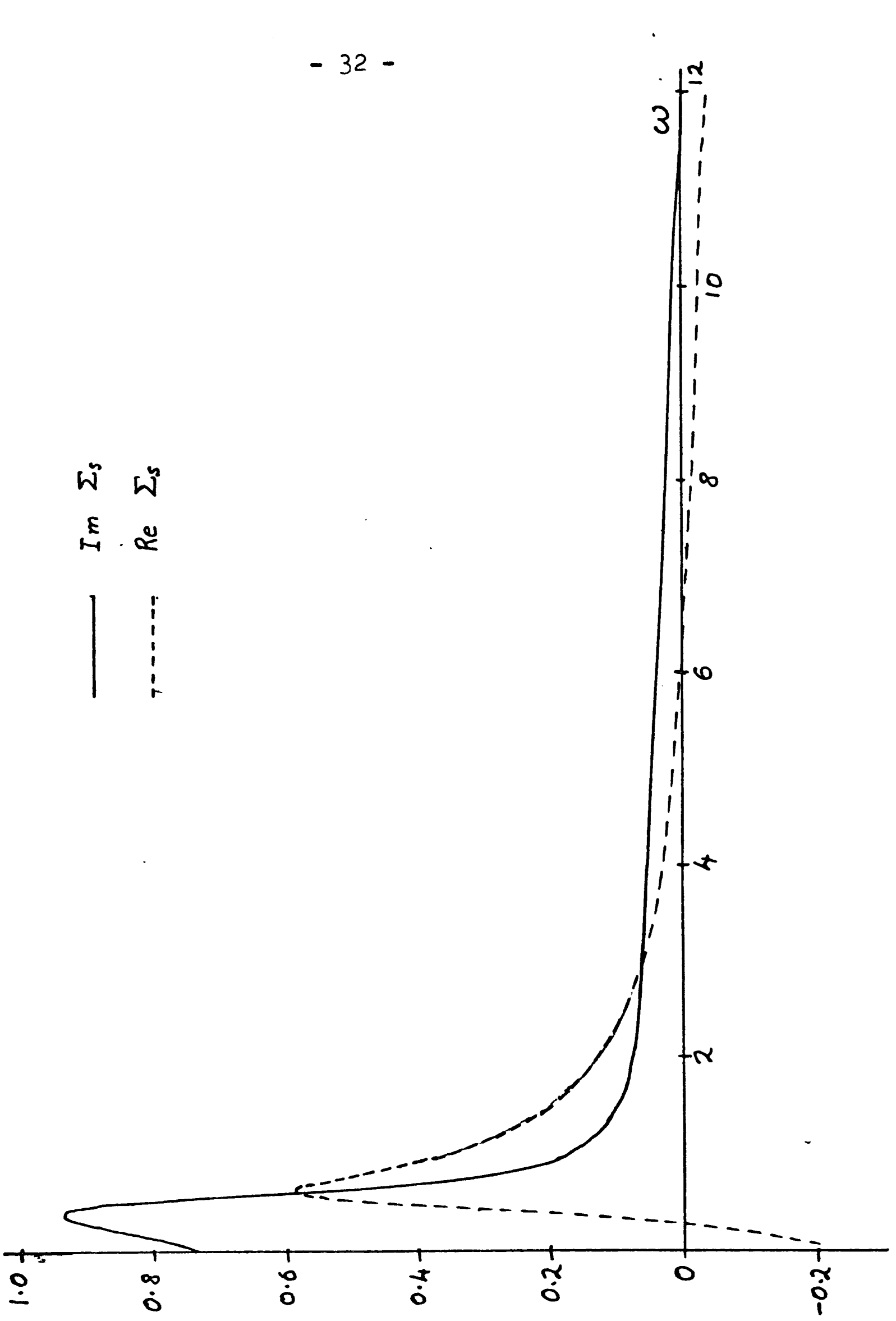


Fig. [1.2]

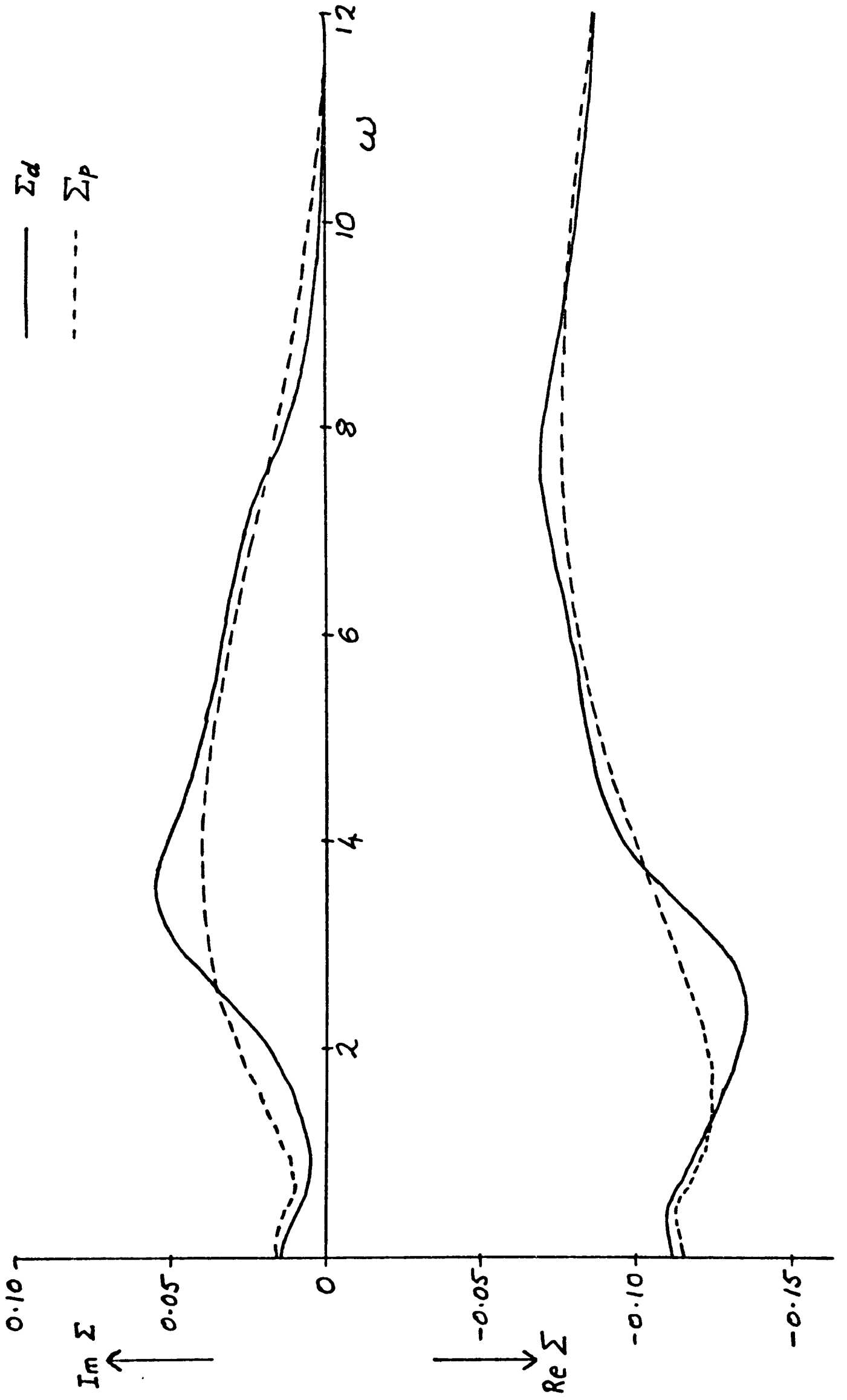


Fig. [1.3]

width is almost constant. The position of the peak, $\omega_m(s)$, as a function of c is shown in fig. [1.4]. When c is small, the resonance occurs at about $\omega = 6c$, as predicted by the ATA; there is a maximum in $\omega_m(s)$ at around c=0.1, and above c=0.3 it falls linearly. When c=0.5, the peak is exactly at $\omega = 0$: above this, it occurs at negative energies. The consequences of the behaviour of Σ_s will be discussed in subsection C.

(2) In figs. [1.5], [1.6] and [1.7] we show the imaginary part of $G(\underline{k}, \omega)$ for a range of concentrations at three points in the Brillouin zone. As we should expect, the peaks become lower and broader as c increases. For c=0.1 and 0.3, the peaks at (0.5, 0.5, 0.5), fig. [1.5], are fairly broad because of the large density of states, and are almost symmetrical; this symmetry is lost for c=0.6 and 0.7, as the spin-waves approach zero energy. At the edge of the zone, fig. [1.6], all the peaks show the same pronounced asymmetry. Close to the zone centre, the peaks for c less than 0.5 are again sharp, fig. [1.7]. For $c > 0.5$, the peaks do not move away from $\omega = 0$ until $\underline{k}$ is some way out into the zone: for c=0.6, in the (ζ, ζ, ζ) direction, the peak is not properly seen until $\zeta = 0.25$. This is a consequence of the behaviour of Σ_s, and will be discussed in the next subsection. In the curves for c=0.1 and 0.3, the effect of the s-resonance can be seen in the presence of small peaks near $\omega = 0$, due to the large imaginary part of Σ_s.

There is no evidence in the results for k = (0.5, 0.5, 0.5) and (1, 1, 1) of any dramatic change occurring at the critical concentration. The peaks are qualitatively similar at concentrations of 0.3 and 0.7, despite the differences in height and width. This is clearly consistent with the way in which we view

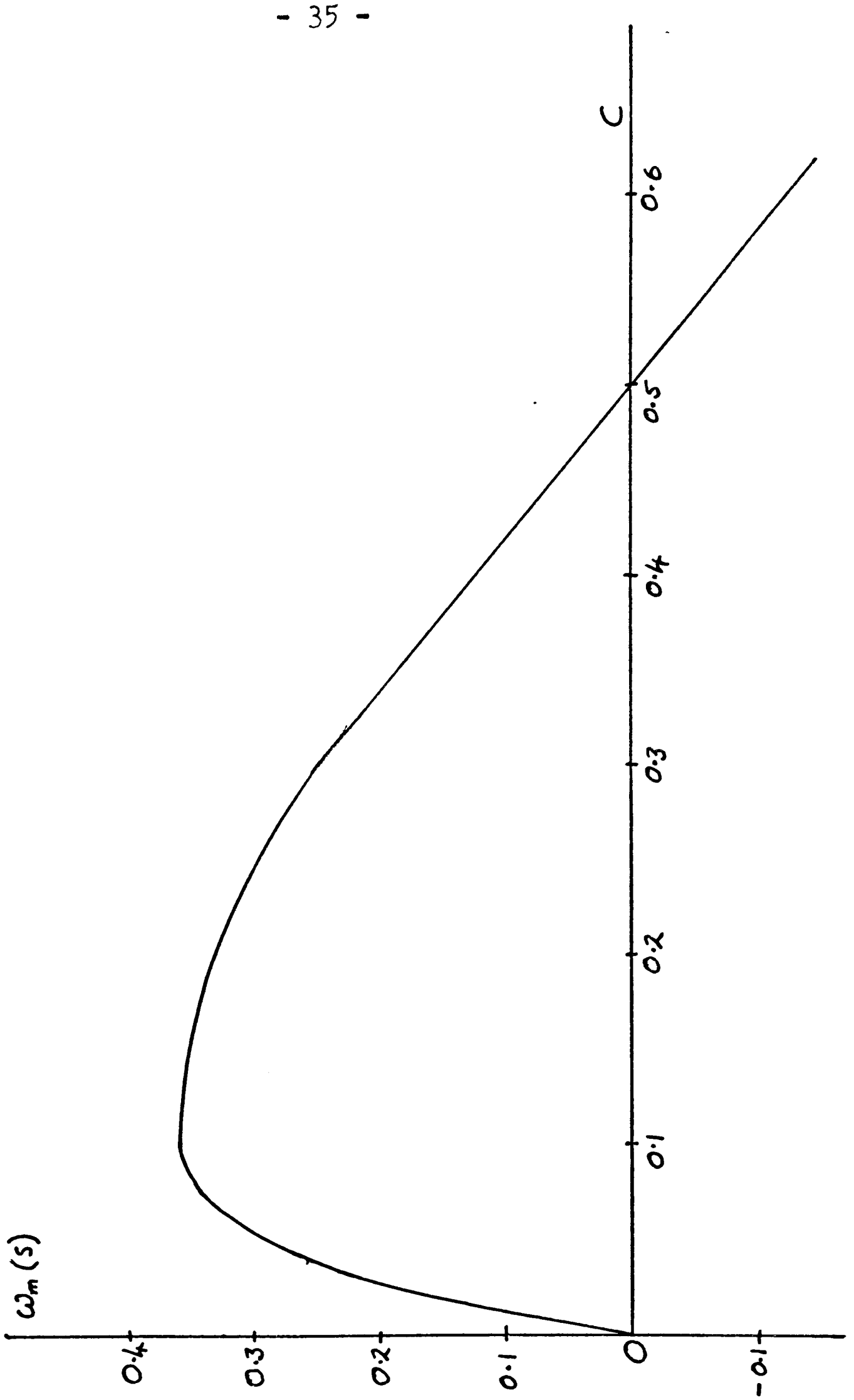


Fig. [1.4]

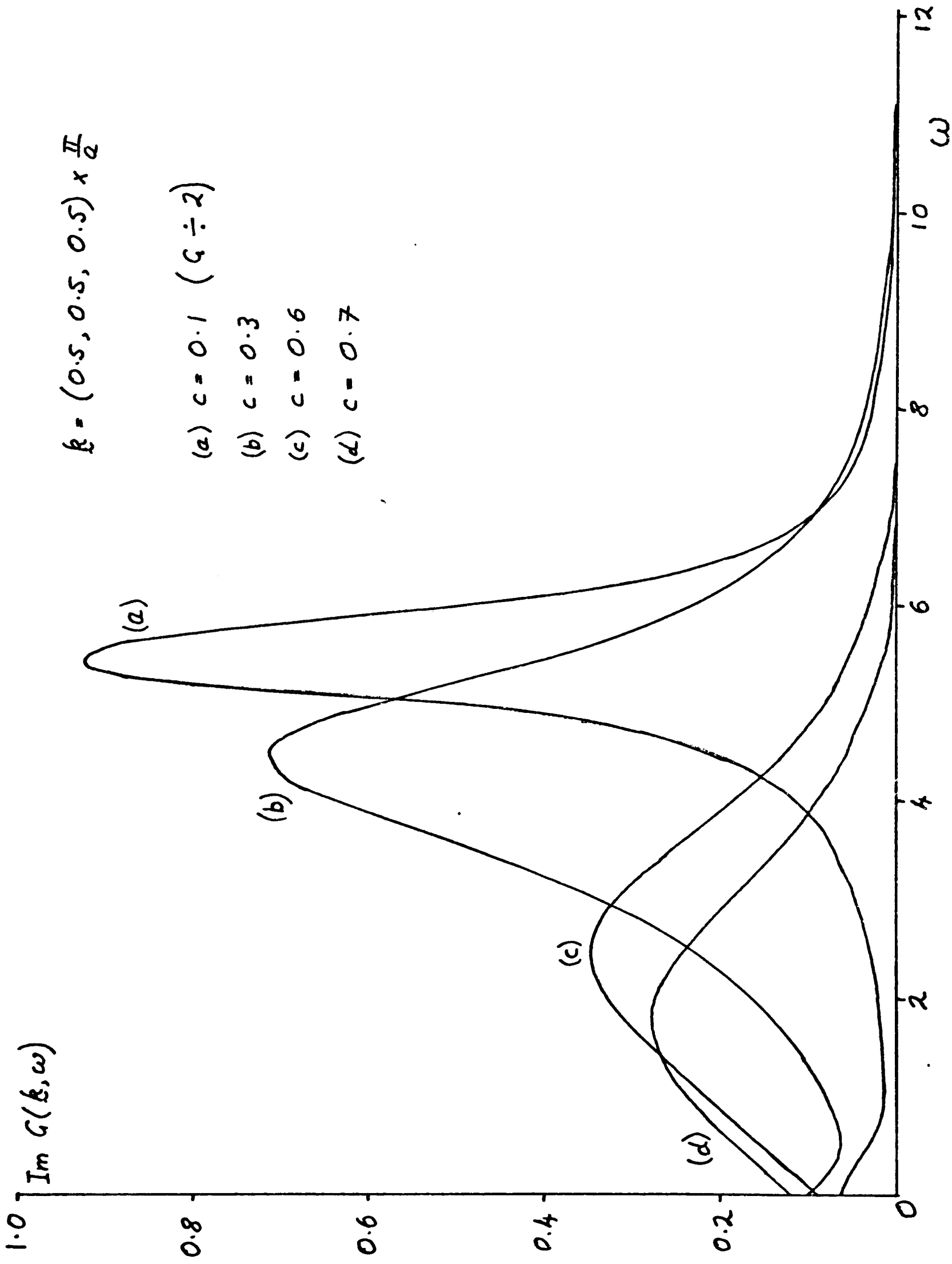

$k = (0.5, 0.5, 0.5) \times \frac{\pi}{a}$
(a) c = 0.1 (G ÷ 2)
(b) c = 0.3
(c) c = 0.6
(d) c = 0.7
Im G(k, ω)
1.0
0.8
0.6
0.4
0.2
0
2
4
6
8
10
12
ω
(a)
(b)
(c)
(d)

Fig. [1.5]

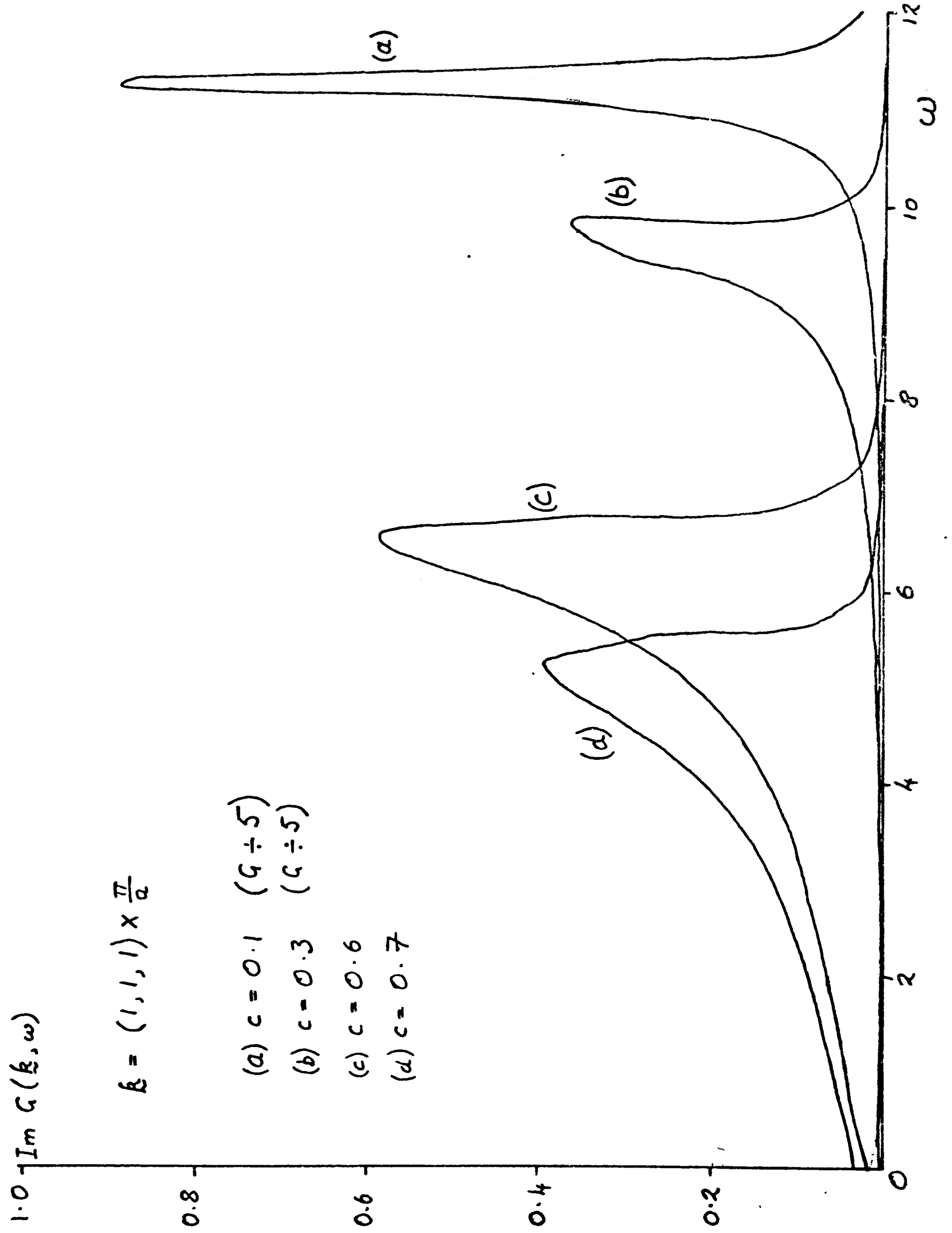

Im G(k, ω)
k = (1, 1, 1) x π/a
(a) c = 0·1 (G ÷ 5)
(b) c = 0·3 (G ÷ 5)
(c) c = 0·6
(d) c = 0·7
1·0
0.8
0.6
0.4
0.2
0
2
4
6
8
10
12
ω
(a)
(b)
(c)
(d)

Fig. [1.6]

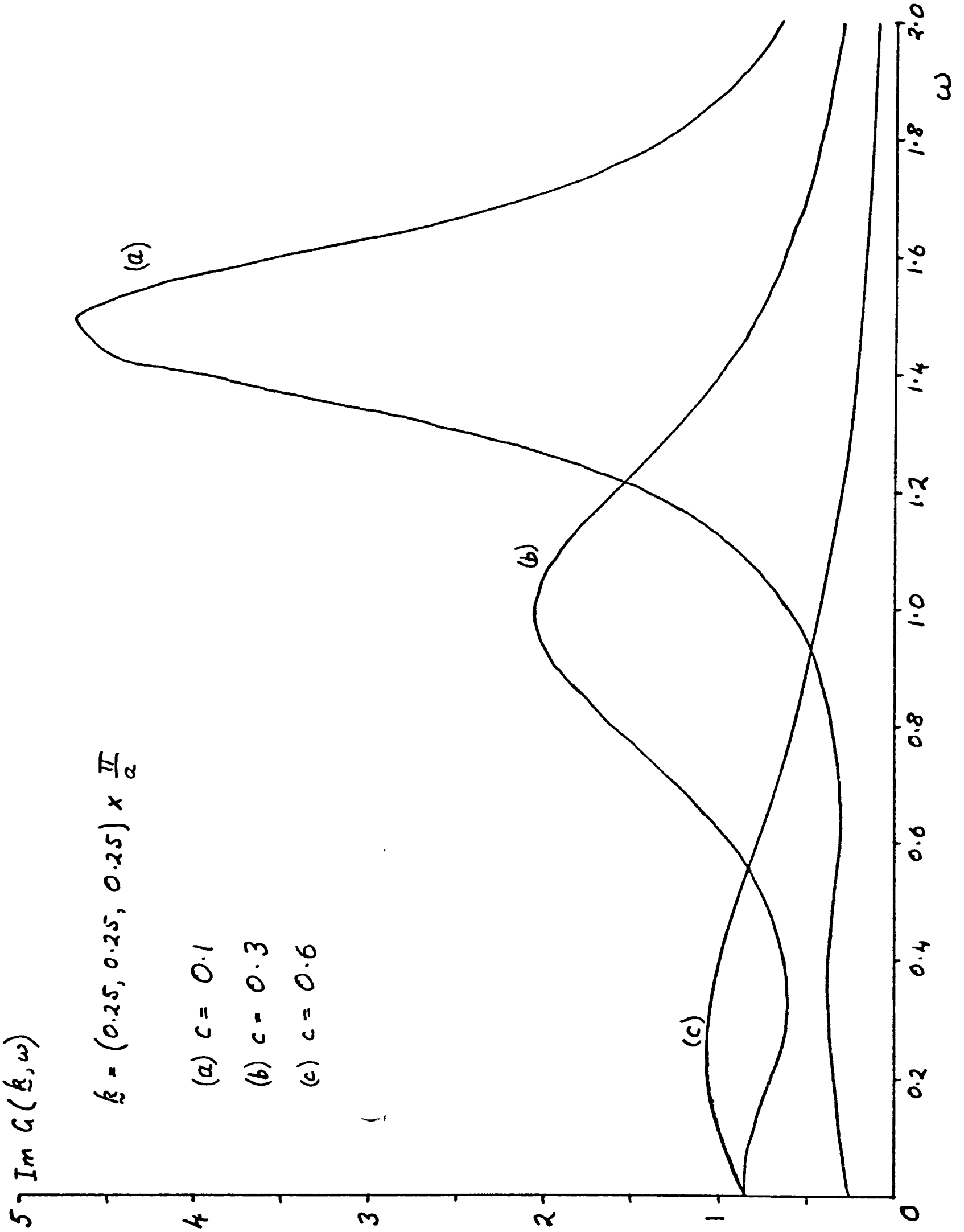

Im G(k, ω)
k = (0.25, 0.25, 0.25) x π/a
(a) c = 0.1
(b) c = 0.3
(c) c = 0.6
(a)
(b)
(c)
ω
0
0.2
0.4
0.6
0.8
1.0
1.2
1.4
1.6
1.8
2.0
1
2
3
4
5

Fig. [1.7]

the breakdown of the ferromagnetism; it is in the long-wave-length spin-waves that the instability appears, and for larger $\underline{k}$ no change is to be expected.

(3) In fig. [1.8] we show spin-wave dispersion relations in impure crystals for several values of c. These were obtained from the peaks in the imaginary part of $G(\underline{k},\omega)$, for $\underline{k}$ in the (ζ,ζ,ζ) direction. For $c<0.5$, the change is much as expected: the curves are essentially scaled by a factor of (1-c), although some distortion does occur, the upper half of the curve moving down rather less than the lower half. For $c>0.5$, the curves intersect $\omega=0$ for $\zeta>0$: this reflects the apparent "sticking" of the spin-wave peaks on $\omega=0$, mentioned above.

The spin-wave density of states is shown in fig. [1.9]; the quantity plotted is in fact the imaginary part of $G_{oo}(\omega)$. At low concentrations, the curve is essentially a scaled form of the density in the pure crystal, with some slight distortion, but as c becomes large the curve is smoothed out and pulled down, and remains finite at zero energy. The s-resonance is clearly visible near $\omega=0$ in the curves for c=0.1 and 0.3. Even the curve for c=0.01 does not go to zero at $\omega=0$, but this is essentially due to the fact that G_{oo} is obtained from a sum over a finite number of points in $\underline{k}$-space, and with the necessary small imaginary part in ω we cannot expect to produce zero imaginary part in the Green function.

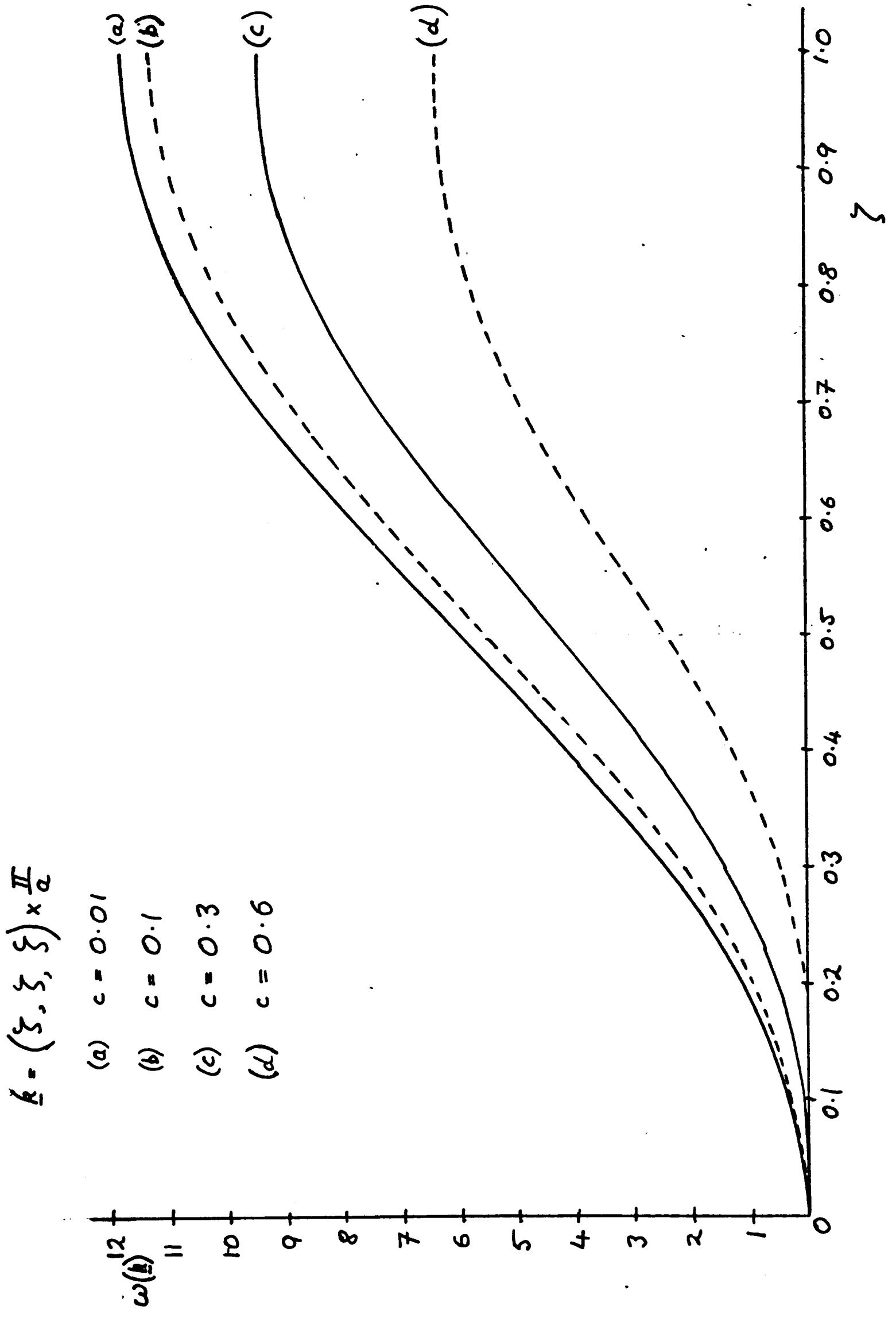

$k = (\xi, \zeta, \zeta) \times \frac{\pi}{a}$
(a) c = 0·01
(b) c = 0·1
(c) c = 0·3
(d) c = 0·6
ω(k)
12
11
10
9
8
7
6
5
4
3
2
1
0
0·1
0·2
0·3
0·4
0·5
0·6
0·7
0·8
0·9
1·0
ζ
(a)
(b)
(c)
(d)

Fig. [1·8]

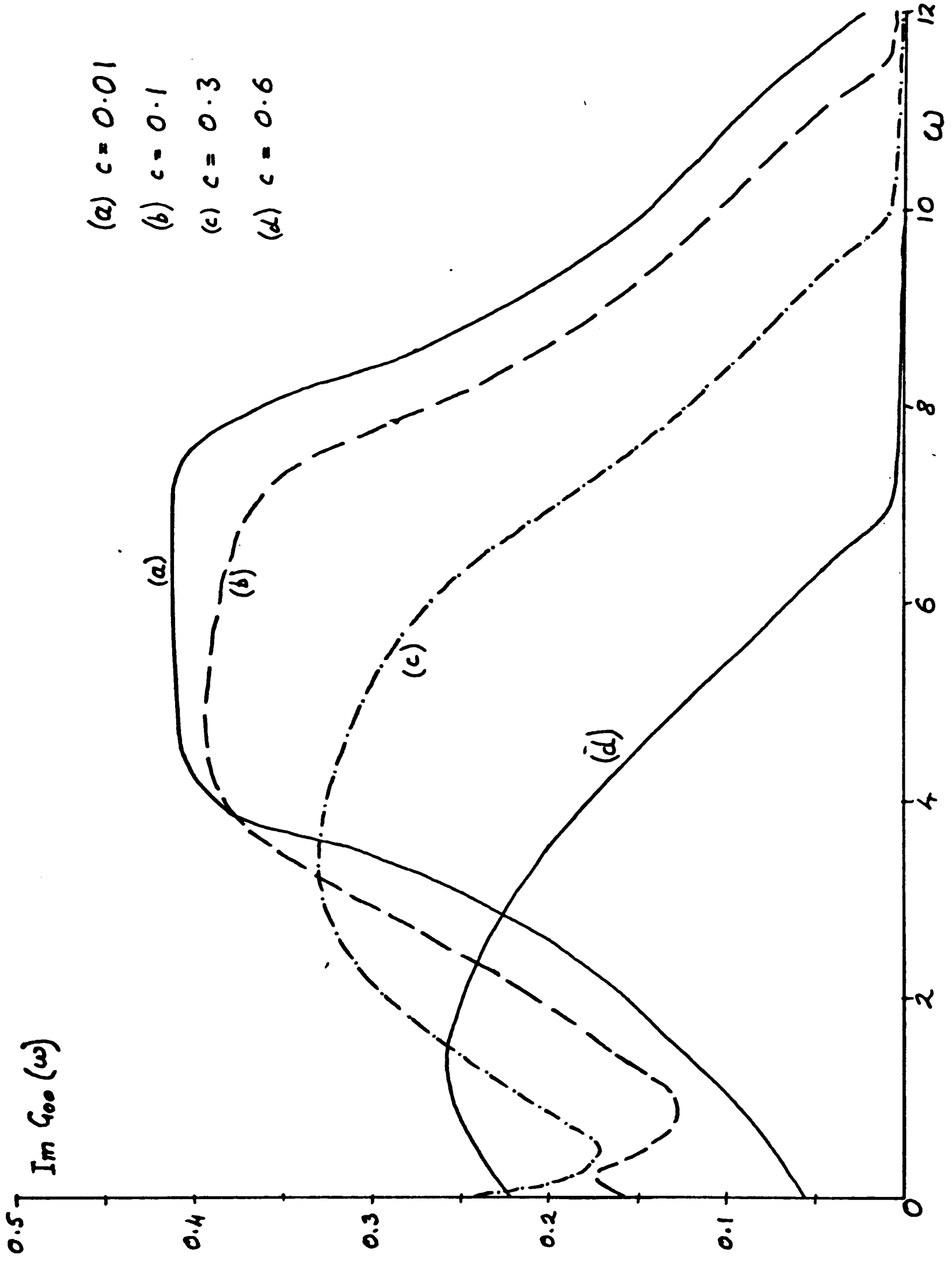


Fig. [] · 9]

C : Discussion

At large energies, the results of the CPA are quite satisfactory; the spin-wave peaks in Im $G(\underline{k},\omega)$ behave sensibly, and the dispersion curves are as we would expect. However, at low energies we observe the same error as that which occurred in the ATA, the failure to keep the s-resonance on $\omega = 0$. For the reasons explained in § 1.2, this means that we cannot use the theory to make a meaningful estimate of the critical concentration.

In order to explain the behaviour of the CPA solutions at high concentrations, we must consider in detail the spin-wave dispersion relation for small $\underline{k}$. From (1.50) and (1.51) :

$$\omega(\underline{k}) \simeq (ka)^2 + \tfrac{1}{6}\Sigma_s'\cdot(ka)^4 + 2\Sigma_p'\cdot(ka)^2 + \Sigma_d'\cdot(ka)^4 \qquad (1.69)$$

where the primes indicate the real parts of the self-energies. If Σ_s' does not diverge as ω^{-1}, then to order $(ka)^2$ we have

$$\omega(\underline{k}) \simeq (ka)^2(1 + 2\Sigma_p') \qquad (1.70)$$

If we take this equation as defining some "critical" concentration in the CPA, then this concentration is clearly that value of c for which $\Sigma_p' = -0.5$. It is found that this occurs for c=0.5 exactly; this result can, in fact, be understood from the CPA equations, as shown in Appendix E.

We see, then, that for $c > 0.5$, the spin-wave energies predicted by the CPA are negative for small $\underline{k}$. The behaviour observed in the numerical results for these concentrations is a consequence of this fact. Any peak in Im $G(\underline{k},\omega)$ for small $\underline{k}$ must now appear for some $\omega < 0$: no peak can be present at positive ω. In fact, this behaviour masks what we would expect

to happen: the spin-waves for small $\underline{k}$ should move to zero energy as we pass through the true critical concentration, as it is through them that the instability sets in. The dispersion relation actually produced goes to negative energy at some finite $\underline{k}$ for all $c > 0.5$. The density of states now includes some states for $\omega < 0$, so that it remains finite into this region.

It is clear that this behaviour is entirely unphysical, and results from the erroneous resonance in Σ_s. It seems that in this respect the CPA is no better than the ATA; if we are to use this general approach we must find a way to eliminate this particular error.

1.4 : ALTERNATIVE APPROACHES

In § 1.3 we developed a theory of the dilute ferromagnet in the coherent potential approximation, and showed that although its behaviour at high energies is satisfactory, it is incapable of giving any information about the critical concentration. In this chapter we describe two alternative approaches which have been tried; both methods continue to use the CPA, but are designed to avoid the low-energy resonance which caused the simple CPA theory to fail. In subsection A, we derive equations aimed at keeping the resonance on $\omega = 0$, using the "defect Green function" formalism; the second approach, described in subsection B, moves the resonance completely out of the spin-wave band - taking it, in fact, to infinite energy. In the final part of this section we give the theory of the magnetic form of the bond problem, and show that the CPA can there be used to derive a value for p_c.

A. Defect Green functions for s-modes

The theory of § 1.3 fails because one of the effects of the configuration-average is to blur the distinction between magnetic and non-magnetic atoms. Physically, the excitations should be constrained to remain on the magnetic sites; but in the CPA (and the ATA) the averaging process allows them to spread on to the impurities. It is clear that this general approach to the problem can only work if such effects can be prevented. One method of doing this involves the use of the defect Green function, $G^{\mathcal{D}}$, of Elliott and Taylor (1967). The original calculation of $G^{\mathcal{D}}$ was simplified by the form of the impurity scattering potential V, which there affected only one

site, whereas in this problem it affects several. We first derive an equation for G^D for this problem, and then show how it can be of use.

The Dyson equation (1.19) can be rewritten, putting in the matrix sums explicitly :

$$G_{ij} = g_{ij} + \sum_{lk} g_{il} V_{lk} G_{kj} \tag{1.71}$$

We can expand the final matrix product in the term on the right to show the contributions from individual impurities. The non-zero elements of $\underset{\sim}{V}$ are elements of $\underset{\sim}{v}$, (1.20); if we write these as v_{oo} , $v_{o\Delta}$, etc., representing the impurity site by 0 and neighbours by Δ , we find :

$$\sum_k V_{lk} G_{kj} = \sum_d{}' \Big\{ \Big(v_{oo}\, \delta_{ld} + \sum_\Delta v_{\Delta o}\, \delta_{l,d+\Delta} \Big) G_{dj} + \sum_{\Delta'} \Big(v_{o\Delta'}\, \delta_{ld} + \sum_\Delta v_{\Delta\Delta'}\, \delta_{l,d+\Delta} \Big) G_{d+\Delta',j} \Big\} \tag{1.72}$$

where the primed summation extends over all impurity (defect) sites d. It is possible to remove the restriction on the sum by defining conditional Green functions :

$$G^D_{ij} = \sum_d{}' G_{ij}\, \delta_{id}\, \delta_{ij} \tag{1.73a}$$

$$G^\Delta_{ij} = \sum_d{}' G_{ij}\, \delta_{i,d+\Delta} \tag{1.73b}$$

G^D_{ij} is non-zero only if i is a defect site; G^Δ_{ij} has elements where i is the neighbour of a defect and is linked to it by the vector $\underset{\sim}{\Delta}$. The factor δ_{ij} in (1.73a) arises because of the particular impurities we are dealing with: a non-magnetic atom is completely decoupled from all surrounding atoms, so that any G_{ij} corresponding to a correlation between impurity and neighbour must be zero. Similarly, G^Δ_{ij} will be zero if j is the impurity site of which i is a neighbour.

We now define translationally invariant matrices $\underset{\sim}{V}^{D}$ and $\underset{\sim}{V}^{\Delta}$, produced by putting appropriate elements of $\underset{\sim}{v}$ at all sites :

$$V^{D}_{ij} = v_{oo}\,\delta_{ij} + \sum_{\Delta} v_{\Delta o}\,\delta_{i,j+\Delta} \qquad (1.74a)$$

$$V^{\Delta}_{ij} = v_{o\Delta}\,\delta_{i+\Delta,j} + \sum_{\Delta'} v_{\Delta\Delta'}\,\delta_{i+\Delta,j+\Delta'} \qquad (1.74b)$$

(1.72) can be rewritten using (1.73) and (1.74) :

$$\sum_{k} V_{ek}\,G_{kj} = \sum_{k}\left(V^{D}_{ek}\,G^{D}_{kj} + \sum_{\Delta} V^{\Delta}_{ek}\,G^{\Delta}_{kj}\right) \qquad (1.75)$$

the sum on the right-hand side now extending over all sites. This is substituted into (1.71) and a configuration average performed; because of the way $\underset{\sim}{V}^{D}$ and $\underset{\sim}{V}^{\Delta}$ were defined, the average affects only $\underset{\sim}{G}^{D}$ and $\underset{\sim}{G}^{\Delta}$, so that

$$\langle G_{ij}\rangle = g_{ij} + \sum_{ek} g_{ie}\left[V^{D}_{ek}\langle G^{D}_{kj}\rangle + \sum_{\Delta} V^{\Delta}_{ek}\langle G^{\Delta}_{kj}\rangle\right] \qquad (1.76)$$

Comparing this with the defining equation for Σ, (1.23), we obtain immediately

$$\sum_{k}\left[V^{D}_{ek}\langle G^{D}_{kj}\rangle + \sum_{\Delta} V^{\Delta}_{ek}\langle G^{\Delta}_{kj}\rangle\right] = \sum_{k}\Sigma_{ek}\langle G_{kj}\rangle \qquad (1.77)$$

which is similar in form to the equation usually derived for G^{D}, but involves also the new quantities G^{Δ}.

We may consider those elements of (1.77) which lie in the usual 7x7 block around an impurity; using the definitions (1.73), and bearing in mind that $G^{D}_{o\Delta} = G^{\Delta}_{\Delta o} = 0$, we obtain the matrix equation

$$\underset{\sim}{v} \times \begin{bmatrix} G^{D}_{oo} & 0 \cdots 0 \\ 0 & \\ \vdots & \langle G^{N}_{o}\rangle \\ 0 & \end{bmatrix} = \sum_{\sim} \langle \underset{\sim}{G}_{o}\rangle \qquad (1.78)$$

where $\langle \underset{\sim}{G}^{N}_{o}\rangle$ is a 6x6 matrix with elements on all neighbours

of the impurity. This equation may be block-diagonalized as before; as explained below, we shall be interested particularly in the equation for the s-like modes, which is :

$$\underset{\sim}{v}_s \begin{pmatrix} G_{00}^D & 0 \\ 0 & G_s^N \end{pmatrix} = \sum_{\sim s} \begin{pmatrix} G_{00} & \sqrt{6}\, G_{01} \\ \sqrt{6}\, G_{01} & G_s' \end{pmatrix} \qquad (1.79)$$

dropping the average brackets $\langle \ldots \rangle$ for convenience.

The object of introducing these equations is to ensure the correct behaviour of the excitations on the impurity. We know that the only possible resonance on the non-magnetic atom is at $\omega = 0$; consequently, we shall impose the condition

$$G_{00}^D = c/\omega \qquad (1.80)$$

the factor c appearing in order to give G^D the weight required by the averaging. Now it is easily seen from the results of Appendix A that the impurity site appears only in the s-type part of the block-diagonal forms; we therefore need consider only this part in order to fix the $\omega = 0$ resonance. Accordingly, we shall leave the p- and d- components of Σ in the form given by the CPA, while using (1.79) to determine $\underset{\sim}{\Sigma}_s$.

It was noted in § 1.3 that $\underset{\sim}{y}_s$ has a peculiar singular structure; as a result, the solution to (1.79) for $\underset{\sim}{\Sigma}_s$ has fewer variables than would otherwise be the case. In fact, $\underset{\sim}{\Sigma}_s$ must have the form

$$\underset{\sim}{\Sigma}_s = \begin{pmatrix} 6\,\sigma_1 & -\sqrt{6}\,\sigma_2 \\ -\sqrt{6}\,\sigma_1 & \sigma_2 \end{pmatrix} \qquad (1.81)$$

with two quantities, σ_1 and σ_2, to be determined. However, although we have specified G_{00}^D, we know very little about G_s^N.

It involves the behaviour of the shell of atoms around an impurity, embedded in a medium comprising both magnetic and non-magnetic atoms. It would clearly not be satisfactory to use a low-concentration theory to determine G_s^N, nor can the CPA provide any information: the low-energy resonance in in that theory appears also in G_s^N, although physically it should not. We are thus unable to solve (1.79) by any method requiring knowledge of G_s^N.

The only other way we can attempt a solution is to eliminate one of σ_1 and σ_2. In the ordinary CPA, the form obtained for $\underset{\sim}{\Sigma}_s$ corresponds to (1.81) with $\sigma_1 = \sigma_2$: we therefore postulate that this condition also applies here. We then obtain from (1.79) the two equations :

$$\frac{c}{\omega} = (G_{01} - G_{00})\,\sigma_1 \qquad (1.82a)$$

$$G_s^N = (6\,G_{01} - G_s')\,\sigma_1 \qquad (1.82b)$$

Equation (1.82a) is then sufficient to determine σ_1 without knowledge of G_s^N.

We can easily check that relations (1.82) are satisfactory in the low-concentration limit. Replacing the Green functions G by their values in the pure crystal, and using equation (B.2) of Appendix B, (1.82a) gives

$$\sigma_1 = \frac{6c}{\omega(1-\omega g_{00})} \qquad (1.83)$$

which agrees with (1.47) and (1.52). Moreover, using (1.83) and (B.5) in (1.82b), we find

$$G_s^N = c\,(1-\omega g_{00})^{-1}\left[1 - (\omega - 6)\,g_{00}\right] \qquad (1.84)$$

so that the impurity's zero-energy resonance does not appear on

the neighbours.

Our new prescription for the self-energy is thus to use (1.64) and (1.65) to determine Σ_p and Σ_α, and to replace (1.67) by (1.82a) for Σ_s. The Green functions needed are again found from (1.68) and similar equations: (1.82a) is still a self-consistent condition for Σ_s. Once again, a numerical solution is necessary to find Σ: the methods employed for this solution were very similar to those used for the ordinary CPA.

It emerges from these calculations that there is no unique solution to (1.82a). Physically, the reason for this is our failure to put in any information about the shell-modes; it seems that we cannot treat the cluster by dividing it into two parts unless we describe both parts adequately. The mathematical difficulty is that the equations seem insufficient to determine Σ_s when treated self-consistently. A large number of possible solutions can be found for any values of ω and c; they appear to merge continuously with one another as ω and c are varied, and there is no one solution which is clearly more physical than the others. We are therefore forced to conclude that, without some prior knowledge of G_s^N, no progress can be made by this approach.

B. Infinite Impurity Potential

We have found that we cannot satisfactorily describe the $\omega = 0$ resonance on the non-magnetic atoms. This difficulty would be avoided if the resonance could be moved away from zero energy, and into a region where it did not affect the spin-waves. One way to achieve this is to add a term to the Hamiltonian (1.1) :

$$-\sum_m \mathcal{D} S_m^z \qquad (1.85)$$

where the sum extends over all impurity sites, and $D \gg 2JSz$. The effect of this is to prevent the spin-waves turning the spins on the impurity sites, because of the very large energy required to do so. The resonance then moves from $\omega = 0$ to $\omega \simeq D$: if we take the limit $D \to \infty$, this resonance will not directly affect the spin-wave energies.

If we work out the Green function equation of motion and Dyson equation for the modified Hamiltonian, we find that the impurity matrix $\underset{\sim}{y}$ is once again given by (1.20), but now with: $\rho = \gamma = -1$, $\varepsilon \to \infty$. We see immediately from this that it is only the s-type states which are affected by the modification. It is straightforward to show that these impurity parameters lead to the same self-energy in the low-concentration limit as did the simple parameters used before. For the s-states we have

$$\underset{\sim}{\Sigma}_s = c \begin{pmatrix} \varepsilon & \sqrt{6} \\ \sqrt{6} & -1 \end{pmatrix} \left[\underset{\sim}{1} - \begin{pmatrix} g_{oo} & \sqrt{6}\, g_{o1} \\ \sqrt{6}\, g_{o1} & g_s' \end{pmatrix} \begin{pmatrix} \varepsilon & \sqrt{6} \\ \sqrt{6} & -1 \end{pmatrix} \right]^{-1}; \quad (1.86)$$

as we require the limit $\varepsilon \to \infty$, we expand this and keep only terms in the numerator and denominator proportional to ε. Cancelling this factor out, we eventually find :

$$\underset{\sim}{\Sigma}_s = \frac{c}{\mathcal{D}} \begin{pmatrix} 1 + g_s' & -\sqrt{6}\, g_{o1} \\ -\sqrt{6}\, g_{o1} & g_{oo} \end{pmatrix} \quad (1.87)$$

$$\mathcal{D} \equiv -g_{oo} + 6 g_{o1}^2 - g_{oo} g_s' = \frac{1}{6}(1 - \omega g_{oo}) \quad (1.87a)$$

Using equation (A.11) to Fourier transform this, we obtain

$$\Sigma_s(\underline{k}) = \frac{c}{\mathcal{D}} \left[1 + g_s' + 6 g_{oo} \gamma_{\underline{k}}^2 - 12 g_{o1} \gamma_{\underline{k}} \right] \quad (1.88)$$

The term in square brackets may be simplified using the results of Appendix B; moreover, because c is very small, the spin-wave energies will not be very different from their unperturbed values,

so that we can replace ω by $6(1-\gamma_{\underline{k}})$. Eventually, we obtain

$$\Sigma_s(\underline{k}) = \frac{6c}{1-\omega g_{oo}}(1-\gamma_{\underline{k}}) \qquad (1.89)$$

The first expression obtained for this quantity in §1.2 was

$$\frac{6c}{\omega(1-\omega g_{oo})} \cdot 6(1-\gamma_{\underline{k}})^2 \qquad (1.90)$$

which is the same as (1.89) if we again replace ω by $6(1-\gamma_k)$. Thus our new formulation leads to the same result for small c, but with Σ_s giving a contribution to order $(ka)^2$ more easily.

There is, however, one problem with this approach: the addition of the term (1.85) effectively destroys the isotropy of the system, so that we can no longer guarantee that the spin-wave energy will go to zero with $\underline{k}$. Clearly, if this does not happen, we cannot define the critical concentration in terms of the coefficient of $(ka)^2$ in the spin-waves. It is apparent from (1.89) that $\omega(\underline{k}) \propto (ka)^2$ for very small c; and one can argue physically that this should be true for all c as the impurity sites, although carrying infinite energy terms, are completely decoupled from the rest of the lattice and should not upset the spin-wave spectrum. There remains the possibility that our approximations will not preserve this behaviour; as in the earlier case of the $\omega = 0$ resonance, it will depend on the cancellation of several terms, and this may not happen correctly to all orders of c.

We can see this danger immediately by considering the ATA. As in §1.2, we set

$$\underset{\sim}{\Sigma}_s = c\,\underset{\sim}{v}_s\left[\underset{\sim}{1} - (1-c)\,\underset{\sim}{g}_s\,\underset{\sim}{v}_s\right]^{-1} \quad ; \qquad (1.91)$$

this equation can be manipulated in the same way as (1.86) to

give

$$\sum_s(\underline{k}) = \frac{c\{1+(1-c)(g_s' + g_{00}\cdot 6\gamma_{\underline{k}}^2) - 12\, g_{01}\gamma_{\underline{k}}\}}{(1-c)\{-g_{00} + (1-c)(6g_{01}^2 - g_{00}g_s')\}} \qquad (1.92)$$

If we simplify this and keep only terms to order $(ka)^2$, we obtain

$$\sum_s(\underline{k}) \simeq c(6c-\omega) + 2c(ka)^2 \quad ; \qquad (1.93)$$

we see that this predicts a gap at $\underline{k}=0$. However, the gap is only of order c^2, and we might hope that the CPA would do better than this; it would even be possible to ignore a very small gap, and still examine the $(ka)^2$ term.

To derive the CPA expressions for this problem we use once again equation (1.62). After block-diagonalization, the p- and d-equations are the same as before; $\underset{\sim}{\Sigma}_s$ is now given by

$$\underset{\sim}{\Sigma}_s \equiv \begin{pmatrix} S_0 & \sqrt{6}\,S_1 \\ \sqrt{6}\,S_2 & S_3 \end{pmatrix} = c\,\underset{\sim}{v}_s\left[\underset{\sim}{1} - \underset{\sim}{G}_s(\underset{\sim}{v}_s - \underset{\sim}{\Sigma}_s)\right]^{-1} \qquad (1.94)$$

with $\underset{\sim}{v}_s$ as in (1.86). As $\underset{\sim}{v}_s$ is no longer singular, there is no restriction on the form of the self-energy. Evaluating the matrix product on the right-hand side of (1.94), and keeping only terms in ε, we obtain the following set of equations for the elements of $\underset{\sim}{\Sigma}_s$:-

$$\begin{aligned} S_0 &= \frac{c}{\mathcal{D}}\left[1 + 6G_{01}S_1 + G_s'(S_3+1)\right] \\ S_1 &= \frac{-c}{\mathcal{D}}\left[G_{00}S_1 + G_{01}(S_3+1)\right] \\ S_2 &= -c\,G_{01}/\mathcal{D} \\ S_3 &= c\,G_{00}/\mathcal{D} \\ \mathcal{D} &= -G_{00} + (S_3+1)(6G_{01}^2 - G_{00}G_s') \end{aligned} \qquad (1.95)$$

These equations must be solved together with (1.64) and (1.65)

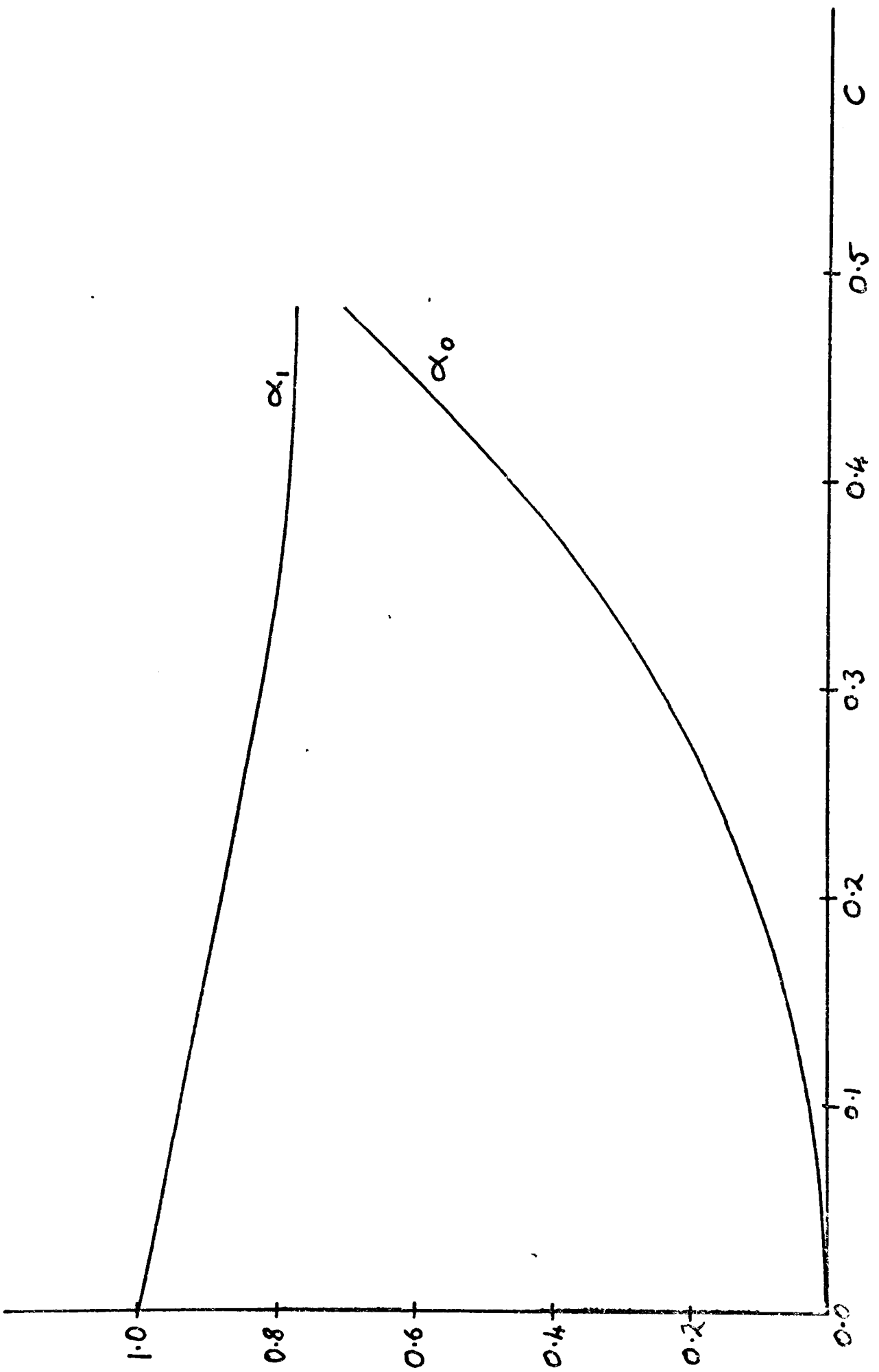


Fig. [1.10]

to find the self-consistent Σ. A numerical solution is once again necessary, using methods described previously.

We find from the calculated solution of these equations that the self-energy does not vary as $(ka)^2$, but has a constant term which increases rapidly with concentration. In fig. [1.10] we show this constant term, and the coefficient of $(ka)^2$, as functions of c. The constant is calculated from the Fourier transform of $\underset{\sim}{\Sigma}_s$; from (1.94) and (A.11), we have

$$\lim_{\underline{k}\to 0} \Sigma_s(\underline{k}) \equiv \alpha_0 = Re\left[S_0 + 6(S_1 + S_2 + S_3)\right] \quad , \qquad (1.96)$$

and the coefficient of $(ka)^2$ in the spin-wave energy is

$$\alpha_1 = 1 - Re\left[S_1 + S_2 + 2S_3 - 2\Sigma_\rho\right] \quad . \qquad (1.97)$$

We see from fig. [1.10] that α_0 is very small for small c, and increases dramatically with c. α_1, which we require to go to zero at c_0, falls only slowly, and appears to be approaching a constant at around c=0.5. Clearly, this behaviour does not permit any deductions about the critical concentration for the ferromagnet.

We must conclude that this approach is entirely unsatisfactory. The unphysical behaviour of the spin-wave spectrum results once again from the imperfect averaging implicit in the CPA: the infinite term (1.85) effectively spreads from the impurity onto the magnetic atoms, and makes the system appear anisotropic.

C. The Bond Problem

We have seen that the application of the CPA to the dilute ferromagnet cannot give an answer for the critical concentration. As mentioned in the Introduction, the problem

considered until now is directly analogous to one of the percolation problems, the site problem: the impurities are placed on the sites in a lattice, and the effect of one impurity is to cut all the bonds terminating on that site. However, we could also consider the analogous situation to the percolation bond problem, in which bonds are cut at random, and one site can have any number (between 0 and z) of intact bonds. Although the application of this idea to the ferromagnet does not correspond to any physical system, it is an interesting test of the CPA to compare its predictions in this case with those of the percolation theory.

The Hamiltonian for this system may be written :

$$\mathcal{H} = -\sum_{(mn)}{}' J\, \eta_{(mn)}\, \underline{S}_m \cdot \underline{S}_n \qquad (1.98)$$

where $\eta_{(mn)}$ takes the value 1 if the bond joining sites m and n is intact, and 0 if it is cut. We can define quasi-boson operators a_m^+ as in (1.2), with S_m=S for all sites m, and use the same Green function as before, (1.5). The equation of motion of G is then

$$\omega G_{mn}(\omega) = \delta_{mn} + \sum_{\rho}{}' 2JS\, \eta_{(m\rho)} \left[G_{mn}(\omega) - G_{\rho n}(\omega) \right] \qquad (1.99)$$

This equation can be converted into matrix form, and then used to produce a Dyson equation, exactly as in § 1.1B. Following the method of equations (1.15) - (1.19), we obtain as usual

$$\underset{\sim}{G} = \underset{\sim}{g} + \underset{\sim}{g}\, \underset{\sim}{V}\, \underset{\sim}{G} \qquad (1.100)$$

with the impurities described by

$$V_{mn} = 2JS \sum_{\rho}{}' \left[\eta_{(m\rho)} - 1 \right] \left(\delta_{mn} - \delta_{\rho n} \right) \qquad (1.101)$$

The effect of cutting one bond is then to produce in $\underset{\sim}{V}$ a single 2x2 block of non-zero elements, given by

$$\underset{\sim}{v} = \begin{pmatrix} -1 & 1 \\ 1 & -1 \end{pmatrix} \quad ; \tag{1.102}$$

if the bond which is cut is (mp), the elements of $\underset{\sim}{V}$ affected are (mm), (pp), (mp) and (pm). We have once again set 2JS=1.

The derivation of the CPA for this system follows just as in §1.3, the result being (1.62); $\underset{\sim}{v}$ is given by (1.102), and $\underset{\sim}{\Sigma}$ is a 2x2 matrix; $\underset{\sim}{G}_o$ is just

$$\underset{\sim}{G}_o = \begin{pmatrix} G_{oo} & G_{o1} \\ G_{o1} & G_{oo} \end{pmatrix} \quad . \tag{1.103}$$

We see that, as before, $\underset{\sim}{v}$ is singular and has equal off-diagonal elements. Consequently, the form of $\underset{\sim}{\Sigma}$ is again restricted, and we may put

$$\underset{\sim}{\Sigma} = \Sigma \begin{pmatrix} -1 & 1 \\ 1 & -1 \end{pmatrix} \tag{1.104}$$

We then obtain the scalar equation

$$\Sigma = \frac{c}{1 + 2(1-\Sigma)(G_{oo} - G_{o1})} \tag{1.105}$$

The Fourier transform of $\underset{\sim}{\Sigma}$ is easily seen to be

$$\Sigma(\underline{k}, \omega) = -z\,\Sigma(\omega)(1 - \gamma_{\underline{k}}) \quad ; \tag{1.106}$$

the factor z arises because each site has contributions from z nearest-neighbour bonds. The Green functions appearing in (1.105) are then given by

$$\Gamma(\omega) \equiv G_{oo} - G_{o1} = N^{-1} \sum_{\underline{k}} \frac{1 - \gamma_{\underline{k}}}{\omega - z(1-\Sigma)(1-\gamma_{\underline{k}})} \quad . \tag{1.107}$$

The simple form of the denominator of $\Gamma(\omega)$ enables us to make considerable simplifications: multiplying by $(1-\Sigma)$

we find

$$(1-\Sigma)\Gamma = N^{-1}\sum_{\underline{k}} \frac{1-\gamma_{\underline{k}}}{\frac{\omega}{1-\Sigma} - z(1-\gamma_{\underline{k}})} \qquad (1.108)$$

the right-hand side now looks like the corresponding Green function for the pure ferromagnet, but at an energy of $\frac{\omega}{1-\Sigma}$ rather than ω. Thus :

$$(1-\Sigma)\Gamma(\omega) = g_{00}\left(\frac{\omega}{1-\Sigma}\right) - g_{01}\left(\frac{\omega}{1-\Sigma}\right) \equiv \Gamma_0\left(\frac{\omega}{1-\Sigma}\right) \qquad (1.109)$$

so that the CPA equation (1.105) becomes

$$\Sigma = \frac{c}{1 + z\Gamma_0\left(\frac{\omega}{1-\Sigma}\right)} \qquad (1.110)$$

This can be simplified further, using the results of Appendix B; from (B.2) we find

$$\Gamma_0(x) = g_{00}(x) - g_{01}(x) = x g_{00}(x) - \frac{1}{z} \quad , \qquad (1.111)$$

which may be substituted in (1.110), setting $x = \frac{\omega}{1-\Sigma}$.

In order to determine the critical concentration, we are interested in the coefficient of $(ka)^2$ in the spin-wave energy; in particular, we require the limit of this quantity as $\omega \to 0$. If we denote the value of the real part of $\Sigma(\omega)$ in this limit by $\Sigma'(0)$, then we see from the denominator of (1.107) that the value of the coefficient is $1 - \Sigma'(0)$. Consequently, in order to obtain c_0 we use (1.110) to find the zero of $1 - \Sigma'(0)$. Now, provided that $Re\,\Sigma < 1$, i.e. provided $c < c_0$, $\frac{\omega}{1-\Sigma} \to 0$ with ω. Thus, from (1.111) and (1.110) we find

$$\Sigma'(0) = \frac{c}{1 - 2/z} \quad ; \qquad (1.112)$$

clearly the critical concentration of <u>cut</u> bonds is

$$c_0 = 1 - 2/z \qquad (1.113)$$

and so p_c is $2/z$. This result is not restricted to the simple cubic lattice, but holds for all lattices.

It will be seen that this result agrees with the rough estimate of the percolation concentration mentioned in the Introduction. However, accurate calculations of p_c for the bond problem (Table II) differ considerably from this figure, and one can argue that a better estimate for this problem is $p_c \simeq (z-1)^{-1}$. While it is possible that p_c for the Heisenberg model is higher than the percolation value, we cannot have much confidence in such a result on the basis of this calculation alone. If we use the first approximation of §1.2B, namely setting $\underset{\sim}{\Sigma}$ equal to c times the single-site t-matrix, and obtain an approximate value for c_o as in §1.2, we again obtain $c_o = 1-2/z$; it seems unlikely that so simple a calculation would give the correct answer. Nevertheless, our result does not necessarily imply that an approach based on the CPA cannot provide an interesting answer to the site problem, and it is encouraging that the method has produced a genuine critical concentration for this model.

TABLE II

Percolation Concentrations for the Bond Problem.

	Diamond	s.c.	b.c.c.	f.c.c.
2/Z	0.5	0.33	0.25	0.17
Monte Carlo [a]	0.390	0.254	-	0.125
Series expansions [b]	0.388	0.247	0.178	0.119

References : (a) Vyssotsky et al., 1961

(b) Sykes and Essam, 1964

1.5 : CONCLUSIONS

We have seen in the previous sections that we are unable to estimate the critical concentration of a dilute Heisenberg ferromagnet using the CPA. The particular error which thwarted our efforts occurs also in the ATA, and this fact suggests that any attempt to sum spin-wave scattering terms by this sort of method is likely to fail in the same way. The failure of the two calculations described in § 1.4 is disappointing, but does not necessarily mean that it is impossible to modify the CPA so as to correct its low-energy behaviour. If we could examine the behaviour of the shell of ions around an impurity, we might hope that the method using defect Green functions would be successful.

The CPA is the best method we have for solving impurity problems with Green functions when c is large. As explained in the Introduction, some improvement upon the results of Edwards and Jones (1971) is certainly needed, and one might reasonably have expected the CPA to provide it. An extension of Edwards and Jones' calculations using their techniques would present serious problems; firstly, to sum a large number of their diagrams would be an extremely lengthy process; secondly, it has been shown by Leath and Goodman (1966) and by Yonezawa (1968) that the use of cumulants in such a calculation produces some highly unsatisfactory features in the self-energy and the excitation spectrum. Indeed, in attempting to avoid these difficulties Yonezawa re-derived the CPA.

One encouraging aspect of the calculations we have described is the satisfactory behaviour of the CPA at energies much higher than the s-resonance. Previous instances of its use were

restricted to diagonal (mass) randomness, or else failed to sum coherently the scattering from all the off-diagonal terms produced by one defect; in this sense our results are an important extension of the approximation. The power of the method lies in its ability to give widths, as well as shifts, for all the excitations and all values of c, whereas low-c theories do not have the same range of validity and produce widths only for those excitations which are within the host band. The CPA is therefore especially useful for calculations of neutron scattering cross sections, although the absence of any experimental data for ferromagnets has prevented a direct test of our theory. However, in Part II we go on to consider impure anti-ferromagnets, and there we are able to make a detailed comparison of theory with experiment.

PART II

IMPURE AND DILUTE ANTIFERROMAGNETS

INTRODUCTION

In Part I we considered an idealized model of a ferromagnet in order to obtain an estimate of one quantity, the critical concentration. We now turn our attention to antiferromagnets, and develop a theory intended to withstand a detailed comparison with experiment. The systems of interest are crystals of MnF_2 and $KMnF_3$ containing impurities - either magnetic ions (Co) or non-magnetic (Zn). Spin-waves in these materials have recently been examined by neutron diffraction techniques at Chalk River (Buyers et al. 1971b; Coombs et al., to be published), and by Raman scattering and infrared absorbtion in Oxford (Buchanan et al., 1972); the calculations described here were performed in order to provide an interpretation of these experimental results.

The salient feature of the observed spectra of $(Co,Mn)F_2$ and $K(Co,Mn)F_3$ is the presence of two branches of excitations. In crystals where the concentration of one of the magnetic species is small one branch appears to be a local mode, but at intermediate concentrations both are dispersive. In $(Mn,Zn)F_2$, on the other hand, only one branch is observed, as the Zn ions are non-magnetic. When the Zn concentration is small a resonance is seen within the spin-wave band, but it disappears as more Zn is added.

Very little theoretical work has been done on this particular impurity problem. Lovesey (1968) and Tonegawa (1968, 1969) calculated the effects of single impurities in antiferromagnets, while Cowley and Buyers (1972) discuss theories for small defect concentrations. None of these theories can account for the experimental observations. Although the local modes in

the (Co,Mn) systems and the resonance in $(Mn,Zn)F_2$ are properly described, the theoretical predictions for higher impurity concentrations do not agree at all with experiment; both the nature of the excitations and their widths are unexplained. Consequently, we have set out to produce a theory which is capable of predicting the observed spectra in some detail.

We have worked once again in the coherent potential approximation, in order to produce results valid for all compositions. In these calculations, in contrast to those in Part I, we are not specifically interested in spin-waves of low energy, and the systems involved are not isotropic. We have therefore abandoned our earlier insistence on summing coherently all the scattering from one impurity, and have concentrated instead on improving the treatment of clusters of neighbouring defects. This seemed particularly necessary as Buyers et al. (1971b) had shown that the large widths of some of the excitations in $(Mn,Co)F_2$ could be explained simply by calculating the effects of these clusters in the Ising model. In making this improvement we were forced to omit from the CPA equations the change in the transverse interaction produced by the impurities, which creates an off-diagonal scattering term. This is, in fact, a good approximation in $(Mn,Co)F_2$, but is unsatisfactory for the other systems studied, and an approximate correction is put in later.

In the first two sections we describe the Green functions used and derive the CPA equations for the self-energy. In sections 2.3 and 2.4 expressions for the neutron scattering and Raman cross sections are given. The methods used to renormalize

the transverse interactions is described in § 2.5, and a detailed comparison of numerical results with experiment is given in § 2.6.

2.1 : GREEN FUNCTIONS

We describe the antiferromagnets by the anisotropic Heisenberg Hamiltonian

$$\mathcal{H} = 2\sum_{m\bar{m}} \left[I_{m\bar{m}}\, S^z_{m1}\, S^z_{\bar{m}2} + \tfrac{1}{2} J_{m\bar{m}} \left(S^+_{m1}\, S^-_{\bar{m}2} + S^-_{m1}\, S^+_{\bar{m}2} \right) \right] ; \quad (2.1)$$

m is the label of a unit cell in the crystal lattice; the magnetic sublattices are labelled 1 (spin up) and 2 (spin down). We treat each ion as coupled to only one set of neighbours on the opposite sublattice; the notation ($\bar{m}2$) indicates those ions on the 2-sublattice which are coupled to ion (m1). The Green functions to be used are defined by

$$G^{\alpha\beta}_{mn}(\omega) = \frac{(-1)^{1+\alpha}}{2\left(S_{m\alpha}\, S_{n\beta}\right)^{1/2}} \ll S^+_{m\alpha} \,;\, S^-_{n\beta} \gg_\omega \quad : \quad (2.2)$$

the notation $\ll \ldots \gg_\omega$ is defined in §1.1. The indices α, β specify the sublattices. The factor on the right-hand side is included for convenience in forming a Dyson equation, as will be seen later.

In the pure crystal, we may write $S_{m\alpha} = S$, $I_{m\bar{m}} = I$ and $J_{m\bar{m}} = J$ for all m and $\bar{m}$; we represent the Green function by $g^{\alpha\beta}_{mn}(\omega)$. The equation of motion of g is :

$$\omega\, g^{\alpha\beta}_{mn} = \delta_{mn}\, \delta_{\alpha\beta} + (-1)^{1+\alpha} 2IS z\, g^{\alpha\beta}_{mn} + (-1)^{\alpha} 2JS \sum_{\bar{m}} g^{\bar{\alpha}\beta}_{\bar{m}n} \quad (2.3)$$

Here, z is the number of neighbours coupled by exchange to a given atom; $\bar{\alpha} = 1$ if $\alpha = 2$, and vice versa. In order to obtain this equation we have made an RPA decoupling on the higher order Green functions :

$$\ll S^+_m\, S^z_n \,;\, S^-_p \gg \;\simeq\; \langle S^z_n \rangle \ll S^+_m \,;\, S^-_p \gg \;\simeq\; \pm S \ll S^+_m \,;\, S^-_p \gg \quad (2.4)$$

Because of the translational invariance of the pure crystal, we may perform a Fourier transform on (2.3); defining

$$g^{\alpha\beta}(\underline{k}) = \sum_{m} g_{mn}^{\alpha\beta} \, e^{i\underline{k}\cdot(\underline{R}_{m\alpha} - \underline{R}_{n\beta})} \tag{2.5}$$

the solution of (2.3) may be written in matrix form

$$\underset{\sim}{g}(\underline{k}) = \begin{pmatrix} g^{11}(\underline{k}) & g^{12}(\underline{k}) \\ g^{21}(\underline{k}) & g^{22}(\underline{k}) \end{pmatrix} = \frac{1}{\omega^2 - \omega_0(\underline{k})^2} \begin{pmatrix} \omega + A & -B\gamma_{\underline{k}} \\ B\gamma_{\underline{k}} & \omega - A \end{pmatrix} \tag{2.6}$$

where

$$\begin{aligned} A &= 2IS z \\ B &= 2JS z \\ \gamma_{\underline{k}} &= z^{-1} \sum_{\Delta} e^{i\underline{k}\cdot\underline{\Delta}} \\ \omega_0(\underline{k})^2 &= A^2 - B^2\gamma_{\underline{k}}^2 \end{aligned} \tag{2.7}$$

and $\underline{\Delta}$ is a vector linking an atom to one of its nearest neighbours. The spin-wave frequencies are then $\omega_0(\underline{k})$.

We now consider the effect of adding impurities to the crystal. We shall deal only with impurities which differ from the host in their longitudinal exchange and spin, in order to simplify the defect matrices appearing in the Dyson equation. This restriction still allows a good description of certain systems - in $(Co,Mn)F_2$ the transverse exchange energies of the two components differ by only $\frac{1}{4}\%$; however, in many cases, notably when the impurities are non-magnetic, it is not satisfactory, and we describe in § 2.5 an approximate way of compensating for it.

Making this restriction, then, and writing the impurity

spin as S' , and the exchange constants as I' between host and impurity and I" between two impurity ions, we place a single defect ion at site $\rho 1$, and find the equation of motion of G to be

$$\omega G^{\alpha\beta}_{mn} = \delta_{mn}\delta_{\alpha\beta} + (-1)^{1+\alpha} A G^{\alpha\beta}_{mn} + (-1)^{\alpha} \frac{B}{z} \sum_{\bar{m}} G^{\bar{\alpha}\beta}_{\bar{m}n} + V^{\alpha}_{m} G^{\alpha\beta}_{mn} \qquad (2.8)$$

where the impurity scattering potential is

$$V^{1}_{m} = 2Sz\,(I'-I)\,\delta_{m\rho}$$
$$V^{2}_{m} = -2\,(I'S'-IS)\,\delta_{\bar{m}\rho} \qquad (2.9)$$

We have here neglected an impurity term which is off-diagonal on m and α and is proportional to S'-S. Because of this, the defect matrix $\underset{\sim}{V}$ is diagonal, which produces a great simplification in the treatment of the many-impurity problem. In the same approximation, a single defect at site $\rho 2$ produces scattering terms $\bar{V}^{\alpha}_{m} G^{\alpha\beta}_{mn}$, where $\bar{V}^{\alpha}_{m} = -V^{\bar{\alpha}}_{m}$.

Because we have obtained a defect matrix $\underset{\sim}{V}$ which is diagonal, we can improve our treatment of clusters of neighbouring defects. It should be noted that although $\underset{\sim}{V}$ is diagonal, an impurity at site $\rho 1$ does nevertheless have scattering terms on neighbouring sites, as in (2.9); this is in contrast with the simple mass-defect problem, where no such neighbouring terms appear. It is straightforward to obtain, from equations of motion like (2.8) above, the scattering term for a site with defects on r neighbouring sites.

The results are as follows :

for a host on a 1-site : $2r(I'S'-IS) \equiv V_H(r)$ (2.10a)

for a host on a 2-site : $-2r(I'S'-IS) = -V_H(r)$ (2.10b)

for a defect on a 1-site : $2(z-r)I'S + 2rI''S' - A \equiv V_0(r)$ (2.10c)

for a defect on a 2-site : $-2(z-r)I'S - 2rI''S' + A = -V_0(r)$ (2.10d)

For a concentration c of impurity ions, the probability of a site having given value of r is

$$P(r) = \frac{z!}{r!(z-r)!}\, c^r (1-c)^{z-r} \qquad (2.11)$$

We have thus produced a situation in which we regard the binary system as though it had 2z+1 different types of impurity, distributed independently and at random; the concentrations of those described by $V_H(r)$ and $V_D(r)$ are (1-c) P(r) and cP(r) respectively. In taking account of neighbouring defects in this way, we have sacrificed the correlation between scatterings from the V' and V^2 terms produced by a single defect; however, this is probably no more serious than our neglect of any change in the transverse interactions, especially for large concentrations of impurities.

We now combine (2.3) with the generalization of (2.8), including contributions from all impurities, to form a Dyson equation in the usual way:

$$\underset{\sim}{G} = \underset{\sim}{g} + \underset{\sim}{g}\,\underset{\sim}{V}\,\underset{\sim}{G} \qquad (2.12)$$

The summations implied by the matrix products in this equation extend over both cell and sublattice indices. The matrix $\underset{\sim}{V}$, as explained above, has elements $\pm V_H(r)$ and $\pm V_D(r)$ distributed along the principal diagonal.

As explained in § 1.1, we must average this equation over all configurations of defects before solving it. The solution

in this case will be of the form

$$\underset{\sim}{G}(\underline{k}) = \underset{\sim}{g}(\underline{k}) + \underset{\sim}{g}(\underline{k}) \sum \underset{\sim}{G}(\underline{k}) \tag{2.13}$$

in which all the quantities are 2x2 matrices, as in (2.6); $\underset{\sim}{G}(\underline{k})$ is, by implication, the configurationally averaged Green function. We have already neglected the off-diagonal terms in $\underset{\sim}{V}$, and shall be working in the single-site CPA; in the same spirit, we assume that $\underset{\sim}{\Sigma}$ has only diagonal elements in the site representation, so that its Fourier transform is independent of $\underline{k}$. In (2.13) we then have

$$\underset{\sim}{\Sigma} = \begin{pmatrix} \Sigma''(\omega) & 0 \\ 0 & \Sigma^{22}(\omega) \end{pmatrix} \tag{2.14}$$

Now, time-reversal symmetry requires that the elements of the averaged $\underset{\sim}{G}$ are related by

$$G''(\omega) = - G^{22}(-\omega) \tag{2.15}$$

the outer minus sign coming from our definition of G, (2.2). Equation (2.14) then implies that a similar result must hold for $\underset{\sim}{\Sigma}$:

$$\Sigma''(\omega) = - \Sigma^{22}(-\omega) \equiv \Sigma(\omega) \tag{2.16}$$

The superscripts will be omitted in the subsequent work. This symmetry can be seen in (2.6) and (2.10). Inverting (2.13) we obtain at last :

$$\underset{\sim}{G}(\underline{k},\omega) = \frac{1}{\mathcal{D}(\underline{k},\omega)} \begin{pmatrix} \omega + A + \Sigma(-\omega) & -B\gamma_{\underline{k}} \\ B\gamma_{\underline{k}} & \omega - A - \Sigma(\omega) \end{pmatrix} \tag{2.17}$$

where

$$\mathcal{D}(\underline{k},\omega) = [\omega + A + \Sigma(-\omega)][\omega - A - \Sigma(\omega)] + B^2\gamma_{\underline{k}}^2 \tag{2.18}$$

2.2 : COHERENT POTENTIAL APPROXIMATION

In order to obtain an expression for $\Sigma(\omega)$, we once again use the CPA. We develop our theory with Appendix C as a starting point; from equation (C.16)

$$\langle t_m \rangle = 0 \tag{2.19}$$

where t_m is the total single-site scattering of the fully perturbed propagator G from one defect. To evaluate (2.19) for this problem, we must allow m to be either a host or a defect, and to have any possible value of r. Summing over all these cases, we obtain the analogous equation to (1.61) :

$$\sum_{r=0}^{z} P(r) \left\{ c \left[V_D(r) - \Sigma(\omega) \right] X_D(r) + (1-c) \left[V_H(r) - \Sigma(\omega) \right] X_H(r) \right\} = 0 \tag{2.20}$$

where

$$X_A(r) = \left\{ 1 - \left[V_A(r) - \Sigma(\omega) \right] \langle G_0''(\omega) \rangle \right\}^{-1} \tag{2.21}$$

for A = D or H. $\langle G_0''(\omega) \rangle$ is the diagonal part of $\underset{\sim}{G}$, and is given by

$$\langle G_0''(\omega) \rangle = N^{-1} \sum_{\underline{k}} G''(\underline{k}, \omega) \quad . \tag{2.22}$$

(2.20) is an implicit equation for $\Sigma(\omega)$ which is a generalization of the one derived by Taylor (1967). It must, as usual, be solved numerically; a more suitable form for an iterative solution is obtained by re-arrangement of the terms :

$$\Sigma(\omega) = \frac{\sum_r P(r) \left[c\, V_D(r) X_D(r) + (1-c)\, V_H(r) X_H(r) \right]}{\sum_r P(r) \left[c\, X_D(r) + (1-c)\, X_H(r) \right]} \tag{2.23}$$

$\Sigma(\omega)$ is then determined self-consistently between (2.17), (2.22) and (2.23).

We can also obtain a simpler form of this theory, rather easier to compute than the preceding one; we refer to it as the <u>average cluster theory</u> to distinguish it from the above <u>multiple cluster theory</u>. Instead of considering the scattering potential for each configuration, V(r), we assume that the spin dynamics are largely determined by the average energies on host and defect sites :

$$W_H \equiv \langle V_H(r) \rangle = \sum_{r=1}^{z} P(r)\, V_H(r) = 2cz\,(I'S' - IS) \qquad (2.24a)$$

$$W_D \equiv \langle V_D(r) \rangle = \sum_{r=0}^{z} P(r)\, V_D(r) = 2cz\, I''S' + 2(1-c)z\, I'S - A \qquad (2.24b)$$

The expansion of (2.19) then becomes

$$c\left[W_D - \Sigma(\omega)\right] X_D(\bar{r}) + (1-c)\left[W_H - \Sigma(\omega)\right] X_H(\bar{r}) = 0 \qquad (2.25)$$

where $X_A(\bar{r})$ is given by (2.21) with $V_A(r)$ replaced by W_A. (2.25) then replaces (2.20) as a condition to determine $\Sigma(\omega)$.

2.3 : NEUTRON CROSS SECTIONS

The differential cross section for neutron scattering may be written in the well-known form (Van Hove, 1954) :

$$\frac{d^2\sigma}{d\omega\, d\Omega} = \frac{1}{4}(r_0 g)^2 \frac{k'}{k}\left(1+\frac{Q_z^2}{Q^2}\right)\frac{1}{2\pi}\int_{-\infty}^{\infty} dt\, e^{-i\omega t} \times \sum_{\substack{mn \\ \alpha\beta}} f_{m\alpha} f_{n\beta}\, e^{-i\underline{Q}\cdot(\underline{R}_{m\alpha}-\underline{R}_{n\beta})}\, \mathcal{S}_{mn}^{\alpha\beta}(t) \tag{2.26}$$

where r_o is the classical electron radius; $g = 1.91$; $\underline{Q} = \underline{k}-\underline{k}'$ is the wave vector transfer; $f_{m\alpha}$ is the form factor of the ion at site $m\alpha$. The final term is the correlation function

$$\mathcal{S}_{mn}^{\alpha\beta}(t) = \left\langle S_{m\alpha}^{+}(0)\, S_{n\beta}^{-}(t) + S_{m\alpha}^{-}(0)\, S_{n\beta}^{+}(t)\right\rangle \tag{2.27}$$

We introduce conditional Green functions G^{HH}, G^{HD}, G^{DH} and G^{DD}, where

$$G_{\alpha\beta}^{HH}(\underline{k},\omega) = \left\langle \sum_{m\alpha=H} G_{mn}^{\alpha\beta}(\omega)\, e^{i\underline{k}\cdot(\underline{R}_{m\alpha}-\underline{R}_{n\beta})}\right\rangle \tag{2.28}$$

$n\beta=H$

the summation being over sites $m\alpha$ and $n\beta$ which are both occupied by host ions; G^{HD}, G^{DD} involve defect atoms and are similarly defined. These are required because of the terms $f_{m\alpha}\, f_{n\beta}$ in (2.26) which ensure that each ion has the appropriate form factor associated with it (Elliott and Taylor, 1967). These conditional Green functions are similar to G^{D} encountered in § 1.4. However, the situation is here complicated by the large number of the defect types, rather than by the size of the defect scattering matrix, and so we give a full derivation of G^{D}, etc. for this case. The cross section now becomes

$$\frac{d^2\sigma}{d\omega\, d\Omega} = \frac{1}{4\pi}(r_0 g)^2 \frac{k'}{k}\left(1+\frac{Q_z^2}{Q^2}\right)\frac{\hbar}{1-e^{\beta\hbar\omega}}\left(\mathcal{J}_{HH}+\mathcal{J}_{HD}+\mathcal{J}_{DH}+\mathcal{J}_{DD}\right) \tag{2.29}$$

where

$$\mathcal{J}_{HH} = \sum_{\alpha,\beta} 5 f_H^2\, \mathrm{Im}\left[(-1)^{1+\alpha} G_{\alpha\beta}^{HH}(\underline{Q},\omega) - (-1)^{1+\beta} G_{\beta\alpha}^{HH}(\underline{Q},\omega)\right] \tag{2.30}$$

and similarly for $\mathcal{J}_{HD}$, etc. We must now find expressions for G^{HH}, etc.

We consider first the case of a lattice with only one atom per unit cell, so that $\Sigma(\omega)$ and $G(\underline{k},\omega)$ are scalars, and let the crystal contain a number of different types of substitutional impurity, described by V_i, (i = 1,2...n), with concentrations c_i. We define the conditional Green function $G^{i}_{mp}(\omega)$, in which site m must be occupied by an atom of type i, and $G^{ij}_{mp}(\omega)$, in which m is an i-atom, and p is a j-atom. The CPA equation corresponding to (2.20) is then

$$\sum_{i=1}^{n} c_i \left[V_i - \Sigma(\omega) \right] X_i - c_o \, \Sigma(\omega) X_o = 0 \qquad (2.31)$$

where

$$X_i = \left\{ 1 - \left[V_i - \Sigma(\omega) \right] \langle G_o(\omega) \rangle \right\}^{-1} ; \qquad (2.32)$$

c_o is the concentration of host atoms, $1 - \sum_i c_i$; and X_o is obtained from (2.32) by putting $V_i = 0$. (2.31) may be arranged to obtain

$$\sum_{i=1}^{n} c_i \left\{ \left[V_i - \Sigma(\omega) \right] X_i + \Sigma(\omega) X_o \right\} = \Sigma(\omega) X_o \qquad (2.33)$$

from which we obtain an equation for the self-energy :

$$\Sigma(\omega) = \sum_{i=1}^{n} c_i V_i X_i \qquad (2.34)$$

Now the Dyson equation (2.12) may be written in the form

$$G_{mp}(\omega) = g_{mp}(\omega) + \sum_{i=1}^{n} \sum_{r} g_{mr}(\omega) V_i \, G^{i}_{rp}(\omega) \qquad (2.35)$$

where the sum over r extends over all lattice sites. This may be averaged over configurations to produce

$$\langle \underset{\sim}{G}(\omega) \rangle = \underset{\sim}{g}(\omega) + \sum_{i=1}^{n} \underset{\sim}{g}(\omega) V_i \langle \underset{\sim}{G}^{i}(\omega) \rangle \qquad (2.36)$$

comparing this with the defining equation for $\Sigma(\omega)$

$$\langle \underset{\sim}{G}(\omega) \rangle = \underset{\sim}{g}(\omega) + \underset{\sim}{g}(\omega) \underset{\sim}{\Sigma}(\omega) \langle \underset{\sim}{G}(\omega) \rangle \tag{2.37}$$

we obtain the result

$$\underset{\sim}{\Sigma}(\omega) \langle \underset{\sim}{G}(\omega) \rangle = \sum_{i=1}^{n} V_i \langle \underset{\sim}{G}^{i}(\omega) \rangle \tag{2.38}$$

Substitution of (2.38) into (2.34) suggests a form of solution for G^i which is consistent, namely

$$\langle \underset{\sim}{G}^{i}(\omega) \rangle = c_i \langle \underset{\sim}{G}(\omega) \rangle X_i \tag{2.39}$$

To find $\underset{\sim}{G}^{ij}$ we iterate (2.12 and (2.37) to obtain

$$G_{mp} = g_{mp} + \sum_{i=1}^{n} \sum_{r=i}^{\prime} g_{mr} V_i g_{rp} + \sum_{i,j=1}^{n} \sum_{r,s} g_{mr} V_i G_{rs}^{ij} V_j g_{sp} \tag{2.40}$$

$$\langle G_{mp} \rangle = g_{mp} + \sum_{r} g_{mr} \Sigma g_{rp} + \sum_{r,s} g_{mr} \Sigma \langle G_{rs} \rangle \Sigma g_{sp} \tag{2.41}$$

If (2.40) is configurationally averaged, comparison with (2.41) yields the equation to be solved for $\underset{\sim}{G}^{ij}$

$$\sum_{i} c_i V_i \underset{\sim}{1} + \sum_{i,j} V_i \langle \underset{\sim}{G}^{ij}(\omega) \rangle V_j = \Sigma(\omega) \underset{\sim}{1} + \Sigma(\omega)^2 \langle \underset{\sim}{G}(\omega) \rangle \tag{2.42}$$

The form of the solution is indicated by (2.39), and we find that (2.42) is satisfied if $\underset{\sim}{G}^{ij}$ has the form

$$\langle \underset{\sim}{G}^{ij}(\omega) \rangle = c_i c_j X_i X_j \langle \underset{\sim}{G}(\omega) \rangle + c_i X_i [\delta_{ij} - c_j X_j] \underset{\sim}{1} \langle G_{oo}(\omega) \rangle \tag{2.43}$$

The last term is necessary to ensure that the diagonal part G_{mm}^{ii} has weight c_i, rather than c_i^2. Thus the diagonal elements of (2.43) also satisfy (2.39).

The extension of these results to the present case is straightforward because of the simple diagonal forms of $\underset{\sim}{V}$ and $\underset{\sim}{\Sigma}$. The G^{MM}, etc. that we require in (2.29) are those obtained by averaging over all possible nearest-neighbour configurations,

and so we include a sum over r in the expressions for these quantities. Thus c_i takes the value cP(r) for a defect site, with $V_i = V_D(r)$, and the value of (1-c)P(r) for a host site, with $V_i = V_H(r)$. Using (2.39) and (2.43) we find

$$\underset{\sim}{G}^{D}_{\alpha\beta}(\omega) = \sum_{r=0}^{z} c\rho(r) \left\langle \underset{\sim}{G}^{\alpha\beta}(\omega) \right\rangle X_D^{\alpha}(r) \tag{2.44}$$

$$\underset{\sim}{G}^{DD}_{\alpha\beta}(\omega) = \sum_{r'=0}^{z} \sum_{r=0}^{z} \Big\{ c^2 \rho(r)\rho(r') \left\langle \underset{\sim}{G}^{\alpha\beta}(\omega) \right\rangle X_D^{\alpha}(r) X_D^{\beta}(r') + c\rho(r) X_D^{\alpha}(r) \left[\delta_{rr'} - c\rho(r') X_D^{\alpha}(r') \right] \delta_{\alpha\beta} \left\langle G_0^{\alpha\beta}(\omega) \right\rangle \underset{\sim}{1} \Big\} \tag{2.45}$$

where, from (2.10)

$$\begin{aligned} V_D^{\alpha}(r) &= (-1)^{1+\alpha} V_D(r) \\ X_D^{\alpha}(r) &= \left\{ 1 - \left[V_D^{\alpha}(r) - \Sigma^{\alpha\alpha}(\omega) \right] \left\langle G_0^{\alpha\alpha}(\omega) \right\rangle \right\}^{-1} \end{aligned} \tag{2.46}$$

The other quantities required in (2.29) are then found from the relations

$$\begin{aligned} \underset{\sim}{G}^{H} &= \underset{\sim}{G} - \underset{\sim}{G}^{D} \\ \underset{\sim}{G}^{DH} &= \underset{\sim}{G}^{D} - \underset{\sim}{G}^{DD} \\ \underset{\sim}{G}^{HD}_{\alpha\beta} &= (-1)^{\alpha+\beta} \underset{\sim}{G}^{DH}_{\beta\alpha} \\ \underset{\sim}{G}^{HH} &= \underset{\sim}{G}^{H} - \underset{\sim}{G}^{HD} \end{aligned} \tag{2.47}$$

2.4 : RAMAN SCATTERING

The original development of the theory of the two-magnon Raman scattering of light in antiferromagnets was made by Fleury and Loudon (1968); a formulation in terms of Green functions was given by Elliott and Thorpe (1969), who also included the effects of magnon-magnon interactions. They show that the Raman cross section is determined by Green functions of the type

$$\Gamma_{mnpq} \equiv \ll S_{m1}^{+} S_{n2}^{-} + S_{m1}^{-} S_{n2}^{+} \; ; \; S_{p1}^{+} S_{q2}^{-} + S_{p1}^{-} S_{q2}^{+} \gg \qquad (2.48)$$

We shall first derive an approximate formula for such a two-particle Green function in terms of the single-particle $\ll S^{+}; S^{-} \gg$, and then use it to write down the Raman cross sections for the systems in which we are interested. The method used in the first part of the calculation is similar to that of Deo and Behera (1966).

The two particle Green function we require has the general form

$$\Gamma_{1234}(t) = \ll a_1^{\dagger} a_2 \; ; \; a_3^{\dagger} a_4 \gg \qquad (2.49)$$

$$= -i\,\theta(t) \left\langle \left[a_1^{\dagger}(t)\, a_2(t),\, a_3^{\dagger}(0)\, a_4(0) \right] \right\rangle \qquad (2.49a)$$

where the a_i are boson operators. By adding and subtracting terms to the commutator, this may be re-written

$$\Gamma_{1234}(t) = -i\,\theta(t) \left\langle a_1^{\dagger}(t) \left[a_2(t), a_3^{\dagger}(0) \right] a_4(0) + a_3^{\dagger}(0) \left[a_1^{\dagger}(t), a_4(0) \right] a_2(t) \right\rangle \qquad (2.50)$$

We define advanced and retarded single-particle Green functions

$$\gamma_{12}^{a}(t) = i\,\theta(-t) \left\langle \left[a_1^{\dagger}(t),\, a_2(0) \right] \right\rangle$$

$$\gamma_{12}^{r}(t) = -i\,\theta(t) \left\langle \left[a_1^{\dagger}(t),\, a_2(0) \right] \right\rangle \qquad (2.51)$$

with Fourier transforms

$$\gamma(\omega) = \int_{-\infty}^{\infty} \gamma(t)\, e^{i\omega t}\, dt = \begin{cases} \gamma^{r}(\omega), & \mathrm{Im}\ \omega > 0 \\ \gamma^{a}(\omega), & \mathrm{Im}\ \omega < 0 \end{cases} \qquad (2.52)$$

Following Zubarev (1960), the correlation functions are :

$$\langle a_1^{\dagger}(t)\, a_2(0) \rangle = i \int_{-\infty}^{\infty} \frac{\gamma(\omega+i\varepsilon) - \gamma(\omega-i\varepsilon)}{e^{\beta\omega} - 1}\, e^{-i\omega t}\, e^{\beta\omega}\, d\omega \qquad (2.53)$$

We may then write approximately for Γ:

$$\Gamma_{1234}(t) \simeq \langle a_1^{\dagger}(t)\, a_4(0) \rangle\, \gamma_{23}^{a}(-t) + \langle a_3^{\dagger}(0)\, a_2(t) \rangle\, \gamma_{14}^{r}(t) \qquad (2.54)$$

$$= i \int_{-\infty}^{\infty} \frac{e^{\beta\omega}\, d\omega}{e^{\beta\omega} - 1} \left\{ \tilde{\gamma}_{14}(\omega)\, \gamma_{32}^{a}(-t)\, e^{-i\omega t} + \tilde{\gamma}_{32}(\omega)\, \gamma_{14}^{r}(t)\, e^{i\omega t} \right\} \qquad (2.55)$$

in which we have separated the correlation functions from the commutators before performing the thermal average, and

$$\tilde{\gamma}(\omega) = \gamma(\omega+i\varepsilon) - \gamma(\omega-i\varepsilon) \qquad (2.56)$$

In the impure crystal, this separation into a product of two γ's involves a further approximation, in that we should perform the configurational average on the complete Γ, rather than on the individual γ's; however, our treatment is in the same spirit as the single-site approximations already made in the CPA. We now take the Fourier transform of $\Gamma(t)$, and consider the system at zero temperature, so that $\beta \to \infty$. Eventually, we have :

$$\Gamma_{1234}(\omega_1) = i \int_{0}^{\infty} d\omega \left[\tilde{\gamma}_{14}(\omega)\, \gamma_{32}^{a}(\omega - \omega_1) + \tilde{\gamma}_{32}(\omega)\, \gamma_{14}^{r}(\omega + \omega_1) \right] \qquad (2.57)$$

For the antiferromagnet, we use (2.57) to expand (2.48); there will be four terms like Γ_{1234} from the various cross-products of $S^{+}S^{-}$ operators. Following Fleury and Loudon (1968), we may write down the absorption coefficient for xy-scattering,

corresponding to the Γ_5^+ representation of the crystal space group of MnF_2, as (Elliott and Thorpe, 1969)

$$I^{xy}(\omega_1) = N^{-1}\sum_{k} \mathrm{Im}\ \Gamma(\underline{k},\omega_1)\sin^2(\tfrac{1}{2}ak_x)\sin^2(\tfrac{1}{2}ak_y)\cos^2(\tfrac{1}{2}ak_z) \quad (2.58)$$

where, using (2.57) and remembering the factor $(-1)^{1+\alpha}$ in the definition of $G^{\alpha\beta}$,

$$\begin{aligned}\Gamma(\underline{k},\omega_1) = i\int_0^\infty d\omega \Big\{ & \tilde{G}^{12}(\underline{k},\omega)\,G_a^{12}(\underline{k},\omega-\omega_1) + \tilde{G}^{12}(\underline{k},\omega)\,G_r^{12}(\underline{k},\omega+\omega_1) \\ & - \tilde{G}^{11}(\underline{k},\omega)\,G_a^{22}(\underline{k},\omega-\omega_1) - \tilde{G}^{22}(\underline{k},\omega)\,G_r^{11}(\underline{k},\omega+\omega_1) \\ & - \tilde{G}^{22}(\underline{k},\omega)\,G_a^{11}(\underline{k},\omega-\omega_1) - \tilde{G}^{11}(\underline{k},\omega)\,G_r^{22}(\underline{k},\omega+\omega_1) \\ & + \tilde{G}^{21}(\underline{k},\omega)\,G_a^{21}(\underline{k},\omega-\omega_1) + \tilde{G}^{21}(\underline{k},\omega)\,G_r^{21}(\underline{k},\omega+\omega_1)\Big\}\end{aligned} \quad (2.59)$$

The terms in the first column correspond to processes in which two magnons are created; those in the second column come from one magnon creation plus one annihilation. Obvious modifications to (2.58) will produce coefficients for xz and yz scattering; however, in our calculations these will not differ from xy, as the anisotropy observed in the spin-wave dispersion relations relies on exchange interactions other than those included in our Hamiltonian (see, for example, Low et al, 1964).

2.5 : RENORMALIZATION OF THE TRANSVERSE INTERACTIONS

Before considering the result of the calculations, we comment on the way in which the transverse interactions were handled. For $K(Mn,Co)F_3$ and $(Mn,Zn)F_2$ our earlier approximation, that changes in these interactions could be neglected, is not justified; in the former JS changes between $KMnF_3$ and $KCoF_3$ by a factor of 3, while in the latter the Zn ions are non-magnetic, so that J′is zero. Dealing with this case first, we postulate that the quantity B, which appears in (2.17) and (2.18), changes with c and ω in the same way as A. We then replace the transverse term $B^2\gamma_k^2$ by $[B+\Sigma(\omega)][B+\Sigma(-\omega)]\gamma_k^2$. For an isotropic system, when A is equal to B, this replacement ensures that the Goldstone theorem is obeyed for all impurity concentrations.

This treatment is not good enough for $K(Mn,Co)F_3$, because of the large difference between B(Co) and B(Mn). Accordingly, we make the above replacement, but substitute for B its average :

$$\bar{B} = (1-c)\,B(Mn) + c\,B(Co) \quad . \qquad (2.60)$$

The correct behaviour is now ensured for both pure limits, and a reasonable interpolation obtained.

2.6 : RESULTS

The preceding theory has been used to calculate the neutron-scattering and Raman spectra for the antiferromagnets $(Co,Mn)F_2$, $K(Co,Mn)F_3$ and $(Mn,Zn)F_2$. These materials are known to be well described by the Heisenberg Hamiltonian (see, for example, Martel et al. 1968 ; Low, 1965; Buyers et al. 1971a); however, the calculations for the impure systems are complicated by the orbital angular momentum of the Co ion, and the consequent need to allow for the variation of the exchange mixing of higher spin-orbit states as the crystal composition is varied. Most of the numerical calculations were carried out by Dr. W.J.L. Buyers, and details of the methods used are not given here; they are fully discussed in Buyers et al. (1972a, 1972b). The experimental results with which the calculations are compared are from the Chalk River Neutron Scattering Group (Buyers et al. 1971b; Coombs et al., to be published).

A : $(Co,Mn)F_2$

The neutron scattering spectra of $Co_cMn_{1-c}F_2$ show two distinct bands of excitations each having, at least in certain concentration ranges, a well-defined dispersion relation. This feature is reproduced in the results of the CPA theory; it is well known (Velický et al. 1968) that the CPA does produce such behaviour in a binary alloy if the component single-site energies are well-separated. Fig. [2.1] shows the dispersion curves predicted by the two forms of the theory for c = 0.3, and compares them with the experimental results. The average cluster theory is in fair agreement with the experiments, but the multiple cluster theory is considerably better, as would be

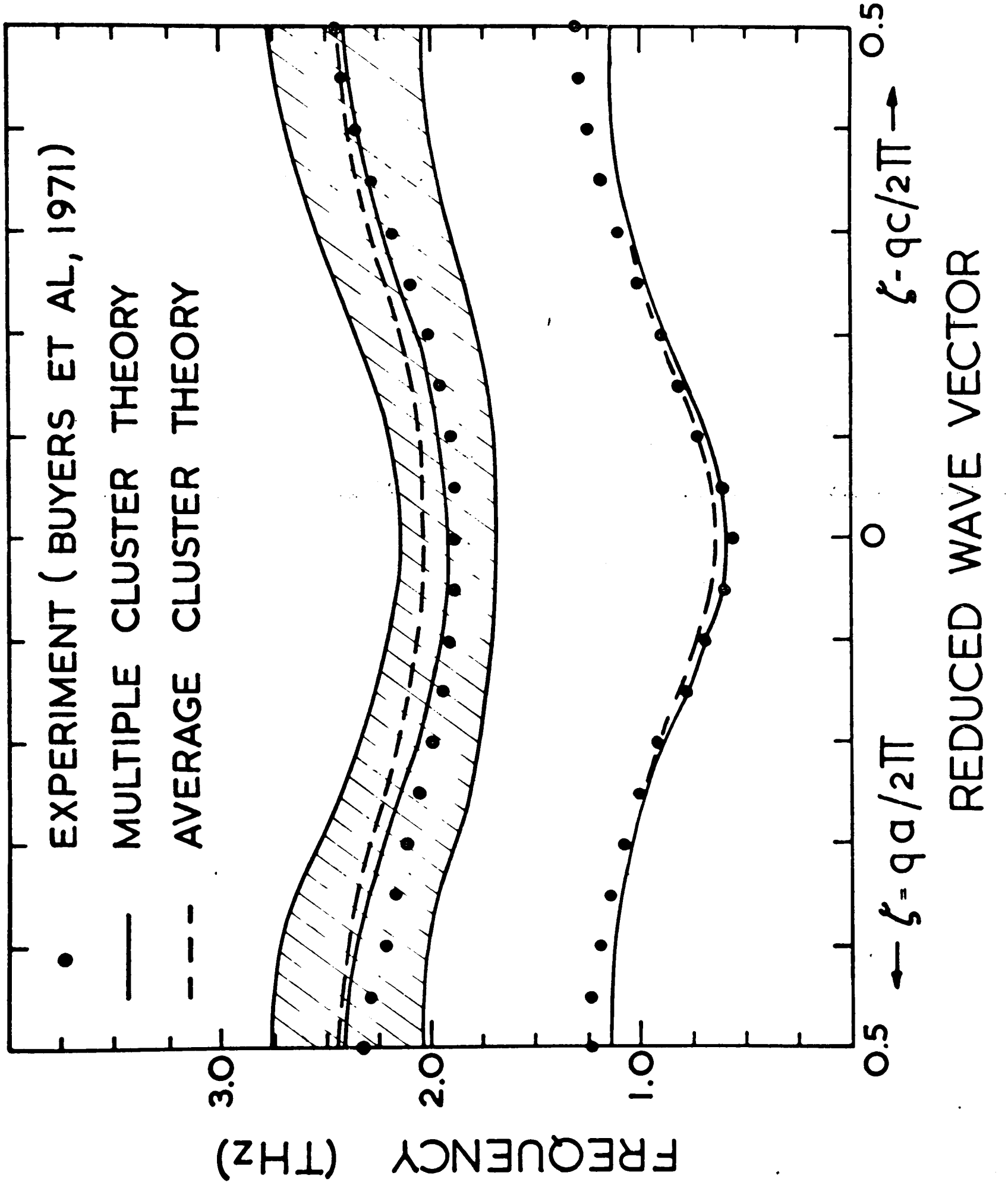

EXPERIMENT (BUYERS ET AL, 1971)
MULTIPLE CLUSTER THEORY
AVERAGE CLUSTER THEORY
FREQUENCY (THz)
3.0
2.0
1.0
0.5
ζ = qa/2π
0
ζ' = qc/2π
0.5
REDUCED WAVE VECTOR

Fig. [2.1]

expected. This superiority is emphasised when the spin-wave widths and line-shapes are taken into account. The average cluster theory predicts that the excitations in both bands are very narrow; experiment, however, shows that those in the upper band are broad, and the multiple cluster theory agrees with this. The width of the spin-waves in the upper band predicted by this latter theory is indicated in the diagram by the shaded area. It is shown by Buyers et al. (1971b) that most of this width can be accounted for simply by considering the excitation energies of the various clusters using the Ising model: we should therefore expect that only a theory which included clustering effects would correctly predict it.

For low c, the upper band becomes very narrow and moves to 3.72 THz, the position of the local mode of Co in MnF_2. For $c \rightarrow 1$, there is a local mode on the Mn, at 0.85 THz. Both these modes are independent of $\underline{k}$.

In Fig. [2.2] we show a comparison of the calculated line-shapes with experiment; the crystal is $Mn_{0.3}\,Co_{0.7}\,F_2$, and the wave-vector is indicated in units of $2\pi(\frac{1}{a},\frac{1}{a},\frac{1}{c})$. The theory used is the multiple cluster form. The overall agreement is seen to be good; the theoretical lines, however, possess some structure which does not appear in the experiments. This is due to the way in which we have included the various clusters, each of which has its own resonance energy. In Fig. [2.3], the same data is shown with experimental resolution added to the results of the theory in an approximate way. The structure has now disappeared, and the theoretical line fits the experimental points well.

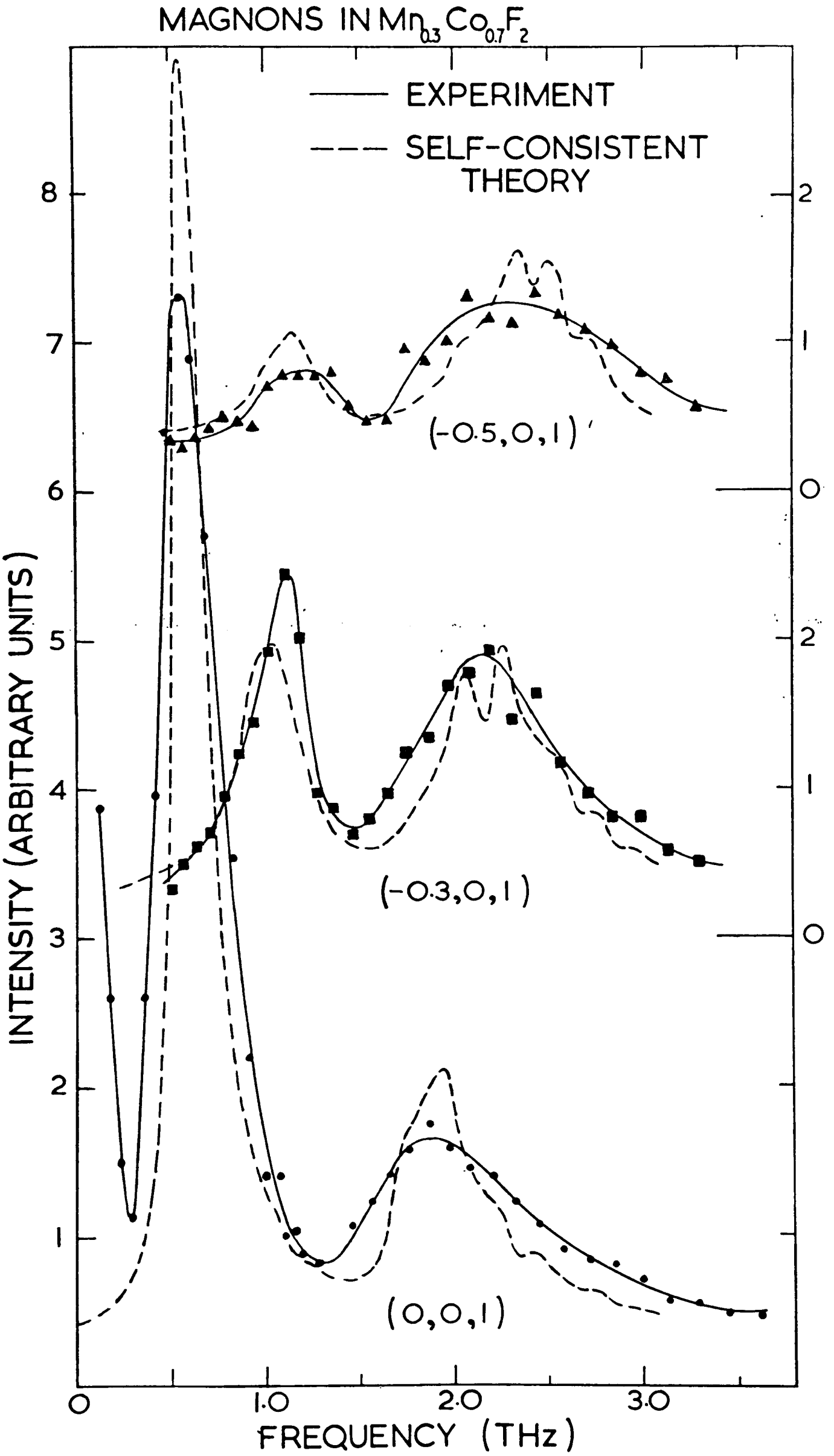

MAGNONS IN $Mn_{0.3}Co_{0.7}F_2$
EXPERIMENT
SELF-CONSISTENT THEORY
(-0.5,0,1)
(-0.3,0,1)
(0,0,1)
INTENSITY (ARBITRARY UNITS)
FREQUENCY (THz)
0
1.0
2.0
3.0
1
2
3
4
5
6
7
8
0
1
2
0
1
2

Fig. [2.2]

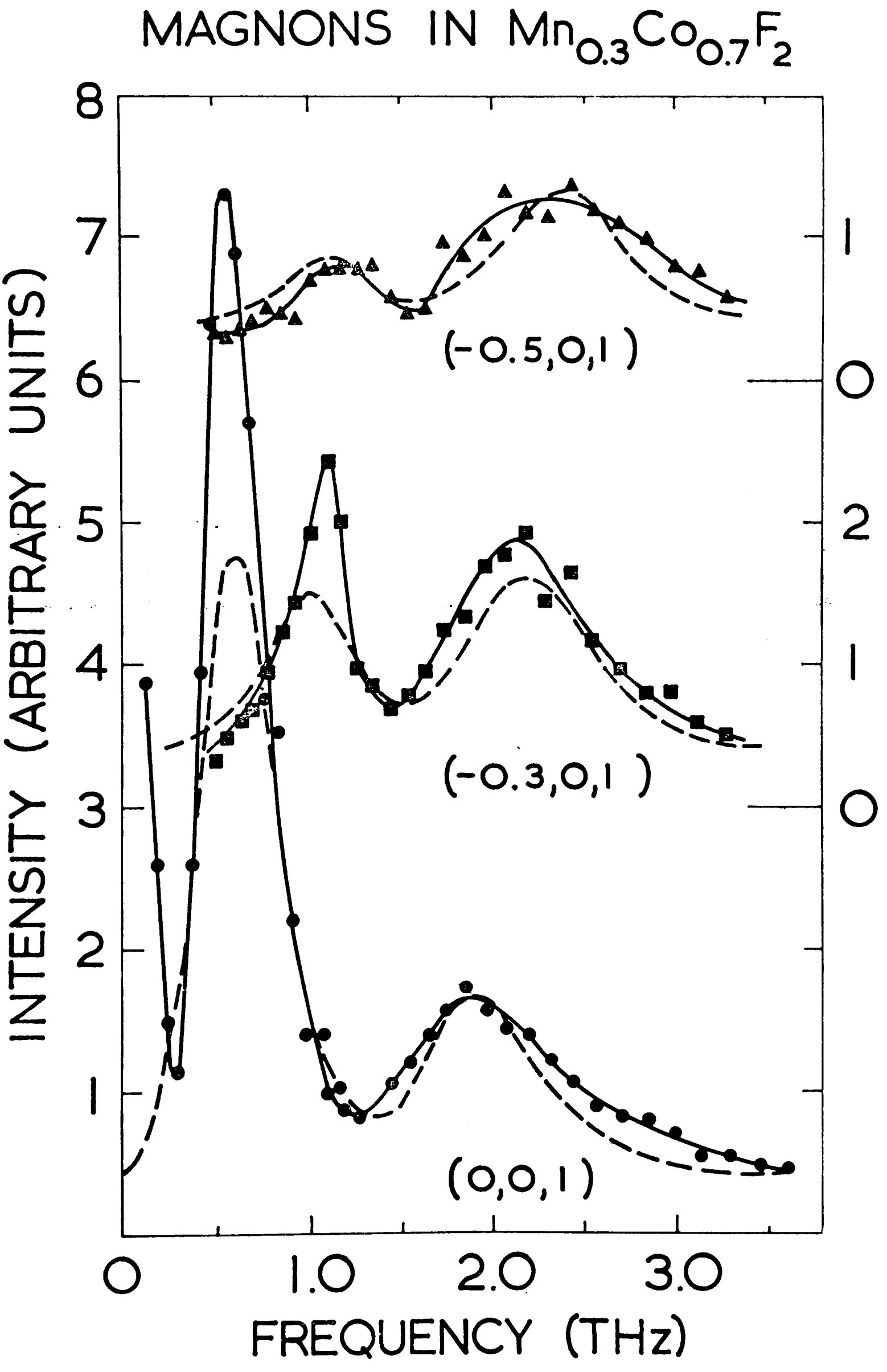

MAGNONS IN $Mn_{0.3}Co_{0.7}F_2$
INTENSITY (ARBITRARY UNITS)
8
7
6
5
4
3
2
1
1
0
2
1
0
(-0.5,0,1)
(-0.3,0,1)
(0,0,1)
0
1.0
2.0
3.0
FREQUENCY (THz)

Fig. [2.3]

B : $K(Mn,Co)F_3$

The behaviour of $KMn_{1-c}Co_cF_3$ is very similar to that of $(Co,Mn)F_2$, although the excitations in the upper band are very much narrower. As before, local modes are observed at both $c \to 0$ and $c \to 1$, and the theory predicts impurity bands with essentially no dispersion in these regions. There is some discrepancy for c = 0.2: the experiments suggest that the Co excitation is still localized, as it has no observable dispersion, whereas in the theory the band falls from 6.5THz at the zone boundary to 5.9THz at the zone centre. However, the nature of the averaging process in the CPA makes it unsuitable for describing localized modes. Further discussion of this point is given by Economou (1972), and by Lyo (1972), both of whom develop theories to describe the change from localized to propagating character of excitations in mixed antiferromagnets. Their predictions agree well with the experimental observations.

In Fig. [2.4] we compare the theoretical dispersion curve with the experimental points for c = 0.71. The agreement is very good for the upper (Co) branch at the zone boundary, and for the lower (Mn) branch at the zone centre. The disagreement at the zone centre of the upper mode is not serious, taking into account the amount by which the mode has risen from its value in pure $KCoF_3$ (see Buyers et al. 1971b). The discrepancy in the lower mode, however, does indicate that some of the approximations made for this system may not be well justified, particularly our treatment of the transverse interactions.

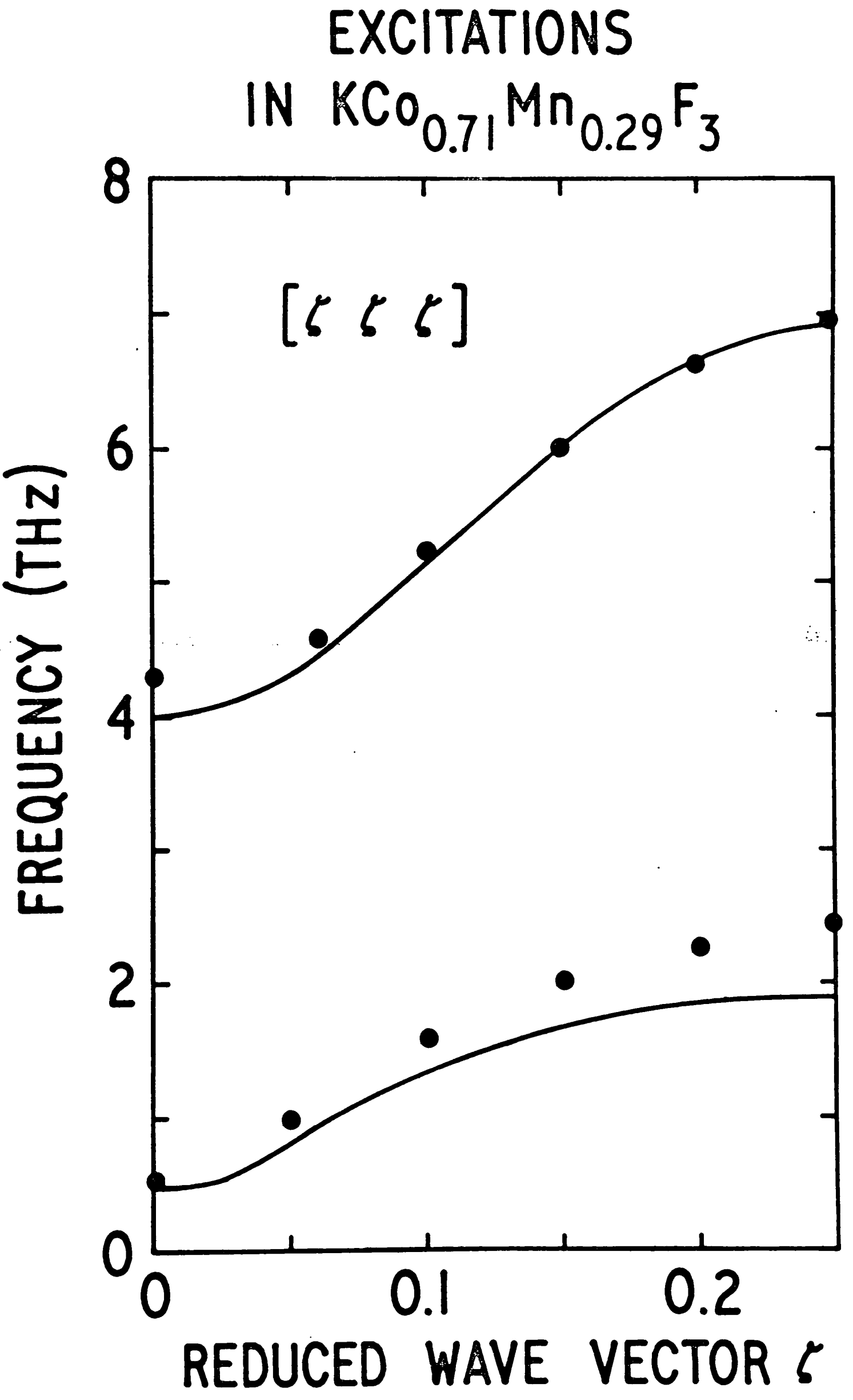

EXCITATIONS
IN $KCo_{0.71}Mn_{0.29}F_3$
[ζ ζ ζ]
FREQUENCY (THz)
8
6
4
2
0
0
0.1
0.2
REDUCED WAVE VECTOR ζ

Fig. [2·4]

C : $(Mn,Zn)F_2$

Before a discussion of the results for $(Mn,Zn)F_2$, one further comment is required on the method employed in the calculations. Because the Zn ions are non-magnetic, we encounter a problem similar to the one which appeared in Part I : if any interaction is permitted between host and impurity, a large resonance occurs at low energy (see also Cowley and Buyers, 1972). In order to avoid this, we place a very large scattering potential on the Zn atoms (i.e. we make $V_0 \gg A$), so that the spin-waves are prevented from turning the spin on an impurity site. In this case, the method does not produce a spurious band-gap, because of the way in which we treat the transverse interactions (§ 2.5).

The spectrum of $Mn_{1-c}Zn_c F_2$ differs from those of the previous systems discussed in that there is only one branch of excitations: the Zn ions are non-magnetic, so that there is no local mode which can become a dispersive band. However, for low c the impurities do give rise to a resonance within the Mn spin-wave band (Svensson et al. 1969). This is effectively a shell mode, produced by a reduction in the molecular field on those Mn ions which have only 7 magnetic neighbours instead of 8. In Fig. [2.5] we show the shift and width of the spin-waves in $Mn_{0.95}Zn_{0.5}F_2$; the solid line is the result of the multiple cluster theory, and the broken line is a low-c theory which includes all transverse and longitudinal interactions exactly to order c (Cowley and Buyers, 1972). The experimental points are from Svensson et al. (1969). The resonance is clearly visible at $\zeta \simeq 0.35$. Although the low-c theory is superior, the CPA results are satisfactory considering the approximations

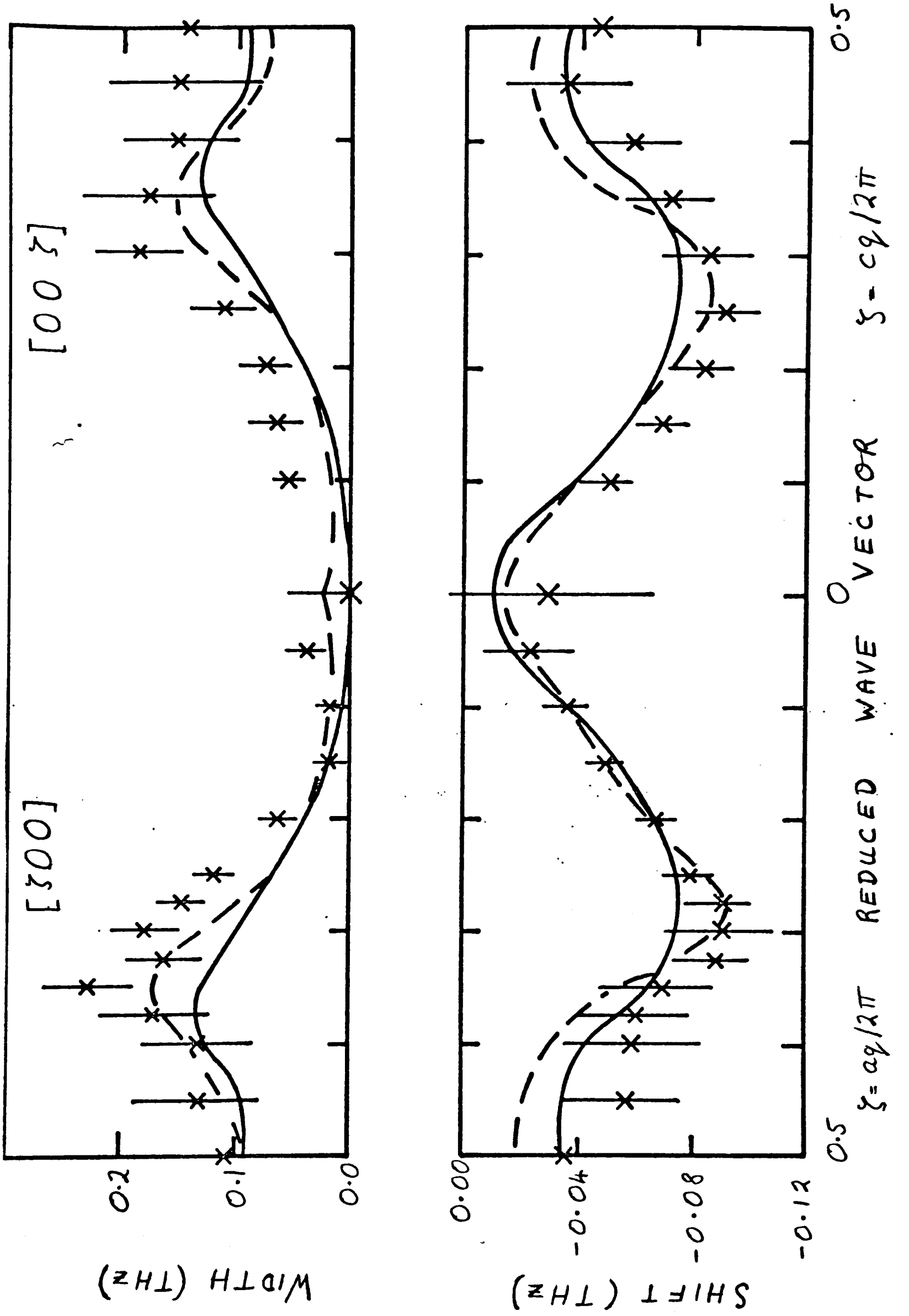

[00ζ]
[ζ00]
0.2
0.1
0.0
WIDTH (THz)
0.00
-0.04
-0.08
-0.12
SHIFT (THz)
0.5
0
0.5
REDUCED WAVE VECTOR
ζ = aq/2π
ζ = cq/2π

Fig. [2.5]

involved, and in particular our treatments of the transverse interactions and of V appear to work well.

As c is increased, the resonance disappears: most Mn ions now have more than one Zn neighbour, and the shell mode produced by a single Zn ion is damped out. The neutron scattering lines become broader and move to lower energies; in Fig. [2.6] the excitation at a reduced wave-vector of (-0.5, 0, 1) for c = 0.22 is shown, and the CPA result is seen to give a good fit to the experimental points (Coombs et al., to be published). Experimental resolution has been added in an approximate way to the theoretical line shape.

The critical concentration of Zn in $(Mn,Zn)F_2$ should be about 0.75, above which we expect no long-range antiferromagnetic order. Fig. [2.7] shows the behaviour of the $\underline{k}$=0 spin-wave as c is increased towards this value; for c = 0.68, the peak has become overdamped because of the breakdown in the long-range order. At the zone boundary, on the other hand, no evidence is observed of a change in the spin-waves, which there reflect mainly short-range order. Fig. [2.8] compares the line shapes for c = 0.68 and 0.75, which are seen to be very similar and well defined. The peak at low energy in the experimental data is probably due to processes described by the $\langle S^z S^z \rangle$ correlation function, involving two magnons; this effect is not included in our theory. We should expect it to appear near the critical concentration as it becomes easier to turn over two adjacent spins.

The theory of § 2.4 has been used to calculate the two-magnon Raman spectra of $(Mn,Zn)F_2$, for comparison with the results of Buchanan et al., (1972). The lines observed decrease

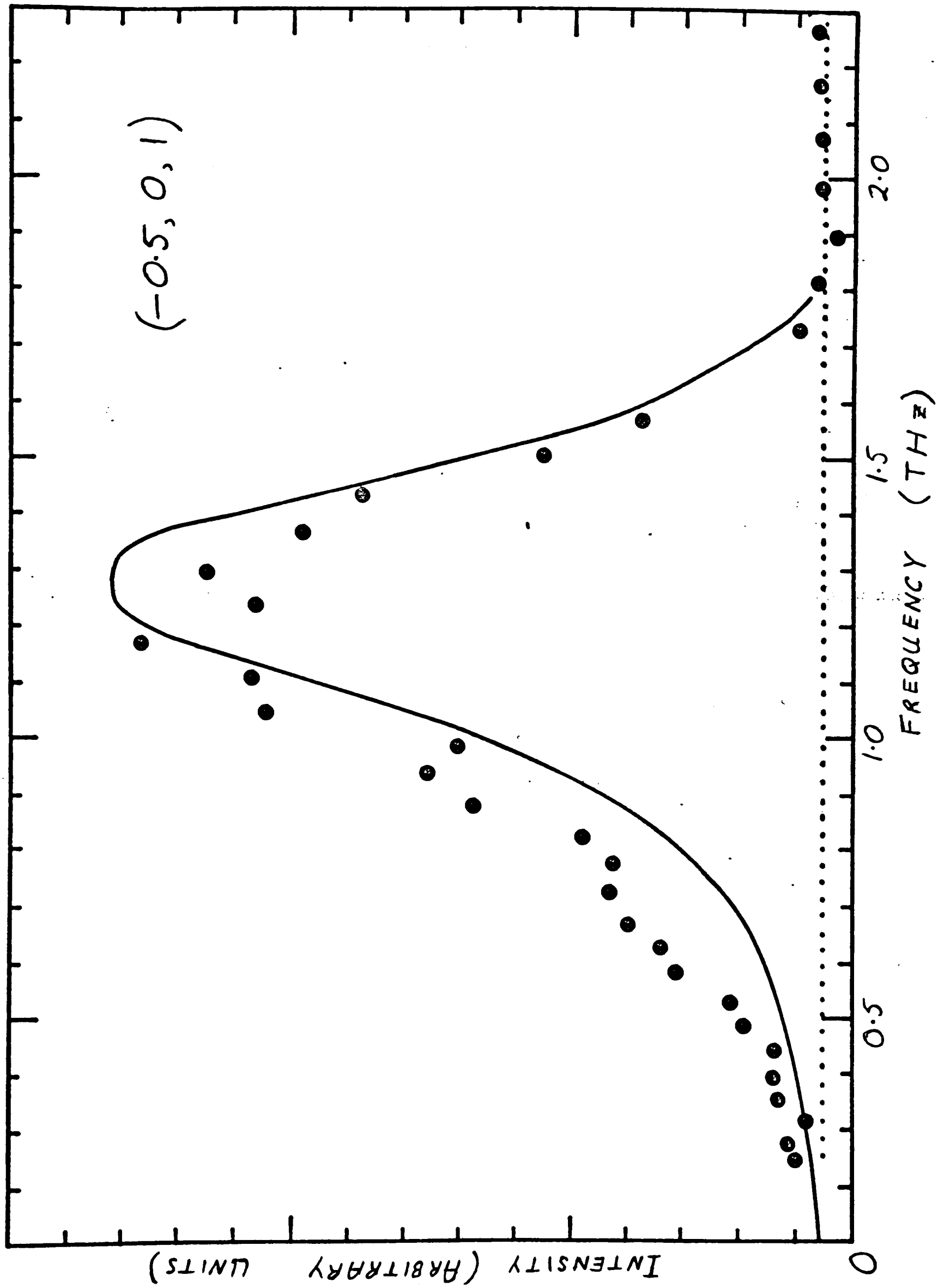


Fig. [2.6]

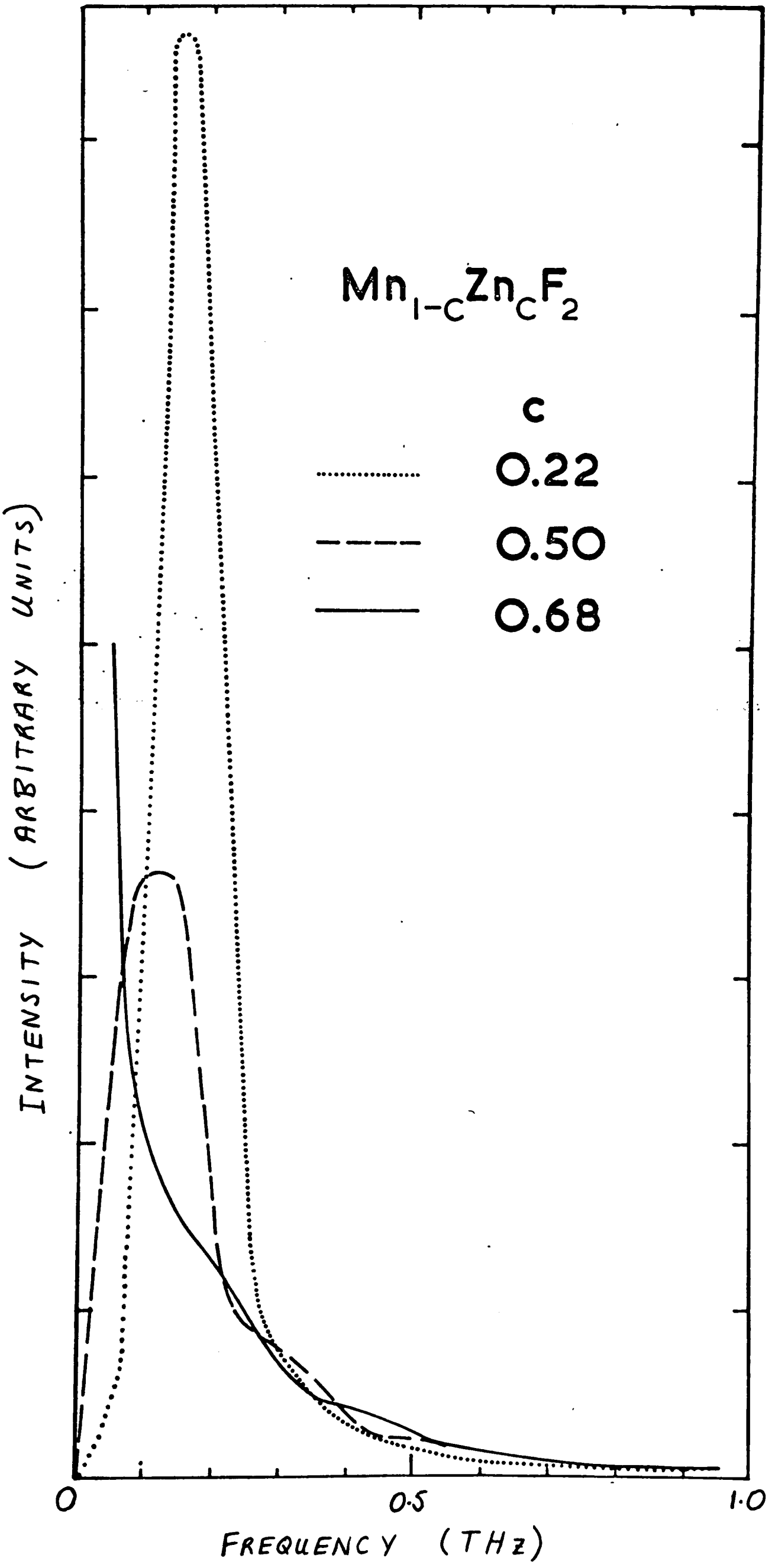

$Mn_{1-c}Zn_cF_2$
c
0.22
0.50
0.68
INTENSITY (ARBITRARY UNITS)
0
0.5
1.0
FREQUENCY (THz)

Fig. [2.7]

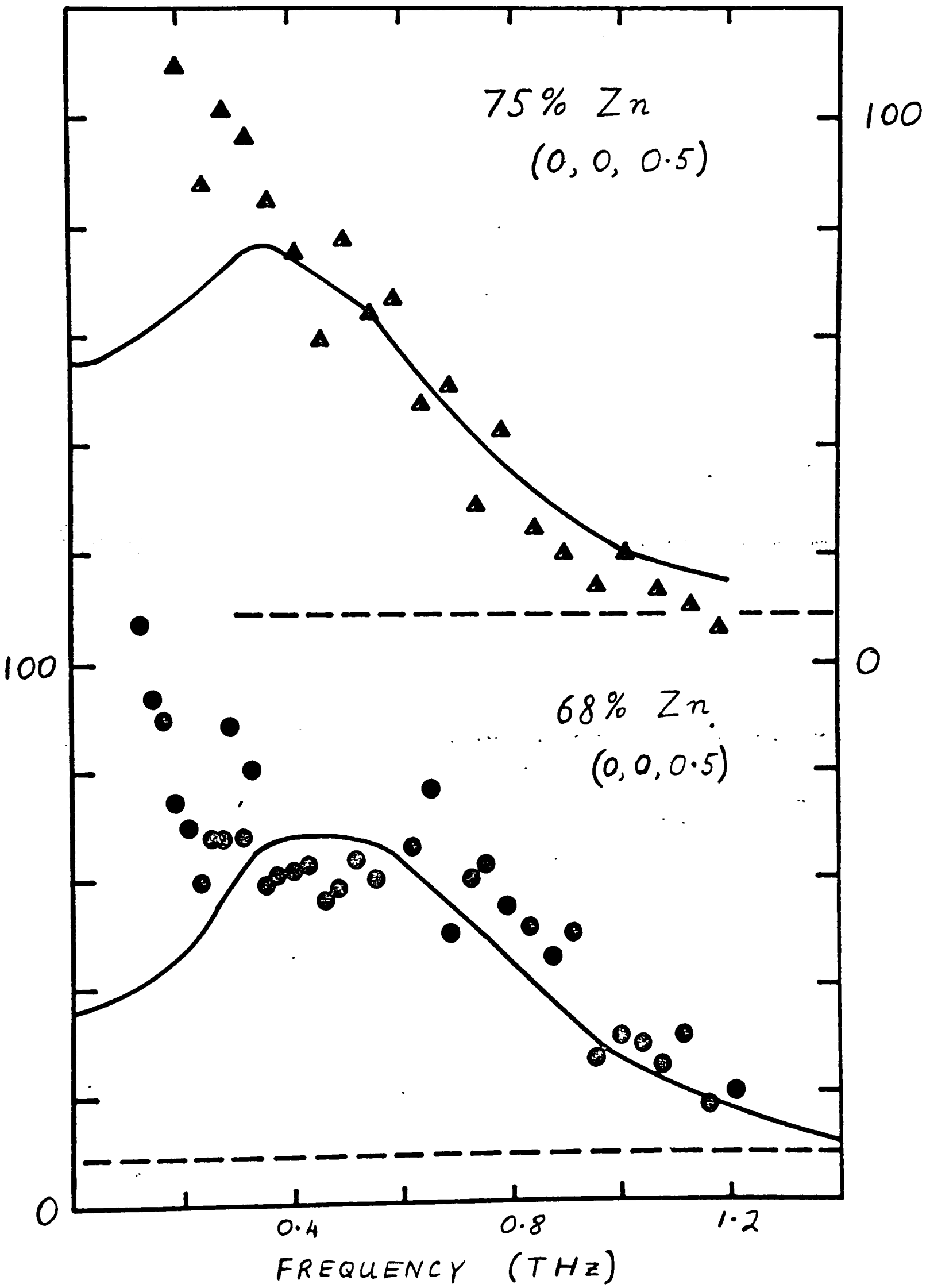


Fig. [2·8]

in frequency and become broader as c is increased. It is shown in the original paper that although the behaviour of the width can be partly accounted for by considering the various defect clusters in terms of the Ising model, the position of the peak falls less fast than would be expected on the same grounds. Our results are generally in agreement with the Ising model predictions, as is to be expected: the greatest contribution to the Raman lines is from zone-boundary magnons, whose energies are mainly determined by the longitudinal interaction. The calculated peak position falls faster than the experiments show, but the line-shapes agree well. Fig. [2.9] shows the variation of width with c, and in Fig. [2.10] we compare the experimental lines for xy-scattering with the CPA (solid line) and Ising model (broken line) theories. The extra width of the experimental lines at low c is probably due to spin-wave interactions, which there dominate the impurity-induced width.

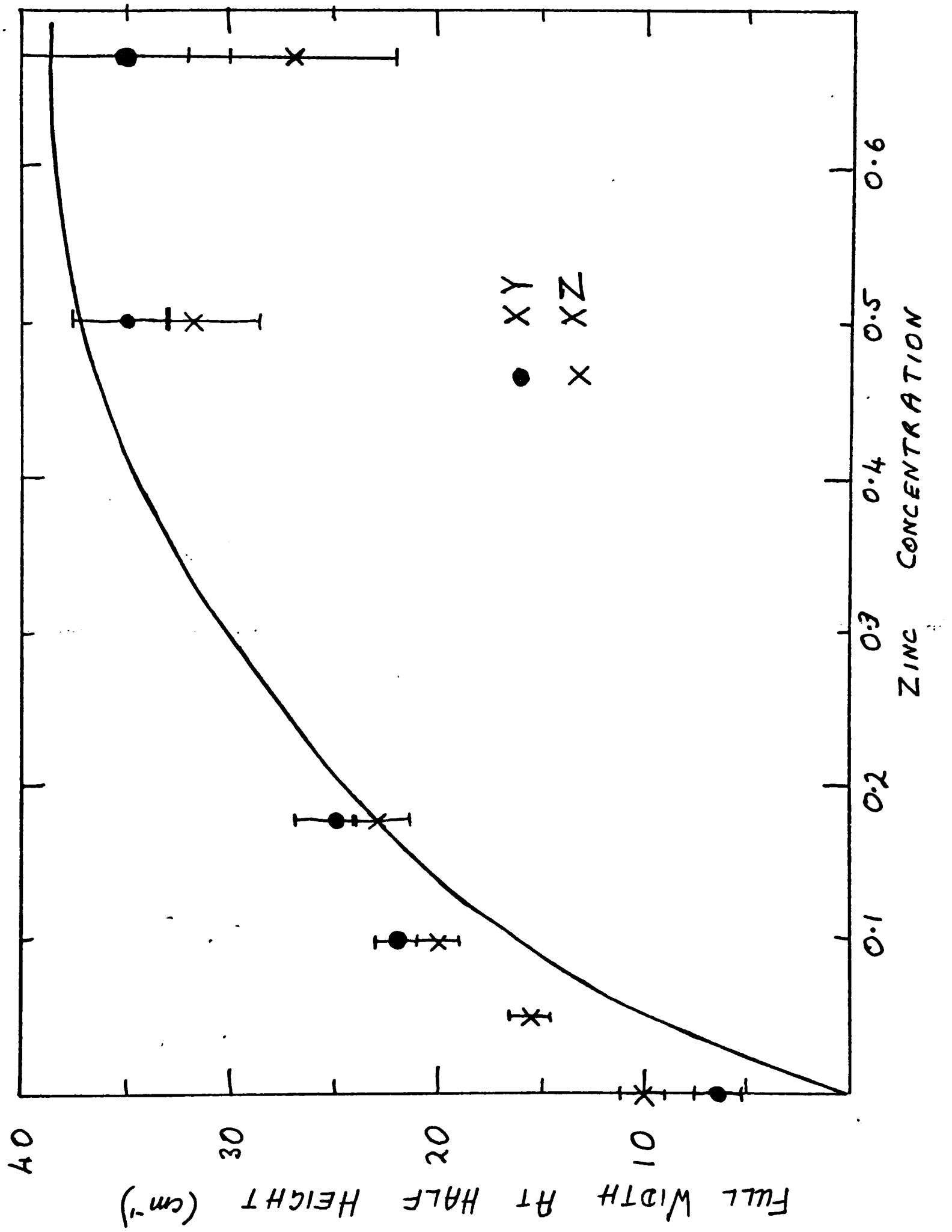

XY
XZ
ZINC CONCENTRATION
0·3
0·4
0·5
0·6
0·1
0·2
FULL WIDTH AT HALF HEIGHT (cm⁻¹)
40
30
20
10

Fig. [2.9]

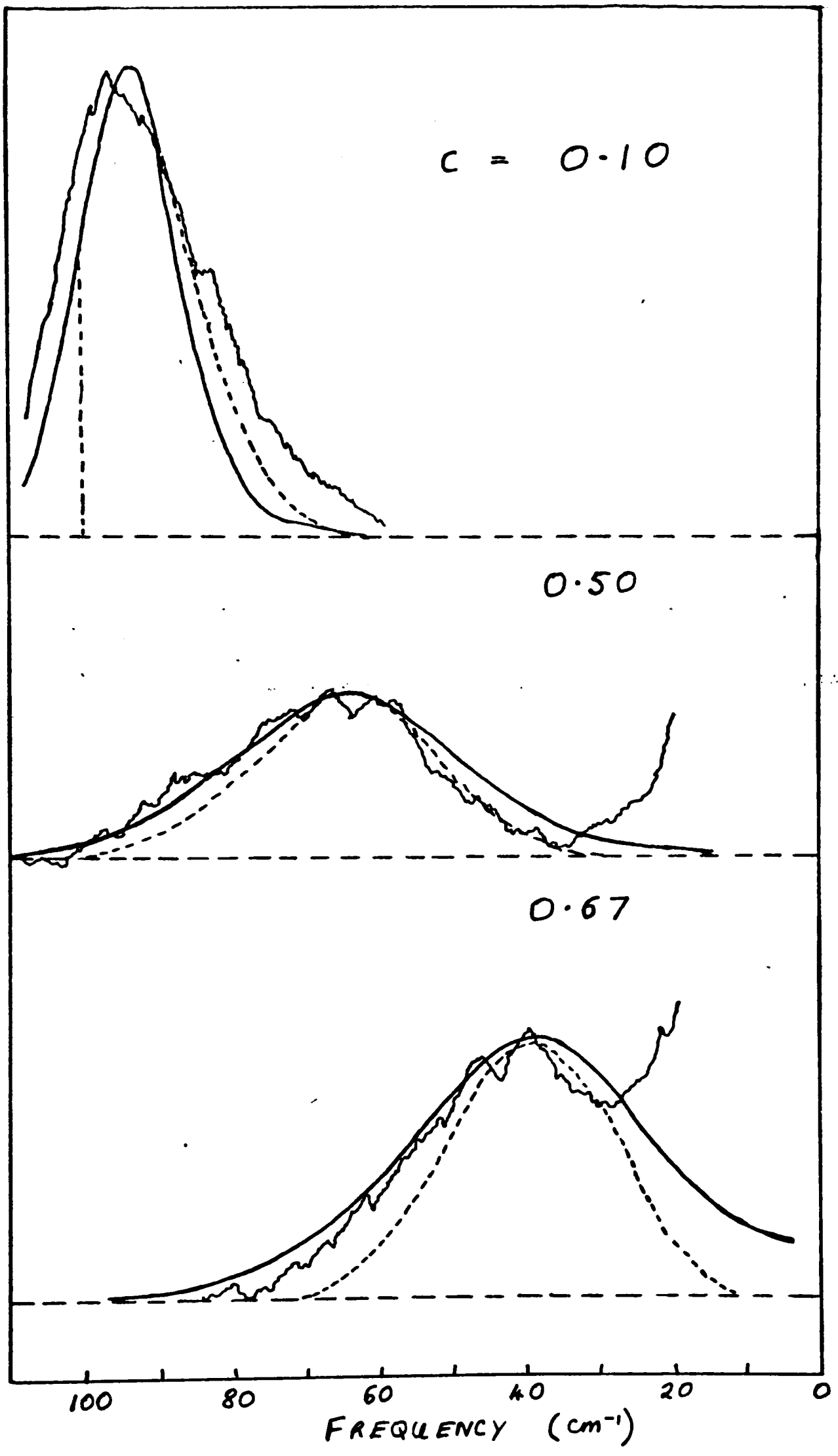


Fig. [2.10]

2.7 : CONCLUSIONS

We have used the CPA to develop a theory of the spin-waves in substitutionally disordered antiferromagnets. The application of this theory to $(Mn,Co)F_2$ is very successful, giving good descriptions of the observed dispersion curves and line shapes. The calculations for this material are essentially unaffected by our neglect of the change in the transverse interaction, because of the similarity of the values of this quantity in MnF_2 and CoF_2 . The most important approximation here is the decoupling of the scattering from an impurity and from its neighbours, and the calculations confirm the validity of this procedure.

For $K(Co,Mn)F_3$ the results are less satisfactory, but this is not surprising in view of the difference between the transverse exchange couplings in the pure crystals, which has been included only very approximately. However, the theory does predict many of the features of the observed spectra, and it seems likely that an improved treatment of the off-diagonal randomness would be necessary to obtain substantially better agreement with experiment.

In the case of $(Mn,Zn)F_2$ the extra problem arises of preventing the non-magnetic atoms from interacting with their neighbours. The method of putting a large energy term on the Zn sites, which failed for the ferromagnet described in Part I, can be used here because the way in which we treat the transverse interactions automatically eliminates any spurious gap at zero wavevector. The agreement between the theory and the neutron scattering data is once again satisfactory. The results

for the Raman spectra are less good, particularly the predicted variation of the position of the peak with c. Two reasons for this may be suggested: firstly, no magnon-magnon interactions are included in the calculation, and these are known to shift the maximum in the spectrum; secondly, only one set of exchange interactions is used in the Hamiltonian, and it is clear that the experimental data cannot be fully explained on this basis.

We may conclude that the CPA is capable of describing in detail the behaviour of the class of impure antiferromagnets considered. This is the most complete test to which it has so far been subjected, and the results indicate its power as a tool in the theory of disordered systems. It also emerges from this work that the approximations in our treatment of the longitudinal and transverse interactions retain all the important features of the observed spectra, while producing great simplifications in the calculations.

APPENDICES

Appendix A : SYMMETRY TRANSFORMS FOR THE SIMPLE CUBIC LATTICE

In this appendix, we show how the 7 x 7 matrices encountered in the treatment of the simple cubic lattice may be reduced to block-diagonal form (Wolfram and Callaway, 1963). The matrices we are concerned with all have the following form:

$$\underset{\sim}{A} = \begin{bmatrix} A_{00} & A_{01} & A_{01} & A_{01} & A_{01} & A_{01} & A_{01} \\ A_{01} & A_{11} & A_{12} & A_{13} & A_{13} & A_{13} & A_{13} \\ A_{01} & A_{12} & A_{11} & A_{13} & A_{13} & A_{13} & A_{13} \\ A_{01} & A_{13} & A_{13} & A_{11} & A_{12} & A_{13} & A_{13} \\ A_{01} & A_{13} & A_{13} & A_{12} & A_{11} & A_{13} & A_{13} \\ A_{01} & A_{13} & A_{13} & A_{13} & A_{13} & A_{11} & A_{12} \\ A_{01} & A_{13} & A_{13} & A_{13} & A_{13} & A_{12} & A_{11} \end{bmatrix} \qquad \text{(A.1)}$$

where 0 signifies the central atom and 1 a neighbour; A_{12} is the element between a pair of opposite neighbours, and A_{13} between nearest neighbours on the first coordination sphere.

Any matrix like $\underset{\sim}{A}$ may be block-diagonalized by a unitary transformation $\underset{\sim}{S}$:

$$\underset{\sim}{S} = \left[\begin{array}{c|cc|ccc|cc} 1 & 0 & 0 & 0 & 0 & 0 & 0 \\ 0 & a & b & 0 & 0 & 0 & d \\ 0 & a & -b & 0 & 0 & 0 & d \\ 0 & a & 0 & b & 0 & c & e \\ 0 & a & 0 & -b & 0 & c & e \\ 0 & a & 0 & 0 & b & -c & e \\ 0 & a & 0 & 0 & -b & -c & e \end{array}\right] \qquad \text{(A.2)}$$

where

$$a = 1/\sqrt{6} \qquad b = 1/\sqrt{2}$$

$$c = 1/2 \qquad d = 1/\sqrt{3} \qquad \text{(A.2b)}$$

$$e = -1/\sqrt{12}$$

The first two columns correspond to the symmetric s-modes, the next three are p-like modes and the last two d-modes. The effect of transforming $\underset{\sim}{A}$ by $\underset{\sim}{S}$ is as follows :

$$\underset{\sim}{S}^{T}\underset{\sim}{A}\,\underset{\sim}{S} = \begin{bmatrix} A_{oo} & \sqrt{6}A_{o1} & & & & & \\ \sqrt{6}A_{o1} & A_s' & & & & & \\ & & A_p & 0 & 0 & & \\ & & 0 & A_p & 0 & & \\ & & 0 & 0 & A_p & & \\ & & & & & A_d & 0 \\ & & & & & 0 & A_d \end{bmatrix} \qquad \text{(A.3)}$$

with

$$\begin{aligned} A_s' &= A_{11} + A_{12} + 4A_{13} \\ A_p &= A_{11} - A_{12} \\ A_d &= A_{11} + A_{12} - 2A_{13} \end{aligned} \qquad \text{(A.4)}$$

It is also necessary to be able to construct the Fourier transform A($\underline{k}$) from the s, p and d components of A. If we write the s-block as

$$\underset{\sim}{A}_s = \begin{bmatrix} A_{oo}^s & A_{o1}^s \\ A_{o1}^s & A_{11}^s \end{bmatrix} \qquad \text{(A.5)}$$

then we may invert (A.3) and (A.4) to obtain the ordinary space-components A_{oo}, A_{11}, etc. in terms of A_s, A_p, A_d, and so produce the Fourier transform :

$$\begin{aligned} A(\underline{k}) &= A_{oo} + 6A_{11} + 12A_{o1}\gamma_{\underline{k}} + 6A_{12}\gamma_{2\underline{k}} + 24A_{13}\Gamma_{\underline{k}} \\ &= \left[A_{oo}^s + 2\sqrt{6}A_{o1}^s\gamma_{\underline{k}} + A_{11}^s(1+\gamma_{2\underline{k}} + 4\Gamma_{\underline{k}})\right] \\ &\quad + 3A_p(1-\gamma_{2\underline{k}}) + 2A_d(1+\gamma_{2\underline{k}} - 2\Gamma_{\underline{k}}) \\ &\equiv A_s(\underline{k}) + 3A_p(\underline{k}) + 2A_d(\underline{k}) \end{aligned} \qquad \text{(A.6)}$$

where

$$\gamma_{2\underline{k}} = \frac{1}{6} \sum_{\Delta_{12}} e^{i \underline{k} \cdot \underline{\Delta}_{12}}$$

$$\Gamma_{\underline{k}} = \frac{1}{24} \sum_{\Delta_{13}} e^{i \underline{k} \cdot \underline{\Delta}_{13}} \qquad \text{(A.7)}$$

It will be useful to express the quantity $\Gamma_{\underline{k}}$ in terms of $\gamma_{2\underline{k}}$ and $\gamma_{\underline{k}}$. Squaring $\gamma_{\underline{k}}$ we obtain :

$$\gamma_{\underline{k}}^2 = \frac{1}{9} \left\{ \cos^2(k_x a) + \cos^2(k_y a) + \cos^2(k_z a) + 2 \left[\cos(k_x a) \cos(k_y a) + \ldots \right] \right\} \qquad \text{(A.8)}$$

Now, Γ_k may be written as a sum of terms like $\cos(k_x a) \cos(k_y a)$, and so (A.8) may be re-arranged as

$$\gamma_{\underline{k}}^2 = \frac{1}{18} \left\{ \cos(2k_x a) + \cos(2k_y a) + \cos(2k_z a) \right\} + \frac{1}{6} + \frac{2}{3} \Gamma_{\underline{k}} \qquad \text{(A.9)}$$

whence

$$\Gamma_{\underline{k}} = \frac{3}{2} \gamma_{\underline{k}}^2 - \frac{1}{4} \left(\gamma_{2\underline{k}} + 1 \right) \qquad \text{(A.10)}$$

Using this in (A.6), we obtain

$$\left.\begin{aligned} A_s(\underline{k}) &= A_{00}^s + 2\sqrt{6}\, A_{01}^s \gamma_{\underline{k}} + A_{11}^s \cdot 6 \gamma_{\underline{k}}^2 \\ A_p(\underline{k}) &= A_p \cdot (1 - \gamma_{2\underline{k}}) \\ A_d(\underline{k}) &= A_d \cdot \frac{3}{2} \left(1 + \gamma_{2\underline{k}} - 2 \gamma_{\underline{k}}^2 \right) \end{aligned}\right\} \qquad \text{(A.11)}$$

Appendix B : PURE CRYSTAL GREEN FUNCTIONS

We show here how certain combinations of off-diagonal elements of $g(\omega)$ can be re-expressed in terms of $g_{oo}(\omega)$. g_{oo} is given by

$$g_{oo}(\omega) = N^{-1} \sum_{\underline{k}} \frac{1}{\omega - z(1-\gamma_{\underline{k}})} \tag{B.1}$$

For any cubic lattice, g_{o1} is then

$$\begin{aligned} g_{o1}(\omega) &= N^{-1} \sum_{\underline{k}} \frac{\gamma_{\underline{k}}}{\omega - z(1-\gamma_{\underline{k}})} \\ &= N^{-1} \sum_{\underline{k}} \frac{1}{z}\left[1 - \frac{\omega - z}{\omega - z(1-\gamma_{\underline{k}})}\right] \qquad \text{(B.2)} \\ &= \frac{1}{z}\left[1 - (\omega - z)\, g_{oo}\right] \end{aligned}$$

In the case of the simple cubic lattice, we are also interested in

$$g_s' = g_{oo} + g_{12} + 4 g_{13} \tag{B.3}$$

$$= N^{-1} \sum_{\underline{k}} \frac{1 + \gamma_{2\underline{k}} + 4\gamma_{\underline{k}}}{\omega - 6(1-\gamma_{\underline{k}})} \tag{B.4}$$

Using (A.10) this may be reduced to

$$g_s' = \left(\frac{\omega}{6} - 1\right)\left[-1 + (\omega - 6)\, g_{oo}\right] \quad . \tag{B.5}$$

Appendix C : COHERENT POTENTIAL APPROXIMATION

We present here one of several possible derivations of the single-site CPA. This one is similar to that given by Velický et al. (1968), and is chosen because it can conveniently be used to generalize the usual theory to the case where a single impurity is described by an extended matrix, as in the dilute ferromagnet. The CPA for such a system has previously been derived by Takeno (1968), but by a different, and more complicated, method.

Throughout this appendix we shall work in an operator formalism: thus the Green function of (1.6) is defined in terms of the operator G by

$$G_{mn} = \langle m | G | n \rangle \qquad (C.1)$$

and similar definitions apply to g, V, etc. The Dyson equation is now written

$$G = g + g V G \qquad (C.2)$$

where the operator V may be written as a sum over impurities :

$$V = \sum_n V_n \qquad (C.3)$$

and V has non-zero matrix elements corresponding to the effective block of a single impurity: such a block for the ferromagnet is given by (1.20). We now define an effective propagator G^e in terms of a self-energy Σ by

$$G^e = g + g \Sigma G^e \qquad (C.4)$$

If g is eliminated between (C.2) and (C.4) we find

$$G = G^e + G^e \tilde{V} G \qquad (C.5)$$

where $\tilde{V}$ describes the scattering of the new propagator G^e, and is given by

$$\tilde{V} \equiv V - \Sigma = \sum_n (V_n - \Sigma_n) \equiv \sum_n \tilde{V}_n \qquad \text{(C.6)}$$

The summation here is over all lattice sites; Σ has a component Σ_n associated with each site, but V_n is zero if n is a host site. (C.5) may be rewritten as

$$G = G^e + G^e T G^e \qquad \text{(C.7)}$$

where T represents the sum of all scattering processes :

$$T = \tilde{V}(1 + G^e T) \qquad \text{(C.8)}$$

$$= \sum_n \tilde{V}_n (1 + G^e T) \equiv \sum_n T_n \qquad \text{(C.9)}$$

Defining the total scattering from a single impurity by

$$t_n = (1 - \tilde{V}_n G^e)^{-1} \tilde{V}_n \qquad \text{(C.10)}$$

we find an equation for T_n :

$$T_n = t_n \left(1 + \sum_{m \neq n} G^e T_m\right) \qquad \text{(C.11)}$$

All the equations so far are exact, and apply to one particular impurity configuration. If we perform an average on (C.7), remembering that G^e is defined to be translationally invariant, then we can ensure that $\langle G \rangle = G^e$ by the condition

$$\langle T \rangle = 0 \qquad \text{(C.12)}$$

which is taken to be the defining equation for the CPA. It means that we determine Σ by the requirement that the effective propagator in the medium representing the impure crystal shall not be affected, on average, by scattering from the impurities.

Using (C.9) and (C.11) we further obtain

$$\langle T \rangle = \sum_n \langle T_n \rangle \tag{C.13}$$

$$\langle T_n \rangle = \langle t_n \left(1 + \sum_{m \neq n} G^e T_m\right) \rangle \tag{C.14}$$

$$= \langle t_n \rangle \left\langle 1 + \sum_{m \neq n} G^e \langle T_m \rangle \right\rangle + \left\langle t_n G^e \sum_{m \neq n} \left(T_m - \langle T_m \rangle\right) \right\rangle \tag{C.15}$$

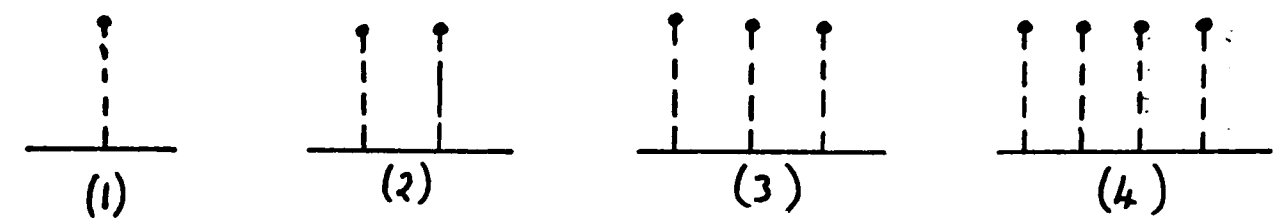
It is clear that the first term in (C.15) represents the average scattering from site n, and the second term represents fluctuations about this average. We now make the so-called single-site approximation (which for our purposes is more accurately called a single-impurity approximation), and neglect the second term in (C.15): thus the determining equation for becomes

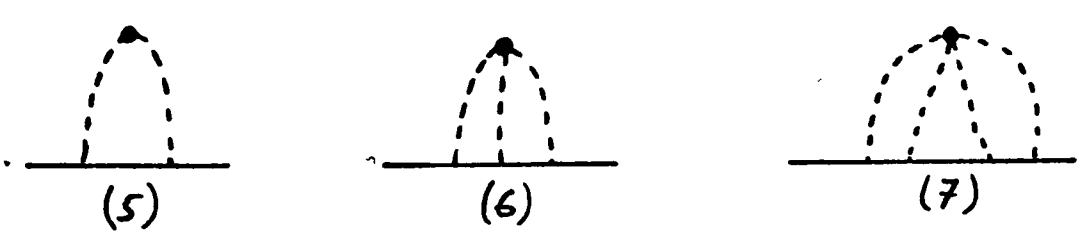
$$\langle t_n \rangle = 0 \tag{C.16}$$

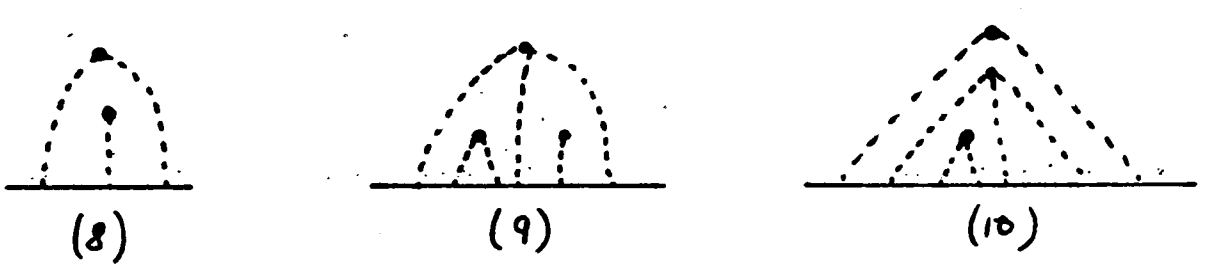
The single-site CPA can be compared with the low-concentration theories of § 1.2 by means of the diagrammatic formalism of Langer (1961). In fig. [C.1] the propagator g is represented by a solid horizontal line, and a scattering V by a broken vertical line. Thus the single-impurity t-matrix is the sum of all diagrams like (1), (5), (6), (7)..... The first approximation in § 1.2B gives correctly all diagrams like (1), (2), (3), (4); errors appear with diagram (5), which is given weight $c + c^2$, instead of c. The ATA improves this by giving the correct weight to (5), but still produces errors in the higher order diagrams.

The CPA, on the other hand, is correct for a much larger class of process. A diagrammatic analysis is made by Leath (1968, 1970) and by Aiyer et al. (1969); they show that it includes correctly all nested diagrams like (8), (9), (10),

representing repeated scattering from one site with intermediate scatterings from other sites. The first errors in the CPA appear in diagrams like (11) with crossing interaction lines, arising from repeated scattering from two or more impurities.







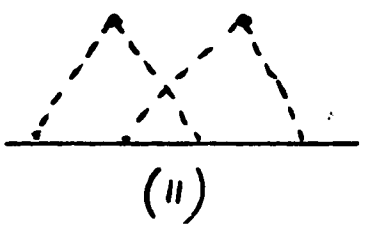


Fig. [C.1]

Appendix D : NUMERICAL METHODS

The various approximations based on the CPA which are used in the text all produce sets of equations like (1.64), (1.65) and (1.67): simultaneous non-linear integral equations in several complex variables. These were solved by the Newton-Raphson method: if the equations to be solved for $\underline{x} = (x_1, x_2, \ldots)$ are written

$$\varphi_i(\underline{x}) = 0 \qquad [i = 1, 2, \ldots] \tag{D.1}$$

and if the matrix $\underset{\sim}{B}$ is defined by

$$B_{ij} = \frac{\partial \varphi_i}{\partial x_j} \tag{D.2}$$

then for an initial estimate of the solution $\underline{x}_0$, the next estimate is given by $\underline{x}_1 = \underline{x}_0 - \underline{\delta}$, where

$$\underline{\delta} = \underset{\sim}{B}^{-1}\,\underline{\varphi} \tag{D.3}$$

the right-hand side being evaluated at $\underline{x}_0$. For a function of only one variable, this method should have quadratic convergence; for functions of several variables, however, the convergence is strongly dependent on the starting point. It was found in practice that if the initial estimate of the solution was good (i.e. within a few per cent of the root), the convergence was extremely fast, taking only two or three iterations to achieve better than 1% accuracy. If, however, the initial estimate was more than about 10% wrong, the iterations often did not converge at all. The first starting point was found by using the ATA equations, (1.55) - (1.57), for very small c; the root was then followed to higher concentrations by changing c slowly and

extrapolating the known roots for lower c to produce trial solutions for higher c. A similar procedure was adopted in order to follow the solution through a range of ω at constant c.

The performance of these calculations involved finding $G_{oo}(\omega)$ and other Green functions, which had to be done by summing over $\underline{k}$-space. The sums were performed over 8000 points of the first Brillouin zone, using the full symmetry of the simple cubic lattice. The calculations were checked by re-summing over 27000 points: the difference produced by the greater number was insignificant. Of much greater importance was the size of the imaginary part added to ω. This must be large enough to ensure that each point used in the sum includes contributions from a large number of neighbouring points. The value adopted was usually between 0.1 and 0.2. The lower value still produced some spurious irregularities in Im $G(\omega)$ as ω is varied, but the higher value caused Re $G(\omega)$ to be appreciably different from its true value, and so appropriate compromises were adopted for various calculations.

Appendix E : SOLUTION OF $\Sigma'_p = -0.5$ IN THE CPA

Each of the three components of the self-energy (Σ_s , Σ_p , Σ_d) is determined in the CPA by an equation :

$$\Sigma_\alpha + c + \Sigma_\alpha (\Sigma_\alpha + 1) G_\alpha = 0 \qquad [\alpha = s, p, d] \qquad \text{(E.1)}$$

where G_α is given by

$$G_\alpha = N^{-1} \sum_{\underline{k}} \frac{\varphi_\alpha(\underline{k})}{\omega - 6(1-\gamma_{\underline{k}}) - [\Sigma_s \varphi_s(\underline{k}) + 3\Sigma_p \varphi_p(\underline{k}) + 2\Sigma_d \varphi_d(\underline{k})]} \qquad \text{(E.2)}$$

The φ_α are given in equation (1.49). If we now write Σ_α as $\Delta_\alpha + i\Gamma_\alpha$, (E.1) becomes

$$\Delta_\alpha + c + [\Delta_\alpha(\Delta_\alpha+1) - \Gamma_\alpha^2] G'_\alpha - \Gamma_\alpha(2\Delta_\alpha+1) G''_\alpha = 0 \qquad \text{(E.3a)}$$

$$\Gamma_\alpha + \Gamma_\alpha(2\Delta_\alpha+1) G'_\alpha + [\Delta_\alpha(\Delta_\alpha+1) - \Gamma_\alpha^2] G''_\alpha = 0 \qquad \text{(E.3b)}$$

separating the real and imaginary parts, and writing $G_\alpha = G'_\alpha + iG''_\alpha$.

Examination of the φ_α shows that

$$\varphi_s + 3\varphi_p + 2\varphi_d = 12(1-\gamma_{\underline{k}}) \ , \qquad \text{(E.4)}$$

so that if $\Delta_s = \Delta_p = \Delta_d = -0.5$, (E.2) becomes

$$G_\alpha = N^{-1} \sum_{\underline{k}} \frac{\varphi_\alpha(\underline{k})}{\omega - i[\Gamma_s \varphi_s(\underline{k}) + 3\Gamma_p \varphi_p(\underline{k}) + 2\Gamma_d \varphi_d(\underline{k})]} \qquad \text{(E.5)}$$

and in the limit $\omega \to 0$, G_α is pure imaginary. If we now put $\Delta_\alpha = c = -0.5$ in (E.3a), we find

$$\left(\Gamma_\alpha^2 + \tfrac{1}{4}\right) G'_\alpha = 0 \qquad \text{(E.6)}$$

which again implies that G_α is pure imaginary. Γ_α is then given by the self-consistent solution of (E.3b) and the imaginary part of (E.2).

We see thus that for $c = -0.5$ and $\omega = 0$, it is consistent to take the solution of the CPA equations to be

$$\Delta_s = \Delta_p = \Delta_d = -0.5 \qquad \text{(E.7)}$$

which is the result required in §1.3C.

It is quite easy to see that this result is true for any cubic lattice. The matrix used for block-diagonalization, corresponding to $\underset{\sim}{S}$ in (A.2) and (A.3), is always (z+1)-square, and the first two columns must have the form $(1, 0, 0 \ldots.)^T$ and $(0, z\ , z\ ,\ldots)^T$ in order to produce the symmetric s-like modes which always occur. The 2x2 matrix describing the s-states is then the same as that in (A.3), with

$$A_s' = \sum_{j=1}^{z} A_{1j} \quad ; \qquad \text{(E.8)}$$

in particular, $\underset{\sim}{v}_s$ is the same for all lattices. The other sub-matrices differ between lattices, but are always diagonal. Because of the singularity of $\underset{\sim}{v}_s$, $\underset{\sim}{\sum}_s$ is constrained to have the form described in the text, equation (1.66). Consequently, the quantity corresponding to the left-hand side of (E.4) is

$$\Phi \equiv (z - 2z\gamma_{\underline{k}} + \sigma_{\underline{k}}) + \sum_{i=2}^{z} \sum_{j,l=0}^{z} S_{ji}\, e^{i\underline{k}\cdot\underline{R}_{jl}}\, S_{li} \qquad \text{(E.9)}$$

where, from (E.8)

$$\sigma_{\underline{k}} = \sum_{l=1}^{z} e^{i\,\underline{k}\cdot\underline{R}_{1l}} \qquad \text{(E.10)}$$

Now, because $\underset{\sim}{S}$ is unitary,

$$\sum_{i=0}^{z} S_{ji}\, S_{li} = \delta_{jl} \qquad \text{(E.11)}$$

so that (E.9) may be re-written

$$\Phi = (z - 2z\gamma_{\underline{k}} + \sigma_{\underline{k}}) + \sum_{j,l=0}^{z} (\delta_{jl} - S_{j0}\, S_{l0} - S_{j1}\, S_{l1})\, e^{i\underline{k}\cdot\underline{R}_{jl}} \qquad \text{(E.12)}$$

Remembering the form of the first two columns of $\underset{\sim}{S}$, we see that $S_{j0}\, S_{\ell 0}$ is equal to $\delta_{j0}\, \delta_{\ell 0}$, and the term in $S_{jl}\, S_{\ell l}$, when summed over j and l, becomes σ_k. Thus, eventually

$$\Phi = 2z\,(1-\gamma_k) \qquad \text{(E.13)}$$

which is the generalization of (E.4). The argument leading to (E.7) follows immediately for all cubic lattices.

REFERENCES

Aiyer R.N., Elliott R.J., Krumhansl J.A. and Leath P.L., 1969, Phys. Rev. 181, 1006.

Baker J.M., Lourens J.A. and Stevenson R.W.H., 1961, Proc. Phys. Soc. 77, 1038.

Blackman J.A., Berk N.F. and Esterling D.M., 1971, Phys. Rev. B4, 2412.

Breed D.J., Gilijamse K., Storkenburg J.W.E. and Miedema A.R., 1970, J. Appl. Phys. 41, 1267.

Broadbent S.R. and Hammersley J.M., 1957, Proc. Camb. Phil. Soc. 53, 629.

Buchanan M., Buyers W.J.L., Elliott R.J., Harley R.T., Hayes W., Perry A.M. and Saville I.D., 1972 (to be published).

Buyers W.J.L., Holden T.M., Svensson E.C., Cowley R.A. and Hutchings M.T., 1971a, J. Phys. C 4, 2139.

Buyers W.J.L., Holden T.M., Svensson E.C., Cowley R.A. and Stevenson R.W.H., 1971b, Phys. Rev. Lett. 27, 1442.

Buyers W.J.L., Pepper D.E. and Elliott R.J., 1972a, b (to be published).

Charap S.H., 1962, Phys. Rev. 126, 1393.

Coombs G.J., Svensson E.C., Holden T.M., Buyers W.J.L. and Jones D.A., (to be published)

Cowley R.A. and Buyers W.J.L., 1972, Rev. Mod. Phys. 44, 406.

Davies R.W. and Langer J.S., 1963, Phys. Rev. 131, 163.

Deo B. and Behera S.N., 1966, Phys. Rev. 141, 738.

Devlin J.F. and Sawatzky G.A., 1972, Phys. Rev. B 6, 208.

Domb C. and Sykes M.F., 1961, Phys. Rev. 122, 77.

Economou E.N., 1972, Phys. Rev. Lett. 28, 1206.

Edwards S.F., 1958, Phil. Mag. 3, 1020.

Edwards S.F. and Jones R.C., 1971, J. Phys. C 4, 2109.

Elliott R.J. and Heap B.R., 1962, Proc. Roy. Soc. A265, 265.

Elliott R.J., Heap B.R., Morgan D.J. and Rushbrooke G.S., 1960, Phys. Rev. Lett. 5, 366.

Elliott R.J. and Taylor D.W., 1967, Proc. Roy. Soc. A296, 161.

Elliott R.J. and Thorpe M.F., 1969, J. Phys. C 2, 1630.

Fisher M.E. and Essam J.W., 1961, J. Math. Phys. 2, 609.

Fleury P.A. and Loudon R., 1968, Phys. Rev. 166, 514.

Foo E., Amar H. and Ausloos M., 1971, Phys. Rev. B 4, 3350.

Foo E. and Wu D., 1972, Phys. Rev.B5, 98.

Frisch H.L., Sonnenblick E., Vyssotsky V.A. and Hammersley J.M., 1961, Phys. Rev. 124, 1021.

Heap B.R., 1963, Proc. Phys. Soc. 82, 252.

Izyumov Y., 1966, Proc. Phys. Soc. 87, 505.

Izyumov Y. and Medvedev M., 1966, Soviet Physics - J.E.T.P. 22, 1289.

Kaneyoshi T., 1969, Prog. Theor. Phys. 42, 477.

Kaneyoshi T., 1970, Prog. Theor. Phys. 44, 328.

Langer J.S., 1961, J. Math. Phys. 2, 584.

Last B.J., 1972, (to be published).

Leath P.L., 1968, Phys. Rev. 171, 725.

Leath P.L., 1970, Phys. Rev. B 2, 3078.

Leath P.L. and Goodman B., 1966, Phys. Rev. 148, 968.

Lovesey S.W., 1968, J. Phys. C 1, 102.

Low G.G., 1965, Proc. of Symposium on Inelastic Scattering of Neutrons (Bombay), (Vienna: IAEA), p.453.

Low G.G., Okazaki A., Stevenson R.W.H. and Turberfield K.C., 1964, J. Appl. Phys. 35, 998.

Lyo S.K., 1972, Phys. Rev. Lett. 28, 1192.

Martel P., Cowley R.A. and Stevenson R.W.H., 1968, Can. J. Phys. 46, 1355.

Morgan D.J. and Rushbrooke G.S., 1961, Mol. Phys. 4, 291.

Morgan D.J. and Rushbrooke G.S., 1962, Mol. Phys. 6, 477.

Murray G.A., 1966a, Proc. Phys. Soc. 89, 87.

Murray G.A., 1966b, Proc. Phys. Soc. 89, 111.

Nickel B.G. and Krumhansl J.A., 1971, Phys. Rev. B 4, 4354.

Onodera V. and Toyozawa Y., 1968, J. Phys. Soc. Japan, 24, 341.

Rushbrooke G.S. and Morgan D.J., 1961, Mol. Phys. 4, 1.

Schwartz L., Brouers F., Vedyayev A.V. and Ehrenreich H, 1971, Phys. Rev. B 4, 3383.

Schwartz L. and Siggia E, 1972, Phys. Rev.B5, 383.

Shante V.K.S. and Kirkpatrick S., 1971, Adv. Phys. 20, 325.

Smart J.S., 1959, J. Phys. Chem. Solids 11, 97.

Soven P., 1967, Phys. Rev. 156, 809.

Svensson E.C., Holden T.M., Buyers W.J.L. and Cowley R.A., 1969, Solid State Commun. 7, 1693.

Sykes M.F. and Essam J.W., 1964, Phys. Rev. 133, A310.

Takeno S., 1968, Prog. Theor. Phys. 40, 942.

Taylor D.W., 1967, Phys. Rev. 156, 1017.

Tonegawa T., 1968, Prog. Theor. Phys. 40, 1195.

Tonegawa T., 1969, Prog. Theor. Phys. 41, 1.

Velický B., Kirkpatrick S. and Ehrenreich H., 1968, Phys. Rev. 175, 747.

Vyssotsky V.A., Gordon S.B., Frisch H.L. and Hammersley J.M., 1961, Phys. Rev. 123, 1566.

Van Hove L., 1954, Phys. Rev. 95,1374.

Wolfram T. and Callaway J., 1963, Phys. Rev. 130, 2207.

Yonezawa F., 1968, Prog. Theor. Phys. 40, 734.

Yonezawa F. and Matsubara T., 1966, Prog. Theor. Phys. 35, 357.

Zubarev D.N., 1960, Soviet Physics - Uspekhi 3, 320.